INTERPOLATION, ANALYSIS, AND ARCHIVAL OF DATA ON SEA ICE TRAJECTORIES AND OCEAN CURRENTS OBTAINED FROM SATELLITE-LINKED INSTRUMENTS

by

Robert S. Pritchard and Dennis J. Hanzlick

IceCasting, Inc.
11042 Sand Point Way, N.E.
Seattle, Washington 98125-5846

Final Report
Outer Continental Shelf Environmental Assessment Program
Research Unit 683

April 1987

ACKNOWLEDGMENTS

This study was funded by the Minerals Management Service, Department of the Interior, through an interagency agreement with the National Oceanic and Atmospheric Administration, Department of Commerce, as part of the Outer Continental Shelf Environmental Assessment Program. The analysis and report were prepared according to NOAA Contract WASC-86-00043.

TABLE OF CONTENTS

Page

ACKNOWLEDGMENTS 123

LIST OF FIGURES 127

LIST OF TABLES 129

1. INTRODUCTION 131

2. BACKGROUND 133

3. APPROACH 138

4. ANALYTICAL METHODS 154

4.1 Optimal Interpolation 154
4.1.1 Estimating Position 154
4.1.2 Parameters for Sea Ice Motions 157
4.1.3 Error Estimate 158
4.1.4 Optimal Estimation of Velocity from Position Measurements 159
4.2 Complex Regression 162

5. RESULTS: NORTON SOUND 164

5.1 Ice Trajectories 165
5.2 High Frequency Oscillations 165
5.3 Wind, Current, and Ice Velocity 165
5.4 Correlations. 168

6. RESULTS: CHUKCHI SEA 182

6.1 Ice Trajectories 182
6.2 Wind, Current, and Ice Velocity 183

7. SUMMARY. 201

8. REFERENCES CITED 204

APPENDIX A. NODC File Type 156 Data Documentation Forms 207

APPENDIX B. Sea Ice Trajectories 219

LIST OF FIGURES

Figure		Page
3.01	Buoy 3608 raw position measurements	145
3.02	Buoy 3608 interpolated position time history	148
3.03	Buoy 3608 velocity time history calculated from interpolated position history.	151
5.01	Buoy 3609 velocity time history calculated from interpolated position history.	170
5.02	Buoy 3607 ice velocity power spectral density	171
5.03	Buoy 3608 ice velocity power spectral density	172
5.04	Buoy 3609 ice velocity power spectral density	172
5.05	Buoy 3607 stick plots ofdaily average wind, ice velocity, current, and relative current	173
5.06	Buoy 3608 stick plots of daily average wind, ice velocity, current, and relative current	174
5.07	Buoy 3609 stick plots of daily average wind, ice velocity, current, and relative current	179
6.01	Buoy 3625 interpolated position time history	188
6.02	Buoy 3625 raw position measurements	190
6.03	Buoy 3625 velocity time history calculated from interpolated position history.	192
6.04	Buoy 3623 ice velocity power spectral density	194
6.05	Buoy 3624 ice velocity power spectral density	194
6.06	Buoy 3625 ice velocity power spectral density	195
6.07	Buoy 3623 stick plots of daily average wind, ice velocity, current, and relative current	196
6.08	Buoy 3624 stick plots of daily average wind, ice velocity, current, and relative current	197
6.09	Buoy 3625 stick plots of daily average wind, ice velocity, current, and relative current	198

LIST OF TABLES

Table		Page
1.1	Buoy locations, sensors, and launch and end dates	135
3.1	Relationship between Julian times and calendar dates	139
4.1	Optimal interpolation parameters	158
5.1	Comparison between wind, ice velocity, and current for Norton Sound drifting buoys	169
6.1	Comparison between wind, ice velocity, and current for Chukchi Sea drifting buoys	187

1. INTRODUCTION

This final report is submitted to NOAA to describe the work performed by IceCasting, Inc.(ICI) under NOAA contract No.WASC-86-00043. The broad objectives of the study were to analyze data taken by ice drifting buoys in Norton Sound and the Chukchi Sea during 1981-82, to describe the atmospheric and oceanic features that occurred during these field programs, and to provide the data in a revised format to NODC. The two field projects that collected these data were conducted by Dr. R. S. Pritchard, now with ICI, and others at Flow Research Company (Flow), and were sponsored by NOAA through the OCSEAP program, as part of RU567. The field program in Norton Sound was jointly sponsored by OCSEAP and a consortium of oil companies.

Both of these field projects used the NOAA Tiros satellite system to receive data. A combination of ARGOS and air-droppable TAD(A) buoys was used, with additional sensors on some buoys to measure environmental parameters. The experiments were designed to obtain broad spatial coverage throughout the winter. Eleven buoys were deployed at three different times in Norton Sound and six were deployed at two different times in the Chukchi Sea.

Under RU567 the data were obtained and validated, but not analyzed. The data were submitted to the National Oceanographic Data Center (NODC) to be archived, but file formats have since changed (from File Type 056 to 156), and standardization of these formats precluded including these data. Therefore, the first objective of the work was to modify the raw data to fit into the File Type 156, and to submit the results for a final quality

assurance check and archival in the NODC data bank. The second objective was to describe the ice behavior and the environmental conditions that existed during the field programs.

In section 2, we discuss the background leading to this work. In section 3, the tasks performed during the study are described. In section 4, the analytical methods used are presented. The discussion is focused on the method of Optimal Interpolation because the method has recently been adapted for analyzing sea ice motion data in the presence of tidal oscillations. In sections 5 and 6, we describe the ice behavior and the environmental conditions that existed in the Norton Sound and Chukchi Sea, respectively. In section 7, the work is summarized.

2. BACKGROUND

The MMS and OCSEAP are responsible for obtaining enough information about the environmental conditions in each lease sale area to ensure that exploration and production of hydrocarbons will be safe and will not have an unacceptable impact on the environment. This responsibility has many aspects, and the data to be analyzed here relate to several of them.

The ice motions and ice conditions affect when and how operations can proceed at a site which might be threatened at some time during the operation. Both variables also affect the design of structures that can operate at each site because thicker ice or multi-year ice can exert larger forces on a structure than thinner or first-year ice, and because the ice strength increases with increasing strain rates.

If a drilling accident were to occur, and oil were released into the ocean, on or under the ice, then the impact of this release must be understood. Since oil may be transported by both the ocean and the ice, it is critical to understand the relationship between wind, water and ice motions.

Observations of the winds, currents and ice motions are of direct value, but the history of accurate, season-long observations is short and they are expensive to make. Therefore, OCSEAP has relied on mathematical and computer models of the ice and ocean dynamics to estimate the expected range of behavior over the lifetime of production from a lease sale area (e.g., Pritchard, 1979; Thomas and Pritchard, 1979, 1982; Liu and Leendertse, 1904). Observations are used primarily to validate

and tune the models, although Colony and Thorndike (1985) have estimated the range of ice motions using a statistical model based directly on observed motions.

The data to be analyzed here are from field experiments that were designed so that ice and ocean dynamics models could be tested and their performance verified. The two largest external driving forces (air and water drag) depend on the winds and currents relative to the ice (e.g. Pritchard, 1981; McPhee, 1982). Therefore, these field experiments measured both winds (or barometric pressure from which winds could be determined) and currents at selected locations.

For the Chukchi Sea experiment, where the large-scale wind fields are driven primarily by gradients in the barometric pressure field, barometers were used to supplement the hemispheric barometric pressure fields normally estimated by the National Meteorological Center (NMC). For the Norton Sound experiment, gradient winds give a less accurate measure of local winds (Kozo, 1984), so winds were measured directly using an anemometer and vane on a 3-m-tall mast.

The ocean currents at the bottom of the mixed layer (some 6- to 10-m below the ice in the shallow waters of both Norton Sound and the Chukchi Sea) were measured relative to the ice by suspending a current meter below the ice floe on which the buoy was deployed. This allowed the absolute current to be determined, if the ice velocity were known, by adding the two quantities vectorially.

If the ice trajectories, and the winds and currents that drive the ice, are determined for each day, then we have a

consistent set of variables to describe the synoptic-scale processes that control long-term behavior. On short time scales, the tides cause ice and water movements. Usually these motions are small over periods longer than a day when compared to the wind- and current-driven drift, although Liu and Leendertse (1984) have concluded that Norton Sound currents result from tidal residuals. Here, we assume that the short-term tidal and inertial oscillations have only a small effect on the daily processes, and so they can be filtered out of the data without affecting the analysis of the synoptic-scale processes.

Table 1 shows the buoys that were deployed, their initial locations, sensors, and start/finish dates of transmission. The dates begin late in 1981 and end by the summer of 1982.

Table 1. Buoy Locations, Sensors, and Launch and End Dates.

Buoy ID	Rough Location	Barom.	Anemom. & Vane	Current Meter	Compass	Dates Launch	Dates End
3607	Norton Sound		x	x	x	2/06	2/19
3608	Norton Sound		x	x	x	2/24	6/11
3609	Norton Sound		x	x	x	2/27	4/06
3610	Norton Sound					12/18	1/16
3611	Norton Sound					12/17	6/29
3612	Norton Sound					1/31	5/31
3613	Norton Sound					2/26	4/11
3614	Norton Sound					3/02	6/15
3615	Norton Sound					3/02	3/25
3616	Norton Sound					3/03	6/18
3617	Norton Sound					3/03	6/11
3420	Chukchi					1/30	2/15
3621	Chukchi					12/19	2/17(a)
3622	Chukchi	x				2/09	6/12
3623	Chukchi			x		2/11	7/13
3624	Chukchi			x		2/15	5/03
3425	Chukchi	x		x		2/16	5/08

Note(a) This buoy continued to transmit until 1983.

Trip reports and a description of buoy operations can be found in Thomas and Pritchard (1982). For completeness, we briefly discuss here the data and the methods used to retrieve the raw data using the NOAA satellites.

The positions of the drifting buoys were measured at irregular intervals throughout the day depending on the timing of satellite passes. The ARGOS and TAD(A) buoys transmitted a short, roughly 400 MHz burst at one minute intervals. This signal was received by the NOAA satellites and transmitted to the Gilmore Creek receiving station, which then re-transmitted it to Service Argos, Toulouse, where it was processed. Buoy positions were determined by observing the Doppler shift in signal frequency. As each satellite passed overhead (at satellite noon, it viewed each buoy for up to twelve minutes), multiple transmissions were received and used by Service Argos to estimate position. The sensor data were encoded into the signal, with 256 bits transmitted each time. Those buoys that contained sensors also contained a clock. At 2-hour intervals, the buoy interrogated each sensor and stored the observations in memory. Wind vectors and current meter speeds were averaged over a 9-minute period and then stored. Current meter directions and barometric pressure were sensed instantaneously at the sampling times and stored. Four sets of sensor observations were stored in memory and transmitted sequentially to the satellite receiver to provide redundancy in the system. In this way each sensor observation was saved and transmitted for a 6-hour period, thereby greatly increasing the probability that a satellite would receive the signal .

Reynolds and Pease (1984) also deployed an array of six ARGOS drifting buoys in Norton Sound during January and February 1982. Their experiment was located approximately between the Norton Sound and Chukchi Sea regions being reported here. Four of the PMEL platforms drifted through the Bering Strait, and in response to alternating winds and currents, oscillated through the strait three or more times. Their other two platforms oscillated north and south on the same time scales, but remained near the western Norton Sound area (Pease and Salo, 1987) ,

3. APPROACH

The objectives of the project were satisfied by dividing the work into the following four tasks.

Task 1. Acquire data from the University of Rhode Island (URI).

A magnetic tape containing all data from the two field experiments was provided to the ICI investigators by Ms. Nancy Clayton, URI. The tape blocking was chosen after consulting with Mr. Pat McCafferty, Flow, to ensure that the data could be read from the magnetic tape into the Flow MASSCOMP computer. The Norton Sound data were written in the older file type 056 format, which interspersed records describing the buoy positions, wind speed and direction, relative currents, ice floe orientation, and other measurement%, so that one file was. available for each buoy. The Chukchi Sea data were written in a modified file type 156 format, with separate files for position, barometric pressure, and current for each buoy.

During this project, the barometric pressure data were averaged over two-hour time periods to obtain estimates at about the same sampling rate as the other variables. These average values were stored at NODC. This filtering process retained all essential information because there are no significant physical processes responding above this frequency.

The raw data were examined for erroneous points by plotting the time history for each position and sensor. Figure 3.01 shows a typical plot of the position estimates from Service Argos, with dots at each time. Similar plots were used to peruse the sensor

data. The time scale represents a decimal measure of time in Julian days. The Julian time of t=1.000 day corresponds to January 1, 1982 at 0000 GMT. Plots have been scaled to present 30-days of data, roughly a month, on a page. For convenience, Table 3.1 presents the Julian time at the start of each month for which data were obtained.

Table 3.1. Relationship Between Julian times and Calendar Dates. All times correspond to 0000 GMT on the dates shown.

Calendar Date	Julian Time
Dec 1, 1981	-30,
Jan 1, 1982	1.
Feb 1, 1982	32.
Mar 1, 1982	60.
Apr 1, 1982	91.
May 1, 1982	121.
Jun 1, 1982	152.
Jul 1, 1982	182.
Aug 1, 1982	213.
Sep 1, 1982	244.
Oct 1, 1982	274.
Nov 1, 1982	305.
Dec 1, 1982	335,
Jan 1, 1983	366.
Feb 1, 1983	397,
Mar 1, 1983	425.

Task 2. Calculate interpolated positions for sensor data points for which such information is missing; and calculate absolute current speeds from current meter and buoy position records.

Approximately 10-12 position measurements are obtained each day. These data points are usually obtained during a twelve to sixteen hour period, with little data available during the remainder of the day. These positions are estimated at irregularly spaced intervals (from a few minutes to more than 6 hours apart), while the current meter measurements are obtained at regular 2-hour intervals. This data sampling density is adequate for determining the buoy (and ice floe) trajectories and

the velocities, but a sophisticated analytical technique is required. Accurate ice velocity estimates are important because they are used in conjunction with the relative current measurements to estimate absolute currents. Ice motion data can contain tidal oscillations with a spatial ampl itude on the order of 10Km. The peak velocity of such a diurnal signal is about 60cm/s. This tidal component is larger than the longer-term, daily average values. A similar argument can be made concerning the semi-diurnal tidal component.

The ice velocity can be accurately estimated at 2-hour intervals because the tidal oscillations are periodic and well-known, and because the atmospheric forces and ocean currents which drive the ice vary on time scales longer than tidal. However, internal ice stresses can vary rapidly, creating an ice stress divergence force that accelerates the ice on shorter-term time scales. We have assumed that the short-term ice motions caused by the ice stress divergence are small and that the associated ice velocity component is also small compared to daily and tidal components. There are no independent data available to test this assumption.

The buoy position data were used to obtain a uniformly-spaced sequence of buoy position and velocity. The Optimal Interpolation method (OI) to be presented in section 4 was used to estimate the buoy positions at 3-hour intervals. The ice velocity was estimated at the same times by forming the difference between interpolated positions and dividing by the averaging interval. Linear interpolation was then used to

calculate the ice velocity associated with each current meter measurement.

The calculated position history of buoy 3608 is presented in Figure 3.02. The data used to calculate these positions are presented in Figure 3.01. The two histories may be compared directly. The OI fit is very good, with the interpolated data curve overlaying the raw data points. The high frequency tidal and inertial oscillations are described accurately, as are the longer-term variations.

The ocean current velocity, c, is estimated by adding the ice velocity, vi, to the relative velocity, v_r, measured by the current meter

$$c = v_i + v_r \quad (3.1)$$

The ice velocity, vi, can be estimated from the buoy positions using the relation,

$$v_i(t) = \frac{x(t+\Delta) - x(t-\Delta)}{2A} \quad (3.2)$$

where A equals one-half of the velocity averaging interval . The method of optimal 1 inear interpolation allows the positions to be calculated at any time.

Figure 3.03 shows the velocity of buoy 3608, calculated from the OI position history. Until about Jd 913 <see Table 3.1 for calendar dates associated with the Jul ian Day), this buoy was located near the mouth of Norton Sound where the diurnal tide is large. The presence of this large tidal velocity, which appears as a rather small oscillation in position, required that we use the sophisticated OI analysis, or else the ocean current estimates would have been swamped by uncertainty. Other simpler

techniques, such as linear interpolation between adjacent data points, could have been used to estimate sensor positions, but the OI method allowed us to estimate both position and velocity at the same time.

Task 3. Describe atmospheric and oceanic features and motions extant during the buoy deployment period.

The winds and currents provide two of the external forces that cause the ice cover to move and deform. The ice responds quickly to changes in these forces so that quasi-static behavior may be assumed on time scales of about a day (e.g. Pritchard, 1981). In addition, tidal forcing and inertial oscillations can drive ice motions at time scales as short as 6-12 hours. But it is the daily and longer-term variations that this project originally sought to measure, and it is these time scales on which our attention is focused. Thus, the time histories of winds and currents have been filtered to isolate the synoptic-scale behavior from the shorter term variations. Daily values of the ice velocities, winds, and currents were determined using a 48-hour cosine bell filter (e.g., Bendat and Pierson, 1980; Bloomfield, 1976).

In Norton Sound, the wind speed and direction at each of the met-ocean buoys were measured directly by an anemometer and vane mounted on a 3-meter-tall mast. The winds were then calculated directly by forming the vector.

In the Chukchi Sea, the two barometers were not adequate to determine winds. To estimate the winds at the respective buoys,

we acquired data from the NOAA Pacific Marine Environmental Laboratory (PMEL), and used their METLIB software package (Macklin, et. al., 1984). Specifically, we obtained atmospheric pressure data on a section of the FNOC 63x63 northern hemisphere grid. This section covered the entire Bering and Chukchi sea region. The data had been interpolated by PMEL to one-quarter of the original grid size, and thus the grid spacing was about 90 km in the Chukchi. We extracted a subsection of the data which covered only the region of interest and used the METLIB program to calculate surface winds. The surface winds were estimated by multiplying the gradient winds by 0.70 and rotating the wind vector 30 degrees to the left. These values are consistent with the results of earlier studies of wind reduction ratios and indraft angles in the Arctic (Overland, 1985). A time series of winds at a selected location in the Chukchi was generated, and these data were compared against pressure map contours and surface observations as a check that the output winds were representative of the actual winds. Finally, a time series of winds along the drift tracks of the buoys was calculated.

Task 4. Prepare digital data in appropriate file type (FT 156) for archival at NODC.

The original FT 156 was not compatible with the data generated by this project because there was no field to accept the currents. Therefore, two new record types (E and F) were developed by the PI and Ms. Nancy Clayton of URI to allow us to archive data from drifting buoys with current meters, Mr. Steve Patterson, NODC, was consulted to ensure that the *new* formats

would be acceptable to NODC, and Dr. Jawed Hameedi, COTR, also concurred. The Data Documentation forms for this data set are presented in Appendix A.

The raw current meter measurements describe the ocean current velocity relative to the ice velocity. This relative velocity was considered to be too difficult to use by other investigators, and so the absolute ocean current was calculated and stored instead. However, the absolute current is a derived variable, and one that depends strongly on the method used to estimate ice velocity. Therefore, the FT 156 format also contains the ice velocity that was used to calculate the absolute current. The ice velocity was included to allow other investigators to reconstruct the original data set if desired, and therefore to use alternate methods to analyze the data.

A magnetic tape was generated in the format of File Type 156 and sent to the COTR for quality assurance testing by URI and transmittal to NODC. This tape satisfied the first of two deliverable products required under terms of the contract. This final report satisfies the second, and final, deliverable product of the project.

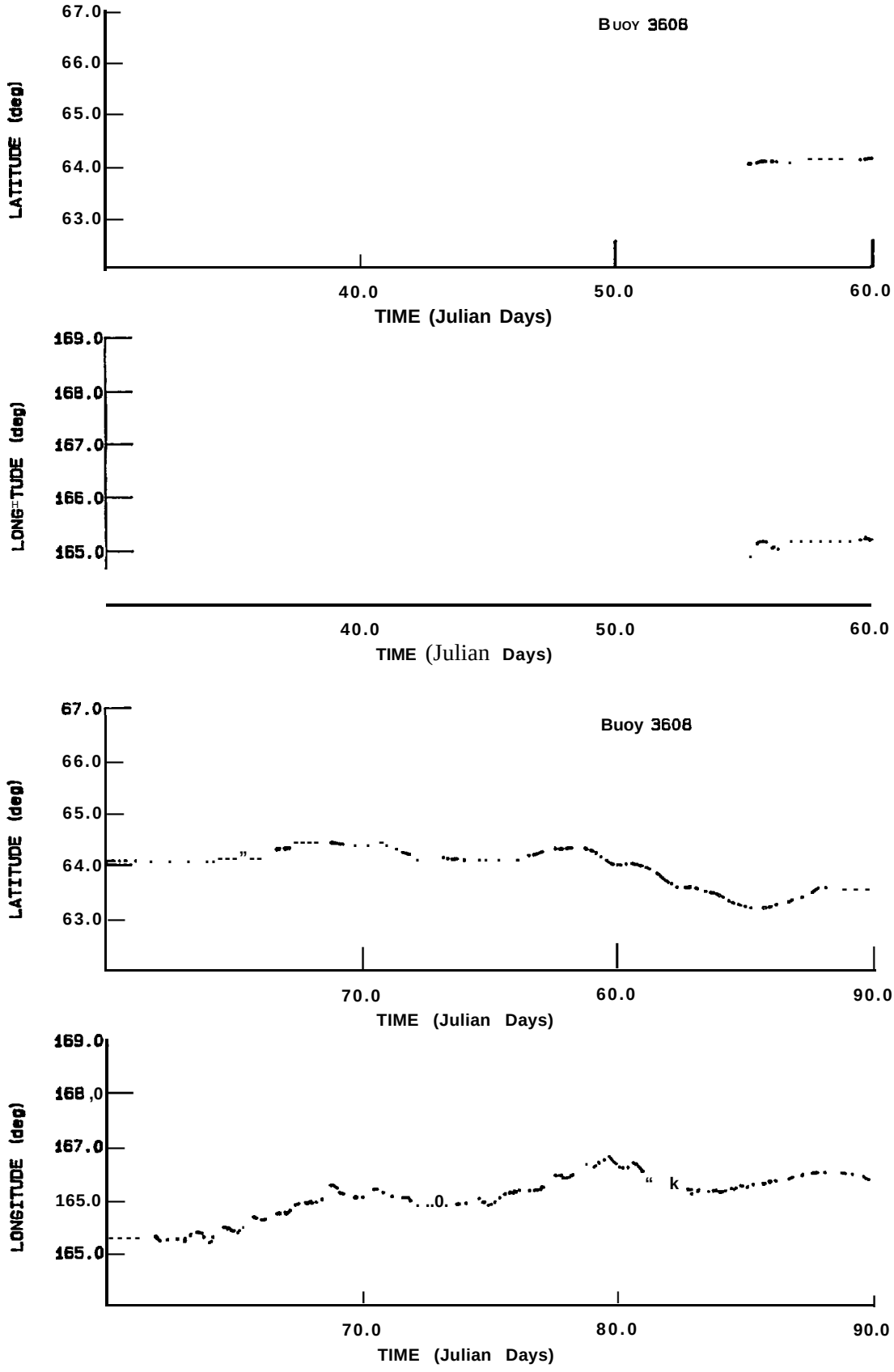

Figure 3.01. BUOY 3608 Raw Position Measurements.

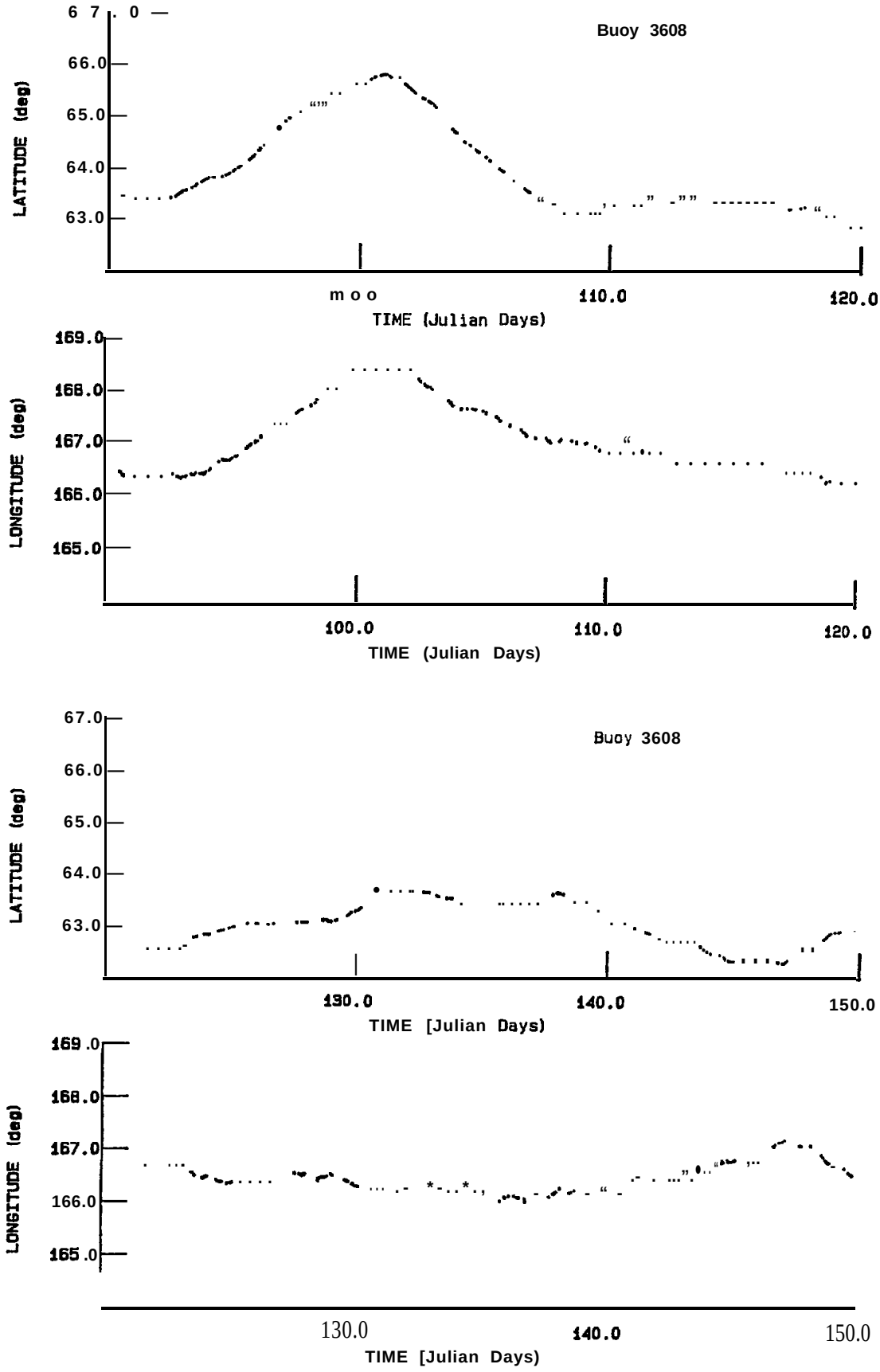

Figure 3.01. Buoy 3608 Raw Position Measurements <cont.)

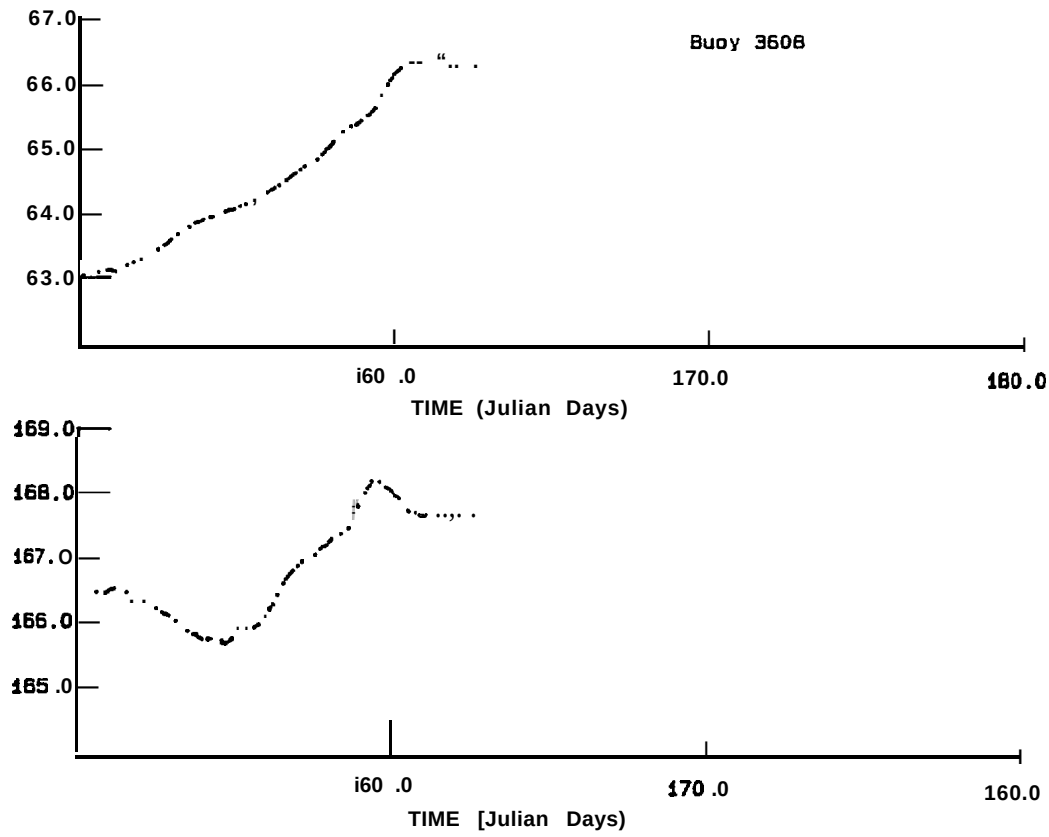

Figure 3.01. Buoy 3608 Raw Position Measurements (concl'd).

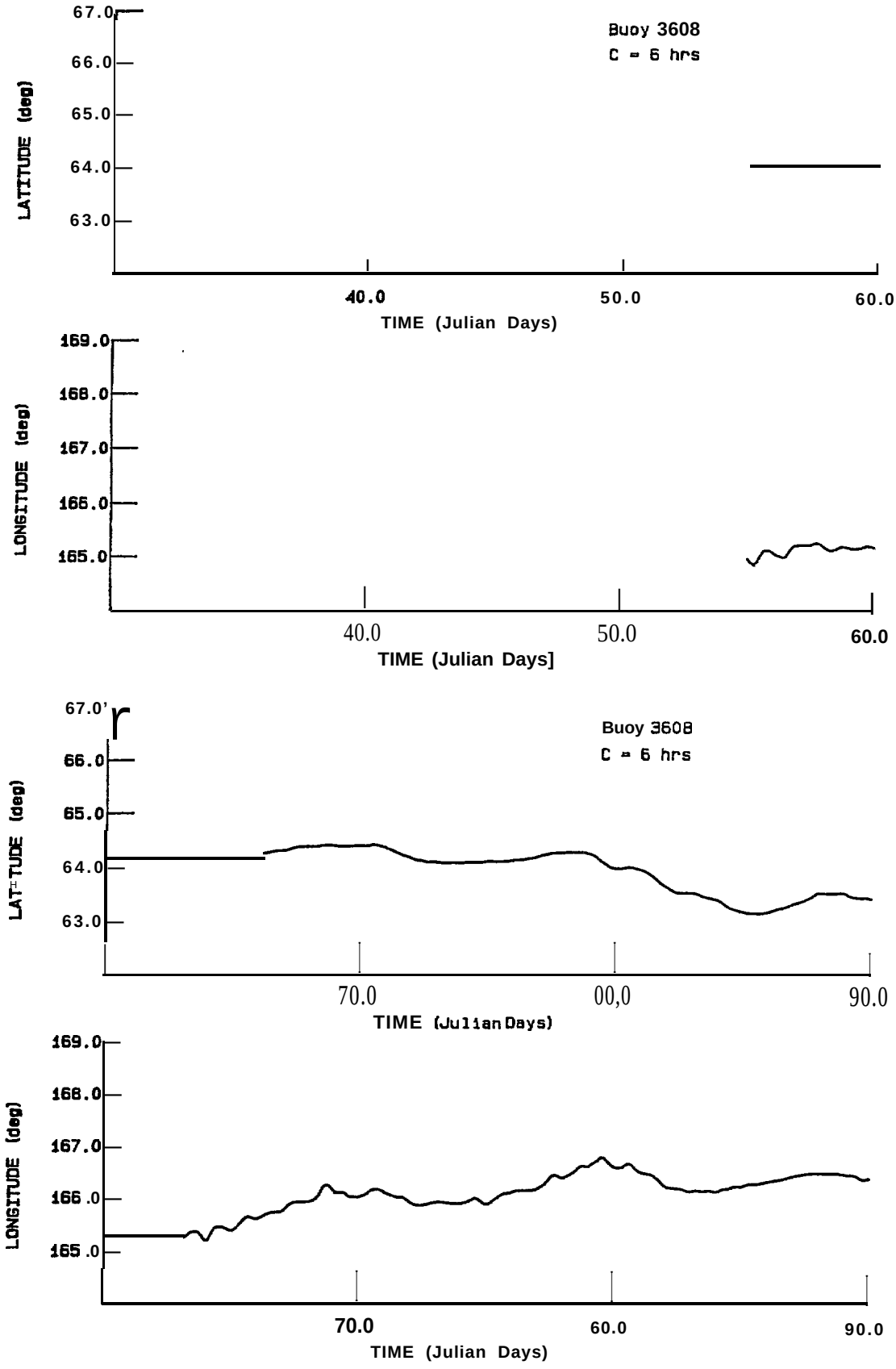

Figure 3.02. Buoy 3608 Interpolated Position Time History.

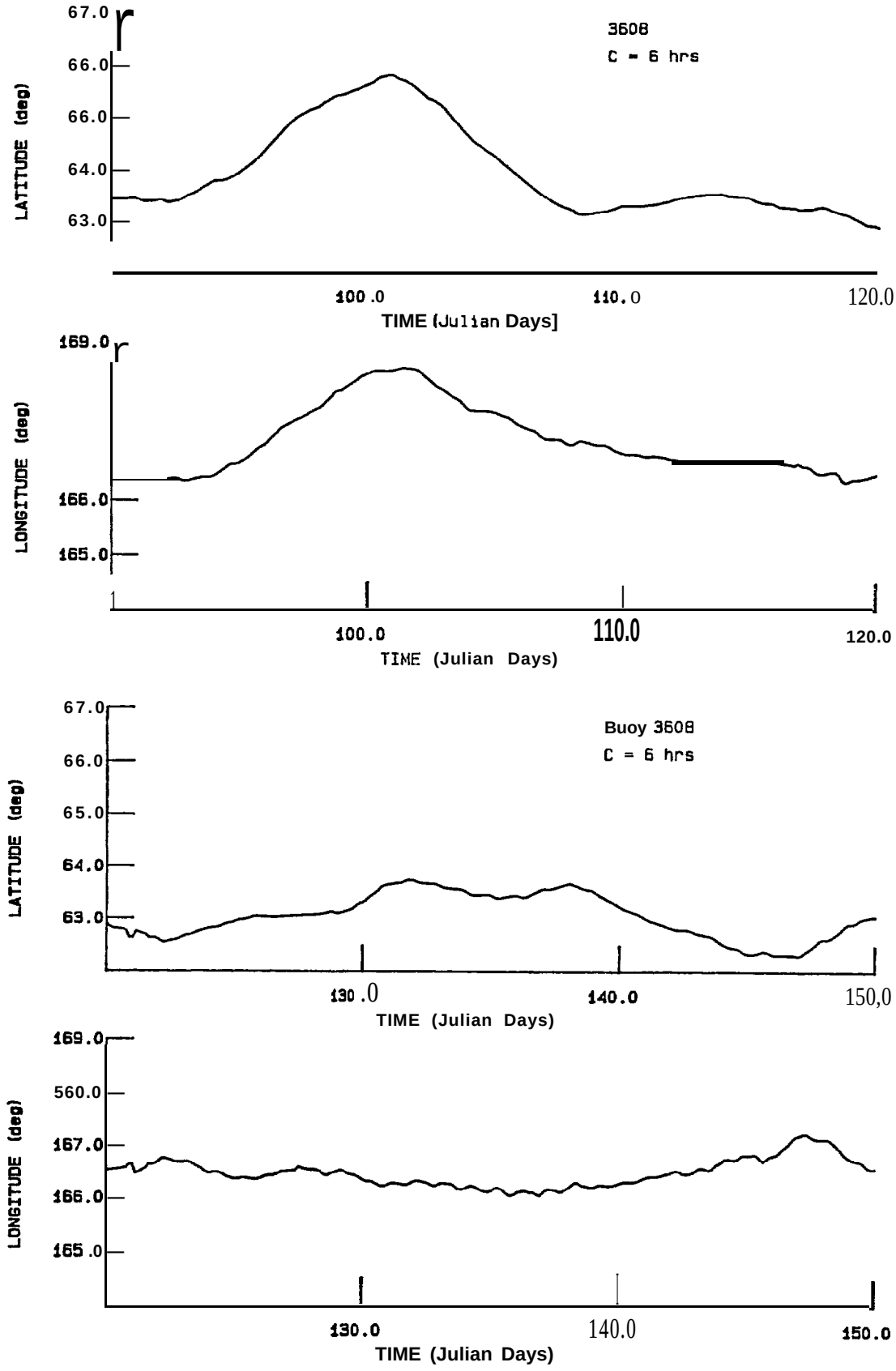

Figure 3.02. Buoy 3608 Interpolated Position Time History (cont.).

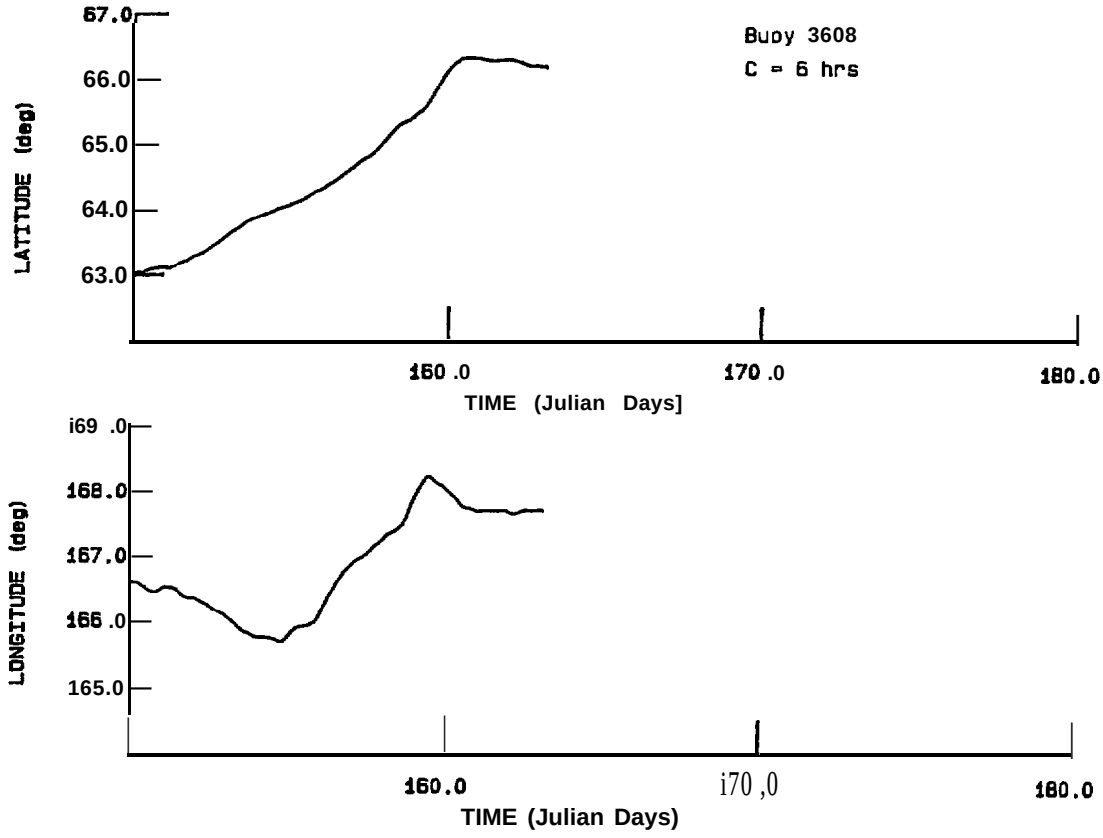

Figure 3.02. Buoy 3608 Interpolated Position Time History (concl'd).

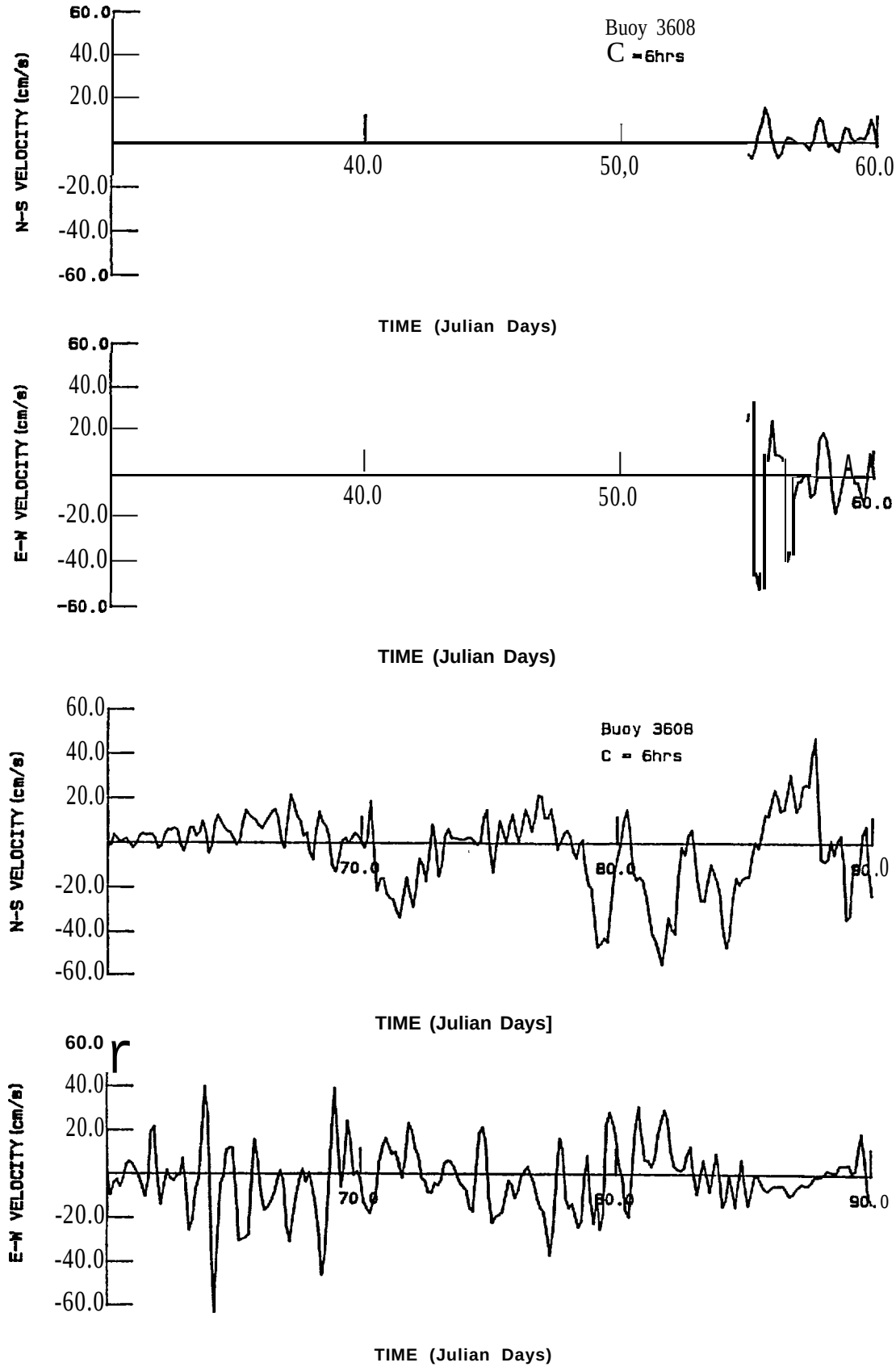

Figure 3.03. Buoy 3608 Velocity Time History Calculated from Interpolated Position History.

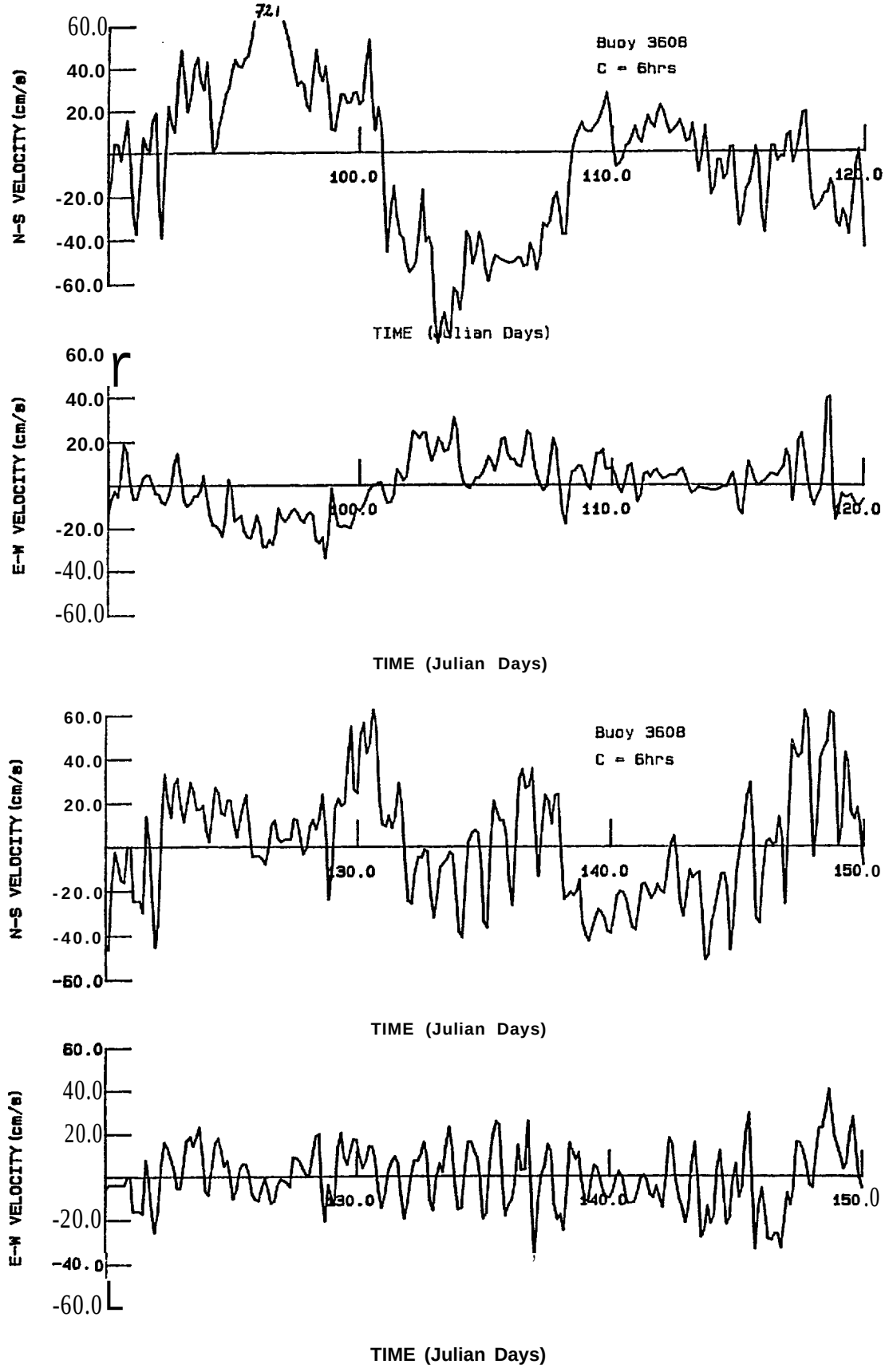

Figure 3.03. Buoy 3608 Velocity Time History Calculated from Interpolated Position History (cont.).

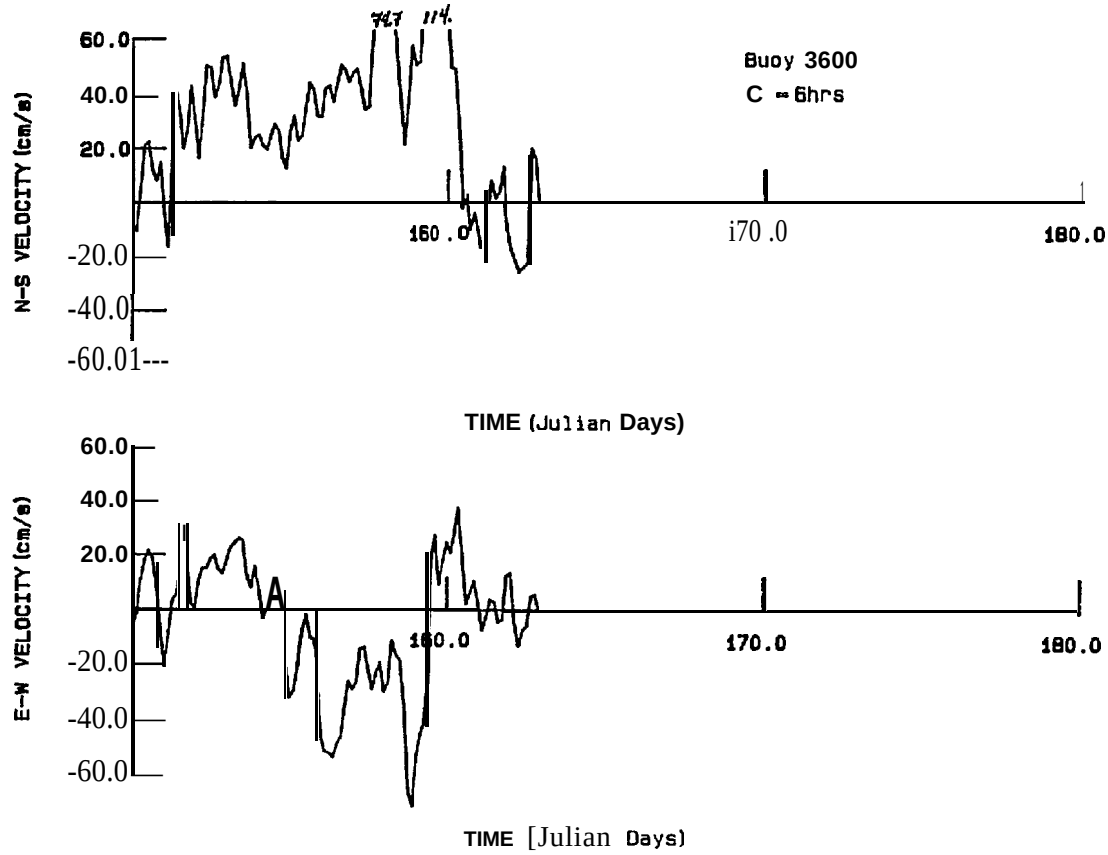

Figure 3.03. Buoy 3608 Velocity Time History Calculated from Interpolated Position History (cone?'d).

4.1. Optimal Interpolation

Assume that the set of N data points Z_i, obtained from an experiment, represents one realization of a random process in time. The data values Z_i are measurements of the dependent variable x that we wish to estimate. Since the data result from one realization of the random process, we consider the statistical properties of the process. The expectation $E(x)$ is a time-dependent ensemble average of all values that the random variable may take weighted by the probability of occurrence. The second moment $E(x^2)$, the expectation of the square of x is found similarly. The variance of the random variable x, denoted by σ_x^2, is the mean squared deviation from its mean. The variance is related to the first two moments by (e.g. Gelb, 1974)

$$\sigma_x^2 = E(x^2) - [E(x)]^2. \tag{4.1}$$

For simplicity, we assume that the average value of the data has been subtracted from the Z_i. Our attention is focused on estimating variations about the average, and we assume that the average is added back at the end of the analysis.

4.1.1. Estimating Position. Let x represent either the latitude ϕ or the longitude λ, and consider each variable separately. We estimate the value of x by forming a linear combination of measured values

$$\hat{x}(t) = \sum_i \alpha_i(t) \; Z_i \tag{4.2}$$

where the coefficients α_i are determined at each time. The relationships that determine the coefficients result from the

assumptions used to make the estimate optimal .

The error between the estimate $\hat{x}$ and the true value x is

$$\varepsilon = \hat{x} - x. \tag{4.3}$$

The expectation of the square of the error ε may be expressed as a function of the coefficients as

$$E(\varepsilon^2) = E([\sum_i \alpha_i(t) \; Z_i \; - x]^2). \tag{4.4}$$

This second moment is minimized at each time to determine the optimal estimate. The minimum value is found by taking the derivative of $E(\varepsilon)^2$ with respect to each coefficient α_j. As a result, for each value of j=1,2,..N, we obtain

$$\sum_i \alpha_i(t) \; E(z_i z_j) - E(xz_j) = 0 \tag{4.5}$$

where the order of the ensemble average and the summation are interchanged because both are linear operators.

The measurements differ from the value xi (which is the value of x at time t_i) by the measurement error ε_i so that

$$z_i = x_i + \varepsilon_i. \tag{4.6}$$

The measurement errors are taken into account by expanding

$$E(z_i z_j) = E(x_i x_j) + E(x_i \varepsilon_j) + \\ + E(\varepsilon_i x_j) + E(\varepsilon_i \varepsilon_j) \tag{4.7}$$

and

$$E(xz_j) = E(xx_j) + E(x\varepsilon_j).$$

But if the error ε_j is uncorrelated with the variable x, and with other errors ε_i , then

$$E(x_i \varepsilon_j) = 0$$

$$E(\varepsilon_i x_j) = 0 \tag{4.8}$$

$$E(x\varepsilon_j) = 0$$

and

$$E(\varepsilon_i \varepsilon_j) = \sigma^2 \delta_{ij}$$

where σ is the standard deviation of the measurement errors. Substituting back into the equations governing the coefficients a, gives

$$\sum_i \alpha_i [E(x_i x_j) + \sigma^2 \delta_{ij}] - E(x x_j) = 0 \qquad (4,9)$$

where the coefficients $\alpha_i(t)$ are evaluated at arty time t by likewise evaluating the function x(t) at the same time.

The second moment of the process $E(x x_j)$ must be specified independently to solve for the coefficients a_i. If the process is stationary, then the correlation between x and X_j is a function of the time difference $t-t_j$. Previous experiments with different functional forms led us to assume that

$$E(x x_j) = (7_x^2 \; R(t-t_j) \qquad (4.10)$$

where the autocovariance function R is the error function

$$R(t-t_j) = \exp[-|t-t_j|/C \; 1^2. \qquad (4.11)$$

The parameter C is a constant that defines the decay of the correlation with time, and σ_x is the standard deviation of x.

This form of the autocovariance function cannot describe the ice motions completely because the motions include both tidal and inertial oscillations (roughly 12 and 24 hour periods) and wind-driven variations (roughly 2-10 day periods). We tried to use an autocovariance function that included both the tidal cosine functions and the longer-term exponential decay, but the OI method failed. The problem arose when two or more data points were too-highly correlated. Even when data were pre-conditioned by averaging nearby data points, the system of linear equations was i n-conditioned, and could not be solved for the

coefficients. To circumvent this problem, the smaller time constants shown in Table 4.1 were used, but the local mean and trend were removed from the signal at each time. This step allowed us to track the short-term oscillations, independent of any knowledge of longer-term behavior. The excellent visual comparison of the interpolated values (Fig. 3.01) with the raw position data (Fig. 3.02) confirm that this approach was reasonable.

4.1.2. Parameters for Sea Ice Motions. The parameter C of the autocovariance function used to estimate either latitude or longitude histories (4.11) typically had a value of 6 hours. This value was chosen primarily by experimenting with the data. First, since roughly 12 data points were available daily, the highest frequency oscillations that could be resolved had a period of about 4 hours, which required C to be at least this order of magnitude. Second, the autocorrelation function for sea ice motions is unknown so we could not objectively define the independent time scale. Third, we tried several values of C ranging from 6 hours to 2 days and found that the power spectral density was unchanged if 6 or 12 hours was used, and that high frequency oscillations were reduced if longer times were used. Therefore, we chose C to be either 6 or 12 hours for most buoys, and used a larger value only when buoy transmissions were irregular or less frequent than normal . The final test on this choice was visual , If the resulting graphs of interpolated positions appeared to describe behavior in a reasonable way, then that set of parameter values was used. The normal position measurement errors were estimated to be 300 meters based on

measurements taken prior to deployments. Buoy 3620 transmitted irregularly and the pre-deployment measurements indicated that errors were on the order of 2km. Table 4.1 describes the constant values used for each buoy.

Table 4.1. Optimal Interpolation Parameters. The constant C represents the autocovariance time constant in equation (4.11), and E represents the estimated standard measurement error.

Buoy	C(hr)	E(km)
3607	6	.3
3608	6	.3
3609	6	.3
3610	12	.3
3611	48	.3
3612	6	.3
3613	6	.3
3614	6	.3
3615	6	.3
3616	12	.3
3617	&	.3
3620	48(a)	2*
3621	12	.3
3622	6	.3
3623	12	.3
3624	6	.3
3625	6	.3

Note (a). The latitude time constant was 48hr, while the longitude time constant was 72hr.

4.1.3. Error Estimate. The variance in the error is estimated by determining the expectation of the square error, given by equation (4.4). The binomial product is expanded into

$$E(\varepsilon^2) = E(\hat{x}\hat{x}) - 2E(\hat{x}x) + E(xx). \tag{4.12}$$

Expanding the first term gives

$$E(\hat{x}\hat{x}) = \sum_j a_j \sum_i a_i \; E(z_i z_j) \tag{4.13}$$

which by equation (4.5) reduces to

$$E(\hat{x}\hat{x}) = \sum_j \alpha_j E(xz_j) \tag{4.14}$$

Similarly, the second term may be expanded into

$$E(\hat{x}x) = \sum_i a_i E(xz_i). \tag{4.15}$$

The combination of the three terms is written as

$$E(\varepsilon^2) = \sigma_x^2 [\ 1 - \sum_i \alpha_i R(t-t_i)\ ]. \tag{4.16}$$

4.1.4. <u>Optimal Estimation of Velocity from Position Measurements</u>. Gandin (1965, pp. 69-70) states that any linear combination of values determined from an optimal estimate at different times is also an optimal estimate of the variable defined by the same linear combination. Therefore, if the velocity is estimated as the difference between two position estimates separated in time by an increment, then this velocity is also an optimal estimate. Furthermore, if the time increment is reduced in the limit to zero, then the resulting derivative is the optimal estimate of the rate of change of position. This important property implies that we can use the optimal estimate of the positions determined from the position measurements to obtain our optimal velocity estimate, and this result holds whether we calculate a time-averaged velocity (as the difference between two positions separated by a time increment 2Δ) or an instantaneous velocity (as the local slope of the position function). In either case, we use a linear combination of position measurements.

Our attention turns toward determining the velocity from the set of position data. Since (4.2) is a continuous function of time, the expression may be differentiated to determine the

velocity. This derivative gives the instantaneous velocity, or the slope of the position curve

$$\hat{v} = \sum_i \beta_i \; z_i \tag{4.17}$$

where

$$\beta_i = dui/dt \tag{4.18}$$

is the derivative of the coefficients in the linear position estimate. These derivatives may be determined by taking the time derivative of (4.9) which defines the coefficients α_i. The velocity coefficients β_i therefore satisfy

$$\sum_i \beta_i \; E(z_i z_j) - d[E(xz_j)]/dt = 0 \tag{4.19}$$

where the derivative of the autocorrelation may be determined explicitly by differentiating (4.10) and (4.11). This allows the slope of the position curve to be determined explicitly in terms of the position measurements. There is no need to approximate the velocity as a difference between two position estimates divided by the time interval.

In the above discussion, the instantaneous velocity, the slope of the position function, was estimated. In the next paragraphs we study the average velocity over a time interval 2Δ, which is estimated by forming the difference between positions separated by this time interval divided by 2Δ. The average velocity over a time interval 2Δ is the difference in position divided by the time interval

$$\bar{v}(t) = \frac{x(t+\Delta) - x(t-\Delta)}{2A} \tag{4.20}$$

The coefficients needed to estimate the average velocity using

(4.17) are no longer the time derivatives of a_i, but are the differences between the coefficients in the position estimate

$$\beta_i(t) = \frac{a_i(t+\Delta) - \alpha_i(t-\Delta)}{2A}. \tag{4.21}$$

The time-shifted coefficients can be determined explicitly at each time when the average velocity is to be estimated.

The expectation of the square of the velocity error $E(\hat{v}-v)^2$ is found using the same analytical methods presented in section 4.1.3 for the position. The result is

$$\frac{E(\hat{v}-v)^2}{\sigma_x^2} = \frac{1-R(2\Delta)}{2\Delta^2} - \sum_i \beta_i \frac{R(t+\Delta-t_i)-R(t-\Delta-t_i)}{2A} \tag{4.22}$$

The velocity calculated by forming differences of the position estimates was insensitive to the choice of averaging times ranging from 10min to 2hrs. This result occurred because of the values of the time constant C used in the OI analysis, and does not imply that shorter-term peaks do not exist. In fact, we know that local cracking of the ice and other processes can cause the ice to accelerate on shorter time scales, but these individual motions are generally small and within the 300-m measurement error of the buoys. We ignored them because the ARGOS-based measurement system cannot describe them accurately.

The position measurements are provided as latitude and longitude values and the estimates described previously are valid for estimating these geographic coordinates and the time rate of change of them. However, the velocity components must be transformed into rates of change of distance along the earth's

surface if we are to give physical meaning to the velocity components, The northward velocity component is determined from the rate of change of latitude by

$$v_Y = \rho \, d\phi/dt \tag{4.23}$$

and the eastward velocity component is determined from the rate of change of longitude by

$$v_X = - \rho \cos\phi \, d\lambda/dt \tag{4.24}$$

where ϕ is the latitude, λ is the longitude (measured positive westward), and we have assumed that the earth is a sphere of radius ρ. The average velocity components are determined by replacing these derivatives with differences and using the average latitude in the cosine function.

4.2. Complex Regression

To evaluate the relative importance of the wind and current on the ice motions, we study the correlations between these variables. Furthermore , since free-drift sea ice models suggest (e.g. Pritchard, 1984) that the ice motion relative to the ocean current (the variable v_r measured by the current meters) is a known function only of the wind, we wish to compare the ice velocity to the relative current velocity.

Although the correlation between two scalar variables is well-understood, it is not so simple to compare two vector variables. The respective correlations between the various velocity components do not give a particularly clear understanding of the relationship between the vectors themselves. To circumvent this difficulty, we use the complex regression, which allows us to study the relationship between pairs of two-dimensional vectors.

The ice velocity vector v may be regressed onto the wind vector w by introducing the 1 inear relationship

$$v = Aw + B \tag{4.25}$$

where A and B are complex constants. The regression is obtained by determining the values A and B that give the best fit to the data in a least squares sense. This is accomplished in the usual way, except that care is required to include the complex conjugate as necessary.

The two complex constants must satisfy the relationships

$$A \sum w_i w_i^* + B \sum w_i^* = \sum v_i w_i^* \tag{4.26}$$

$$A \sum w_i + B N = \sum v_i \tag{4.27}$$

where w_i^* is the complex conjugate of W_i. These equations can be solved for coefficients A and B using standard complex algebra.

The mean-squared error between all data points and the regression curve is

$$\sigma_\varepsilon^2 = \sum \varepsilon_i \varepsilon_i^* / N \tag{4.28}$$

where $\varepsilon_i = v_i - (Aw_i + B)$ is the error at each data point.

The variance explained by the regression is equal to the total variance of the variable

$$\sigma_v^2 = \sum v_i v_i^* / (N-1) \tag{4.29}$$

less the unexplained variance shown in the error. Therefore, the variance explained by the regression σ is

$$\sigma^2 = \sigma_v^2 - N\sigma_\varepsilon^2/(N-1). \tag{4.30}$$

A similar analysis may be performed for each pair of two-dimensional vectors.

5. RESULTS: NORTON SOUND

5.1. Ice Trajectories

Eleven buoys were deployed in Norton Sound during three different time periods. The deployment pattern was designed to obtain ice motion, wind and current data over broad areas throughout the winter. The ice trajectories for each buoy, obtained after filtering tidal and other high frequency oscillations from the data, are presented in Appendix E.

In general within Norton Sound, the ice drifts westward, until it passes a 1 ine roughly connecting Nome and the Yukon delta. Then the ice tends to moue northward and southward in episodes of roughly 3-15 days. These large-scale reversals appear to be related primarily to the currents existing at the time. Since the long-term average current is northward, one should expect this to be the direction most 1 ikely taken by the ice floes. This conjecture is confirmed by the drift of buoys 3608, 3611, 3613, and 3616. However, the southward movement of buoy 3612 shows that other trajectories are possible.

The slow westward drift of ice as indicated by the movement of buoys 3607 and 3609 points toward Norton Sound as a site for production of sea ice and its subsequent export into the northern Bering Sea where it is transported by the prevailing winds and currents. The strong north-south movements of buoy 3609 as it neared the mouth of Norton Sound indicate that the circulation inside the sound is different from that on the eastern Bering Sea proper .

These trends agree with observations by other investigators taken during different years (e.g. Stringer and Henzler, 1981; Thomas and Pritchard, 1981), and with the PMEL buoy data taken concurrently (Reynolds and Pease, 19S4).

5.2. High Frequency Oscillations

High frequency oscillations in the ice motion arise from tidal and inertial oscillations, and from ice stress divergence. In Norton Sound we assume that ice stress divergence is not important, although nearshore ice motions can feel its influence.

The tidal oscillations in the northeastern Bering Sea and Norton Sound introduce large periodic oscillations to the ice velocity. Figures 3.03 and 5.01 depict the ice velocity observed by buoys 3608 and 3609, respectively. These results are consistent with the observations of Sale, Schumacher and Coachman (1983) and Mofjeld (1984) who have studied the tidal behavior in this region. The power spectral densities of the ice velocity for all three current meter buoys are presented in Figures 5.02 - 5.04.

5.3. Wind, Current and Ice Velocity

Buoys 3607 and 3609 were deployed in the interior of Norton Sound, while 3608 was deployed near the mouth of the sound, In addition to position measurements, these three buoys provided measurements of ocean current, wind, and air temperature every two hours.

Buoy 3607 transmitted for 13 days after deployment on February 6, and in that time, moved roughly 50 km southwestward.

The drift track showed one lateral excursion of 20 km which appeared to be due to a reversal of the wind over a 10-day period. Winds were northward over the first half of the deployment interval, shifting to southward during the second half. Both the currents and the ice drift reflected some influence of the wind, but neither was solely wind-driven (Fig. 5.05). The spectrum of ice velocity (Fig.5.02) showed energy at the diurnal tidal frequency and also at frequencies less than about 0.5 cycles/day. The ice velocity time history indicated that the tidally-driven motion of buoy 3607 was mainly east-west, along the axis of Norton Sound. The trajectory of buoy 3607 thus reflects the influence of the winds at longer periods and currents at tidal periods.

Buoy 3608 was deployed on the ice near the mouth of Norton Sound on February 24 (Jd 55) and provided position and wind data until June 11 (Jd 162). The current meter operated until about Jd 100, ceased, and then resumed again for eight days just after Jd 150. The mean wind direction was toward the south, but there were intervals of strong winds toward the north (Fig. 5.06). For the first two weeks, the ice moved northwest out of Norton Sound, and then moved southward until about Jd 913. Beginning on Jd 92, when a major reversal of both the wind and current toward the north occurred, the ice moved over 250 km northward into Bering Strait by Jd 10CI. Both wind and current reversed again, and the ice moved about the same distance southward by Jd 110. After oscillating primarily north and south outside the mouth of Norton Sound, the ice began a major northward translation on Jd 147 and

passed through Bering Strait on about Jd 158. The wind and current reversed and set northward at the same time. The ice velocity during the major north-south episodes reached nearly 100cm/s. Currents relative to the ice remained small, generally less than 10cm/s, indicating that the currents and the ice moved similarly. Thus, the wind, current, and ice motion in the vicinity of Bering Strait tended to coincide. The reason is that all are likely related to the large scale, alongshore atmospheric pressure gradient. This agrees with Aagaard, et. al. (1985), who found that the meridional wind was well-correlated with the stericheight difference between the Bering and Chukchiseas.

Buoy 3609 recorded wind and position data for five weeks beginning on February 27 (Jd 58). During that time, the net drift was about 120 km westward, ending at the mouth of the sound. Most of this westward translation took place in the first 20 days. Stick plots (Fig. 5.07) suggest only a weak relationship between the wind and the ice velocity for the first 20 days. The winds were primarily north-south while the ice motion was primarily toward the west. After about March 21 (Jd so), the ice velocity showed a very different pattern which was characterized by three episodes of northward movement separated by three episodes of southward movement. Each episode lasted between two and three days. The concurrent winds were weak and variable. These ice motions after March 21 were clearly dominated by the stronger north-south currents outside of Norton Sound. The current meter of buoy 3609 failed about a week after deployment, so that there is no information about water motion over most of the deployment interval . However, the spectrum of

ice velocity (Fig. 5.02) showed energy at both the diurnal and semi-diurnal tidal frequencies, which in turn implies that the currents influenced the ice motion in this frequency range.

5.4. Correlations

Since free-drift models of ice motion indicate that the ice velocity relative to the current v_r is a function of wind velocity w, the correlation between these two variables is an indicator of the effect of the wind on the ice drift. Table 5.1 shows that 27, 35, and 0% of the relative ice velocity variance is related to the wind by this measure. This is less that the correlation between the ice velocity and wind directly, and the difference is probably caused by the correlation between wind and current.

A regression of the ice velocity onto the wind and current at buoy 3608 showed that the current accounted for 80% of the variance in the ice motion (see Table 5.1), while the wind accounted for 43% for the interval when current measurements were available. This implies that the current affected the ice motion significantly more than did the wind. The spectrum of ice velocity showed that most of the energy was at periods of about 5 days and longer, and that there was a relatively small contribution due to the diurnal tides. Similar correlations occur for buoys 3607 and 3609.

These correlations show that the current provides the dominant driving force for the longer-term ice motions.

Table 5.1. Comparison Between Wind, Ice Velocity, and Current for Norton Sound Drifting Buoys. Linear Regression Constants for Ice Velocity onto Wind (V-W), Ice Velocity onto Current (V-C), Current onto Wind (C-W), and Relative Current onto Wind (R-W). The parameters in this table satisfy $A = m \exp(i\theta)$ and $B = b_r + ib_i$, where A and B are used in equation (4.25), σ_y^2 and σ_x^2 are the variance of the dependent and independent variable respectively in the linear fit, and f is the fraction of variance of x described by y.

Buoy	N	m	θ	b_r	b_i	σ_y^2	σ_x^2	f
3607	15							
v-w		1.33	-25.9	-1.27	.56	94.2	23.0	.39
V-C		.89	28.3	-.11	1.46	94.2	70.2	.56
c-w		.97	-66.5	-2.15	-.98	713.2	23.0	.25
R-W		.87	-159.5	-.88	-1.55	54.2	23.0	.27
3608	54							
v-w		3.43	-.5	-3.44	8.80	650.2	24.2	.43
v-c		1.03	2.9	-1.26	2.75	650,2	4%7 .3	.80
C-W		2.65	-6.6	-2.14	6.16	487.3	24.2	.34
R-W		[redacted]70	-166.0	.32	-.72	32.7	24.2	.35
3609	6							
v-w		1.35	-92.8	-.54	-1.59	28.7	7.8	.37
v-c		.81	15.0	-1.43	-3.14	28.7	34.3	.73
c-w		1.14	-111.9	1 .(I5	1.66	34.3	7.8	.12
R-W		.31	113.1	.75	3.79	4.1	7.8	.00

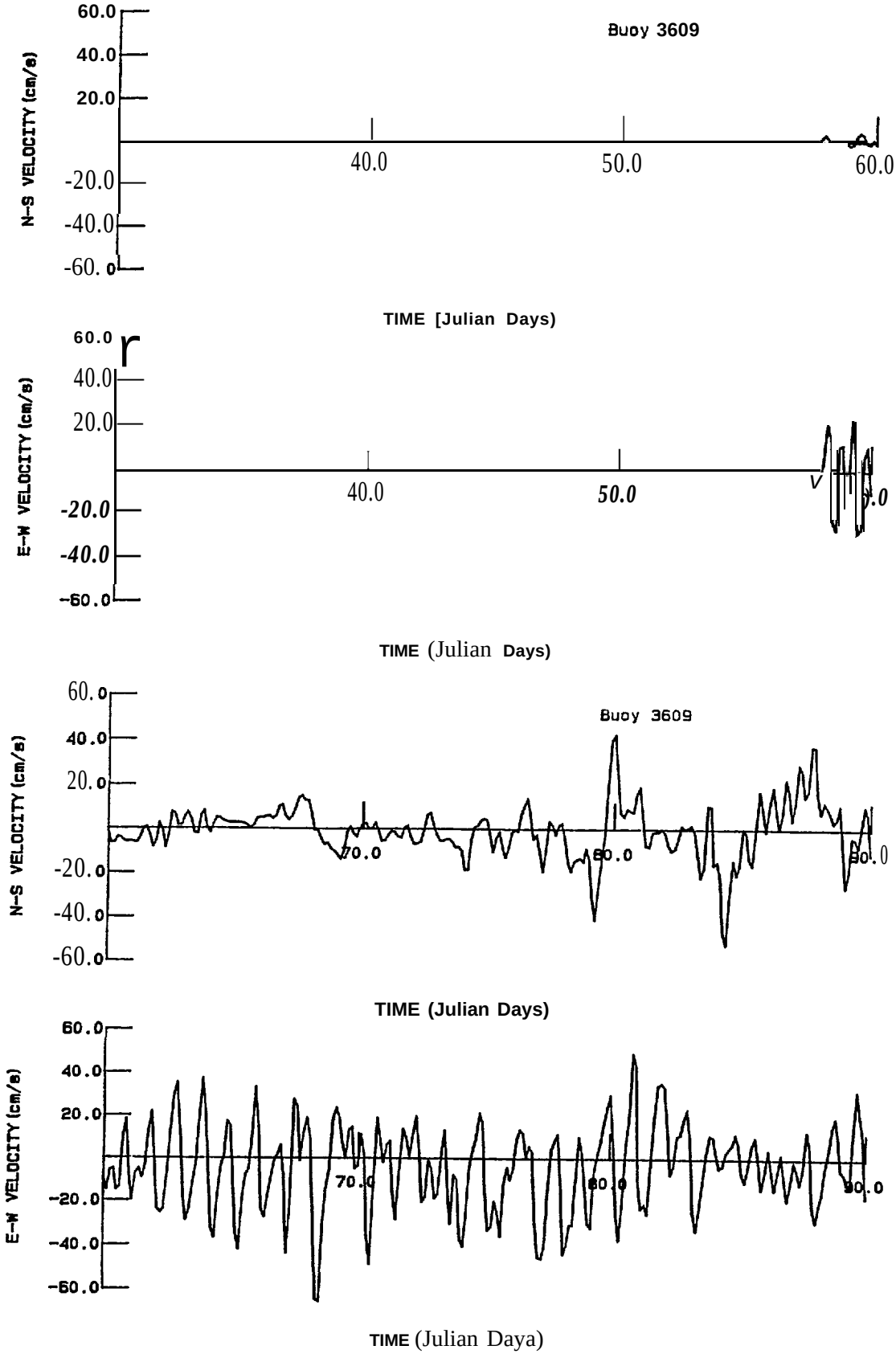

Figure 5.01. Buoy 3609 Velocity Time History Calculated from Intercalated Position History.

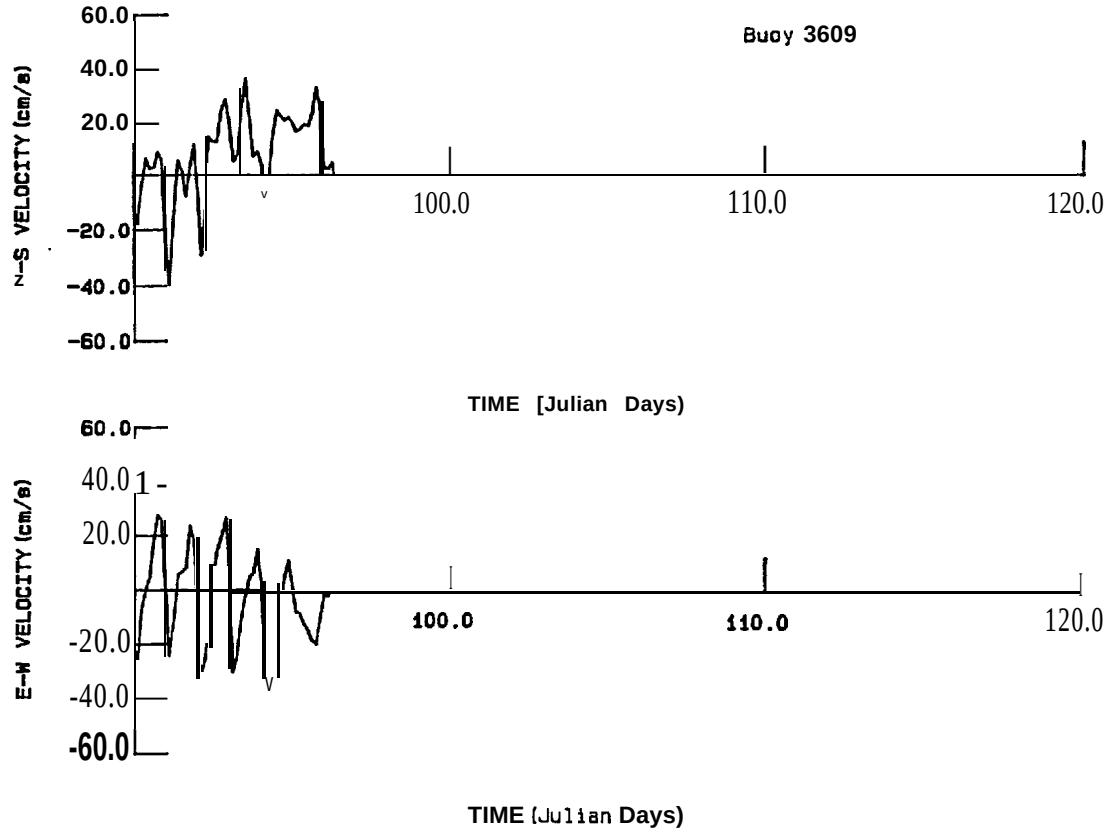

Figure 5.01. Buoy 3609 Velocity Time History Calculated from Interpolated Position History (concl'd).

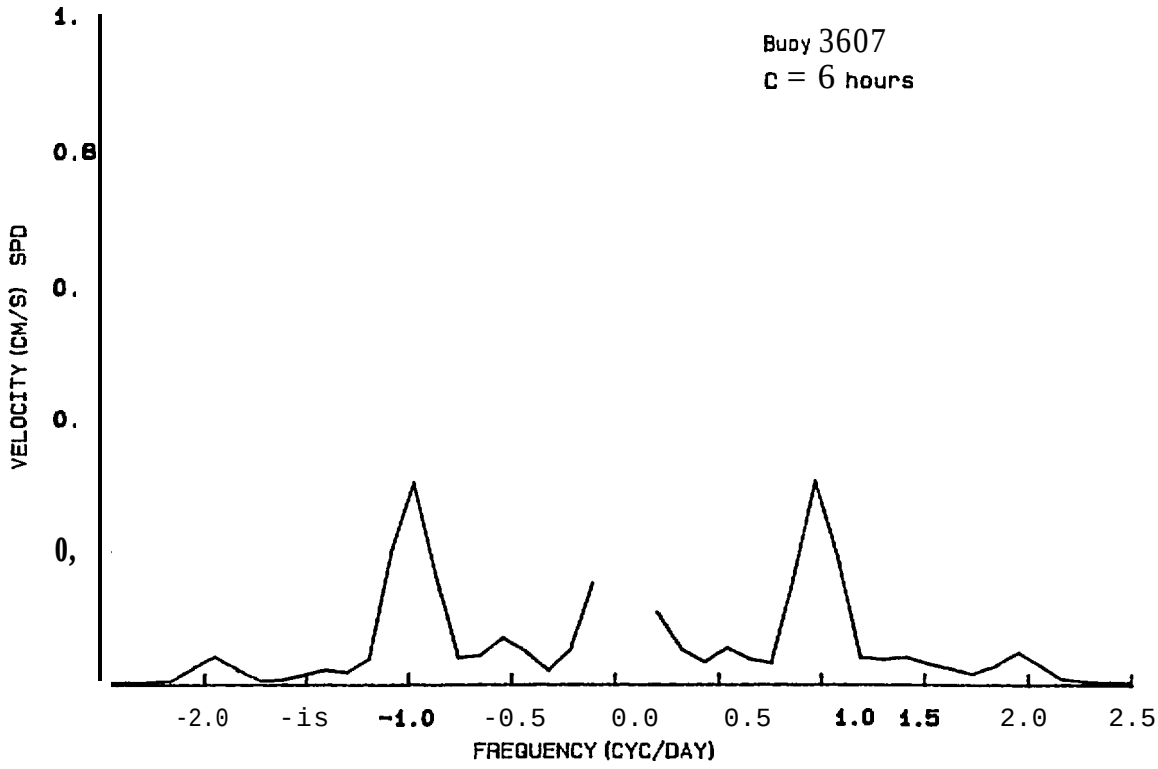

Figure 5.02. Buoy 3607 Ice Velocity Power 'Spectral Density.

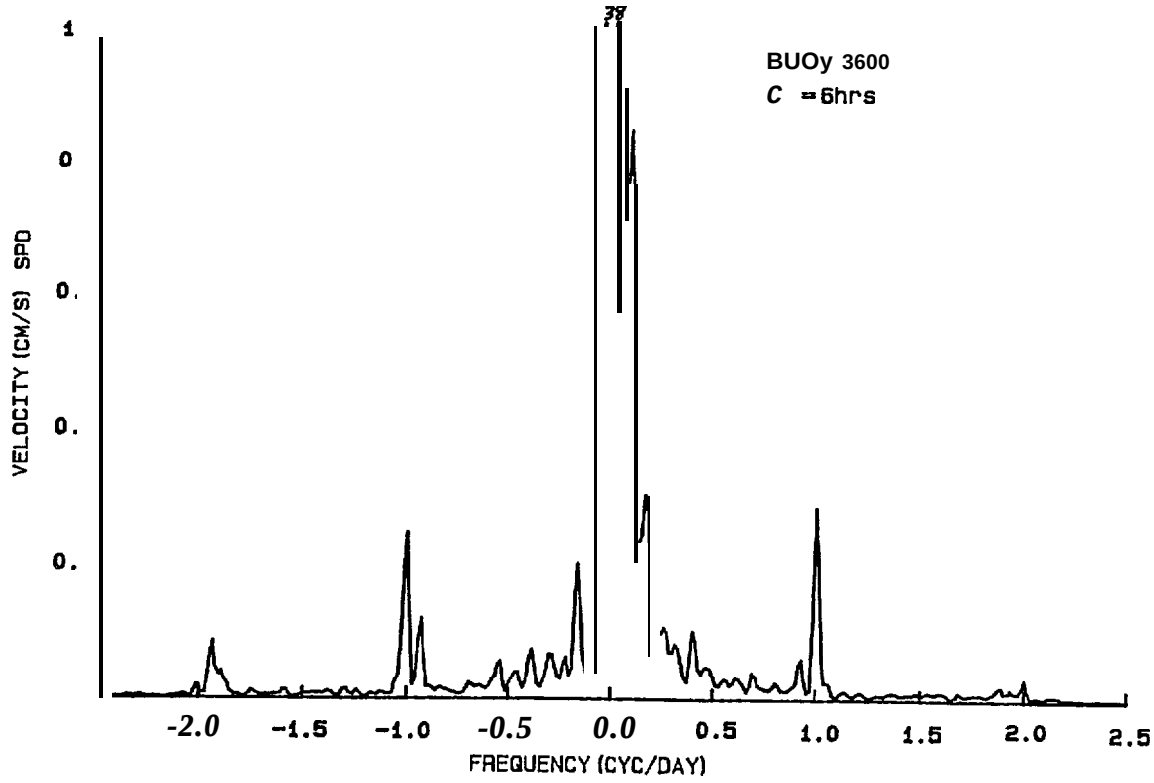

Figure 5.03. Buoy 3608 Ice Velocity Power Spectral Density.

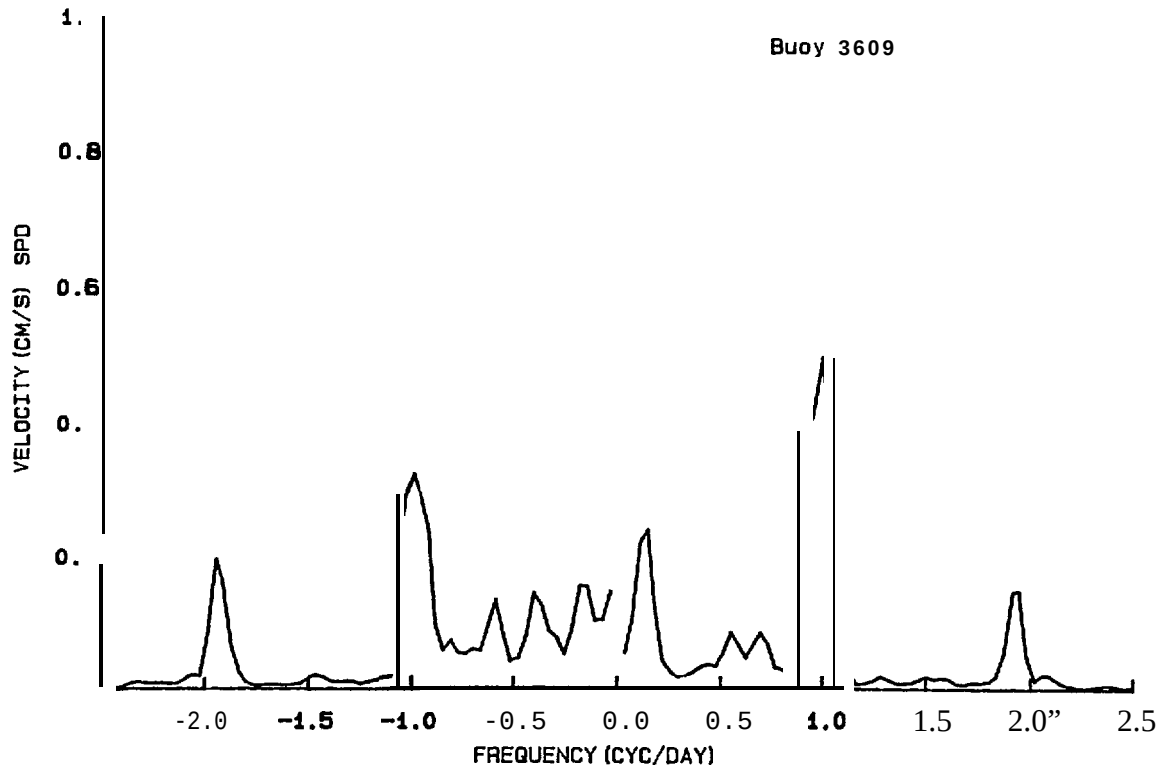

Figure 5.04. Buoy 3609 Ice Velocity Power Spectral Density.

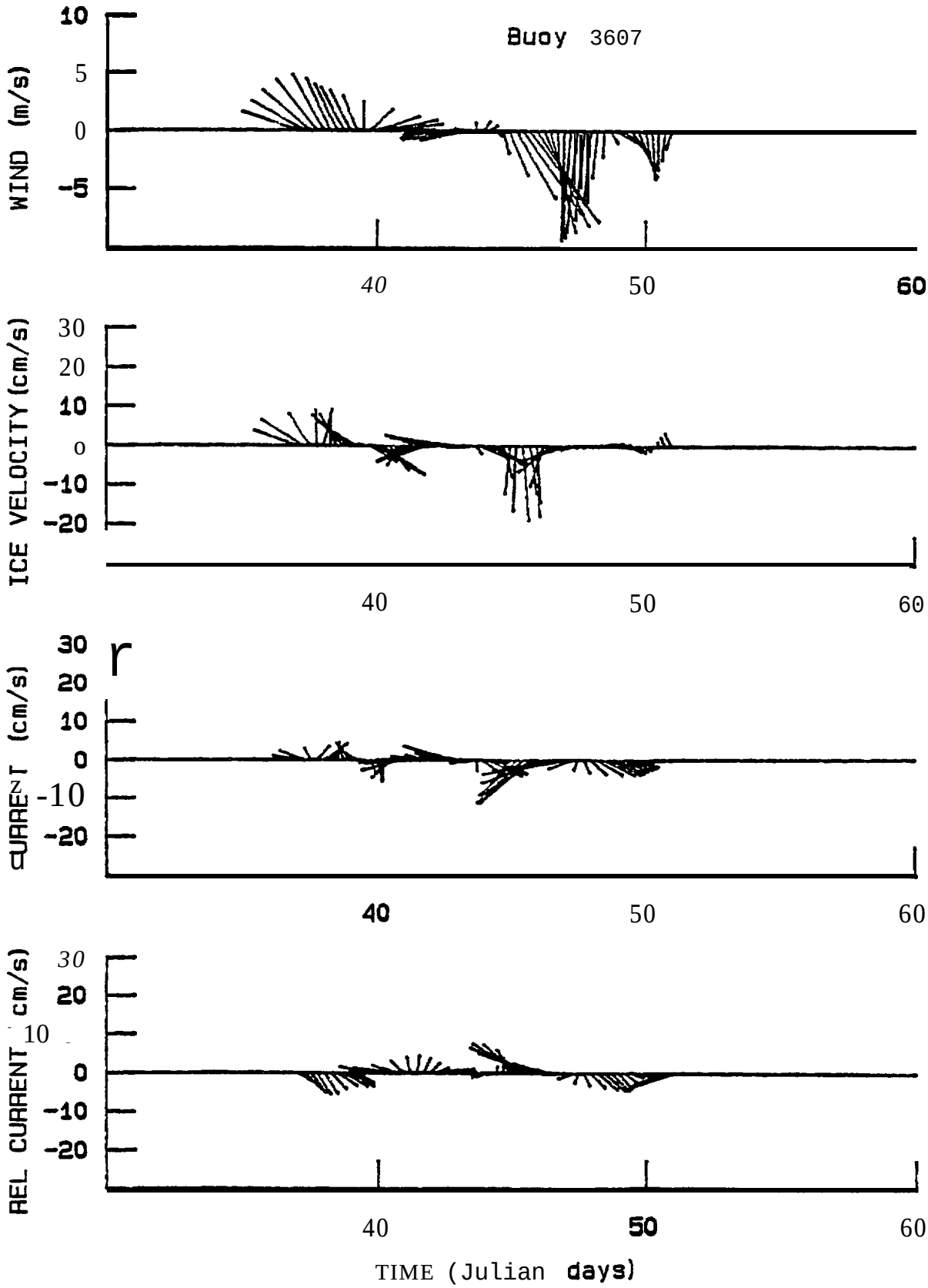

Figure 5.0S. Buoy 3407 Stick Plots of Daily Average Wind, Ice Velocity, Current, and Relative Current.

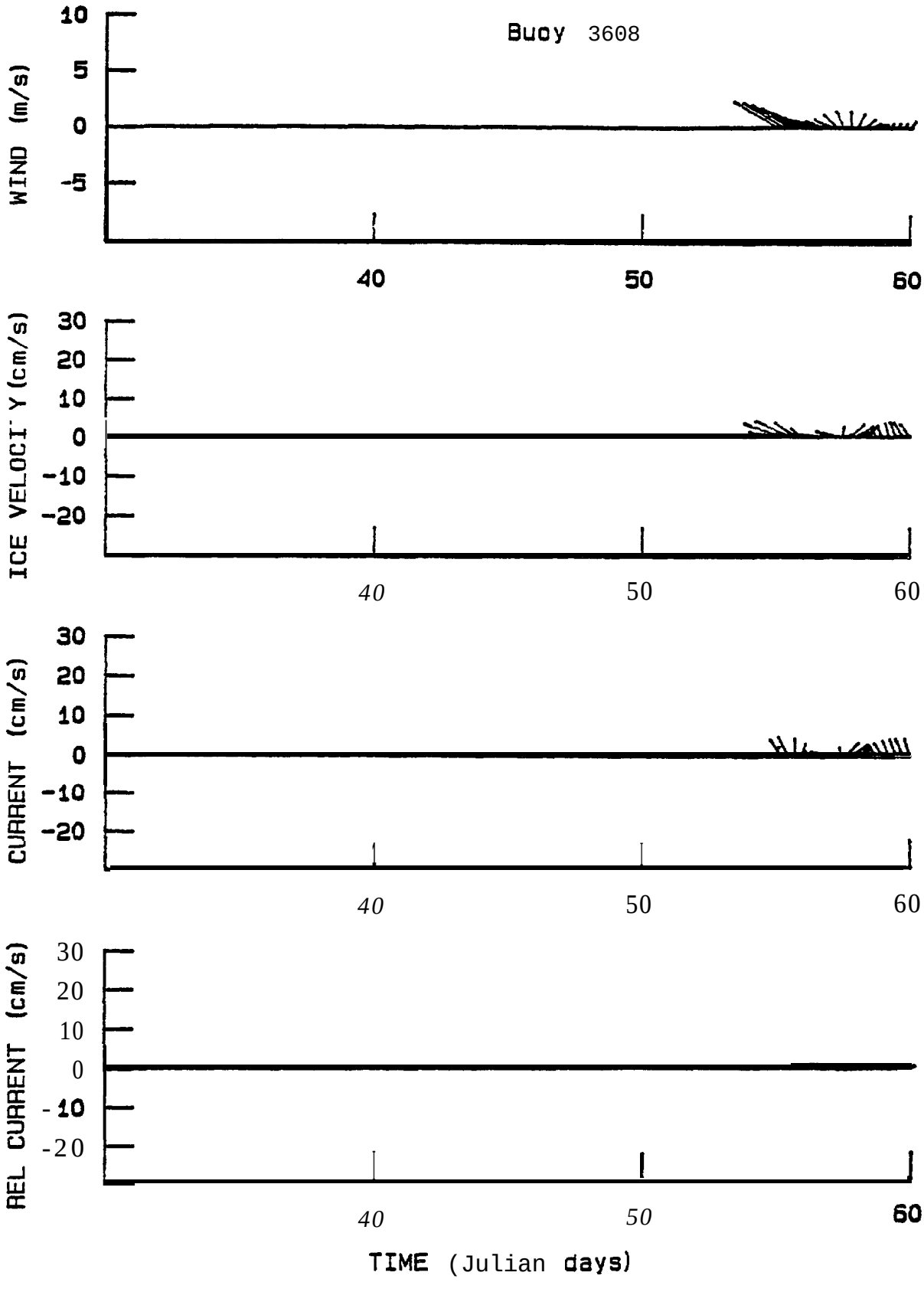

Figure 5.06. Buoy 3608 Stick Plots of Daily Average Wind, Ice Velocity, Current, and Relative Current.

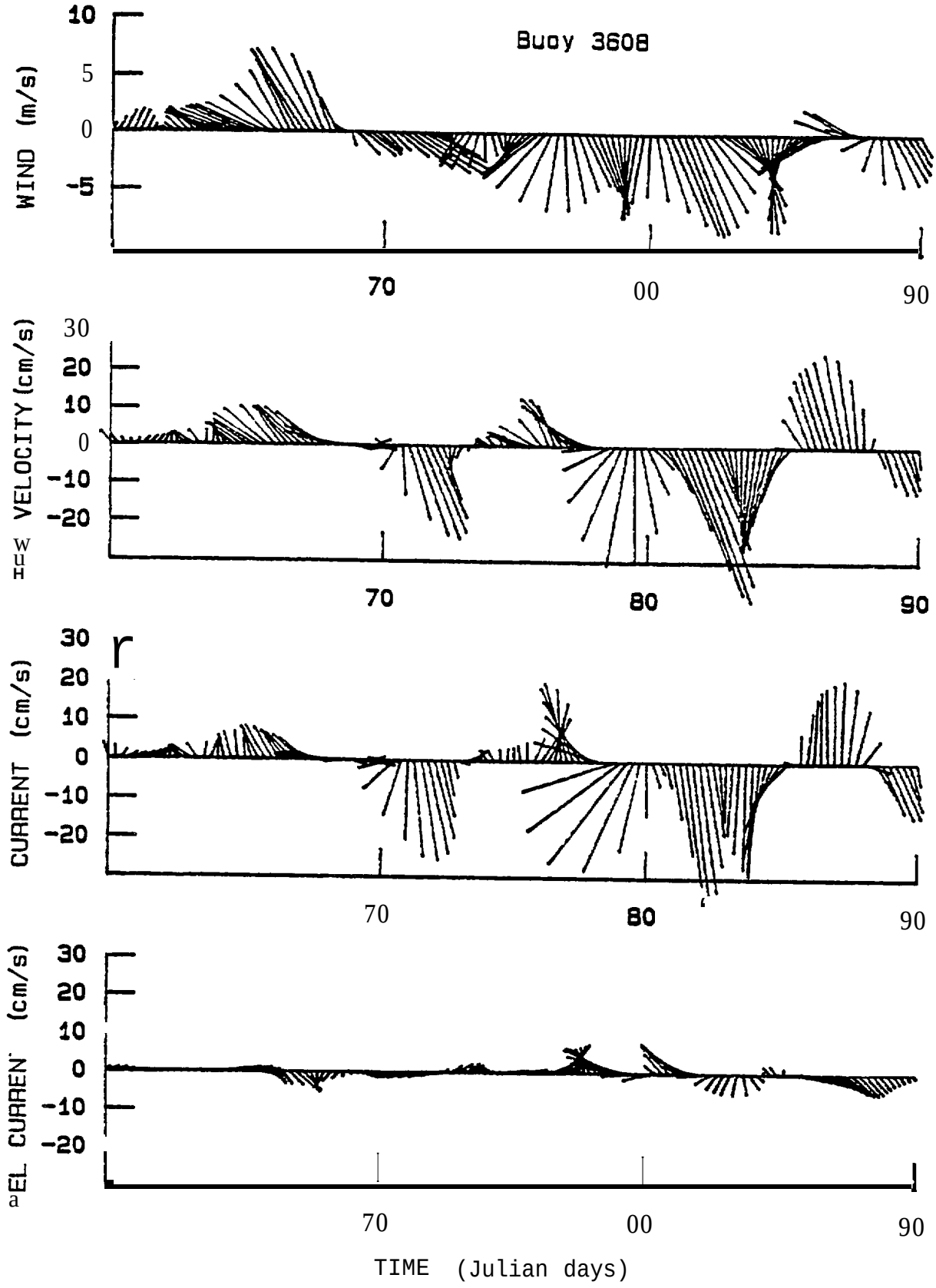

Figure 5.06. Buoy 3608 Stick Plots of Daily Average Wind, Ice Velocity, Current, and Relative Current (con t.) .

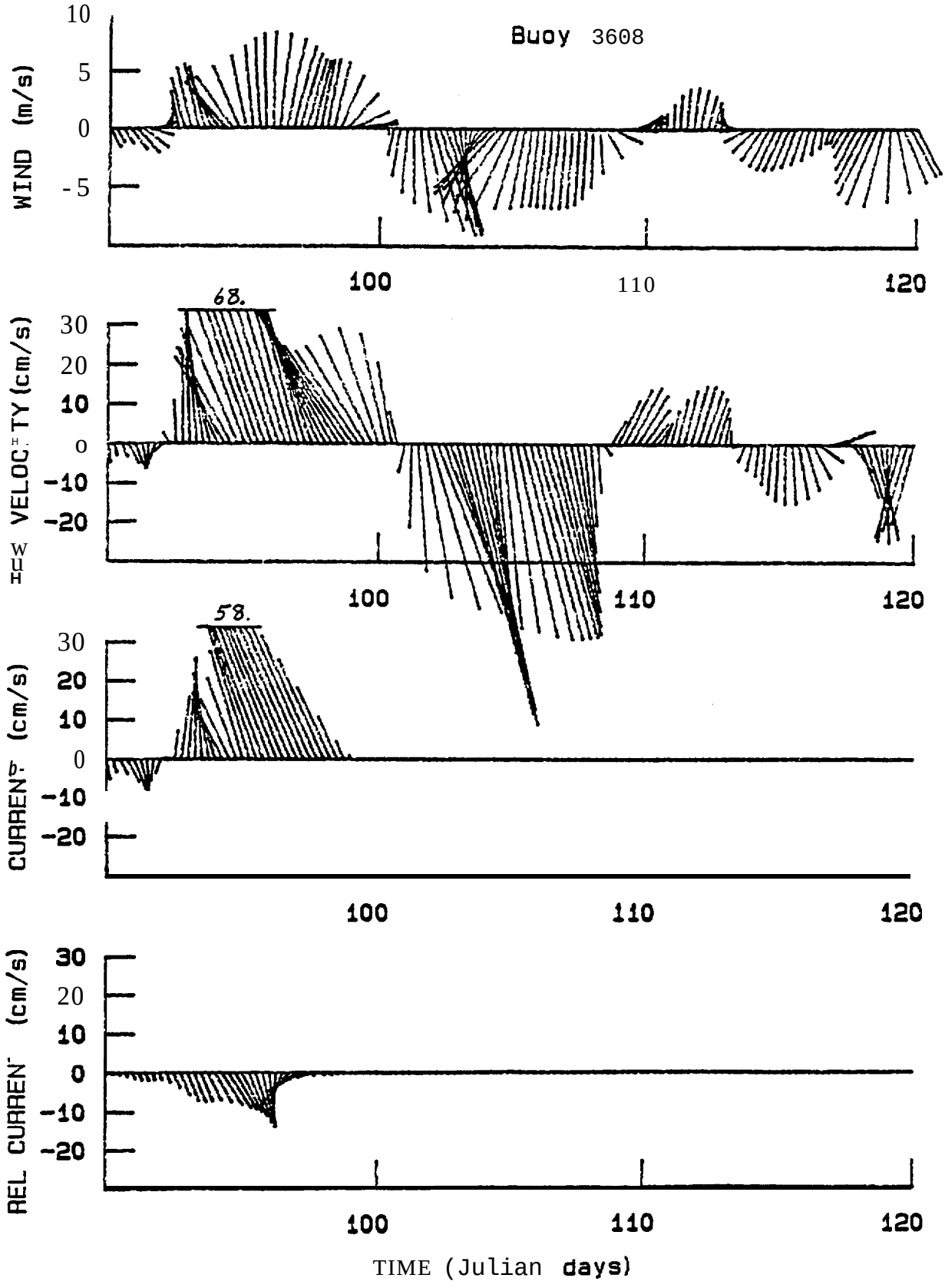

Figure 5.06. Buoy 3608 Stick Plots of Daily Average Wind, Ice Velocity, Current, and Relative Current (cont.).

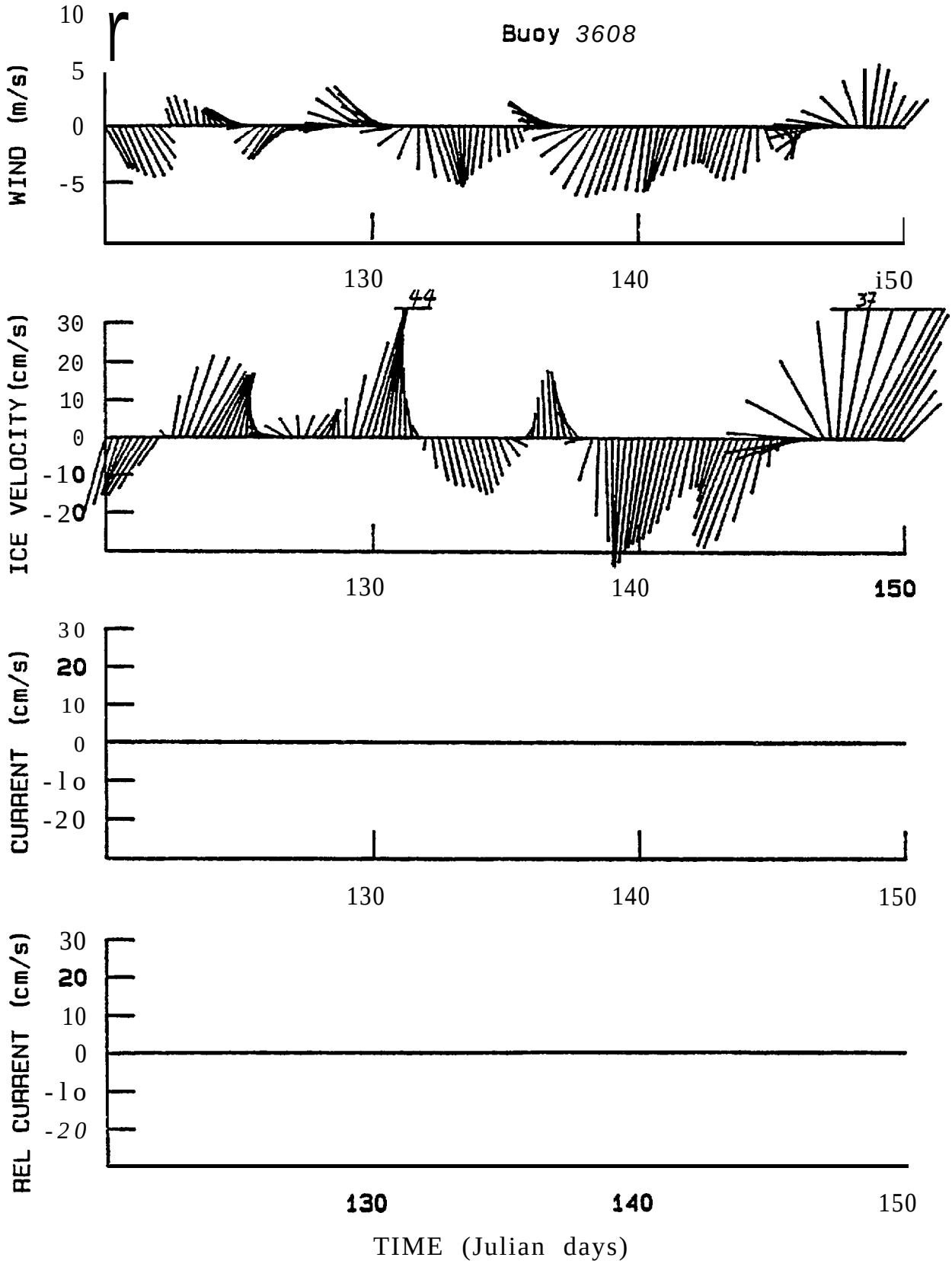

Figure 5.06. Buoy 3608 Stick Plots of Daily Average Wind, Ice Velocity, Current, and Relative Current (cant.).

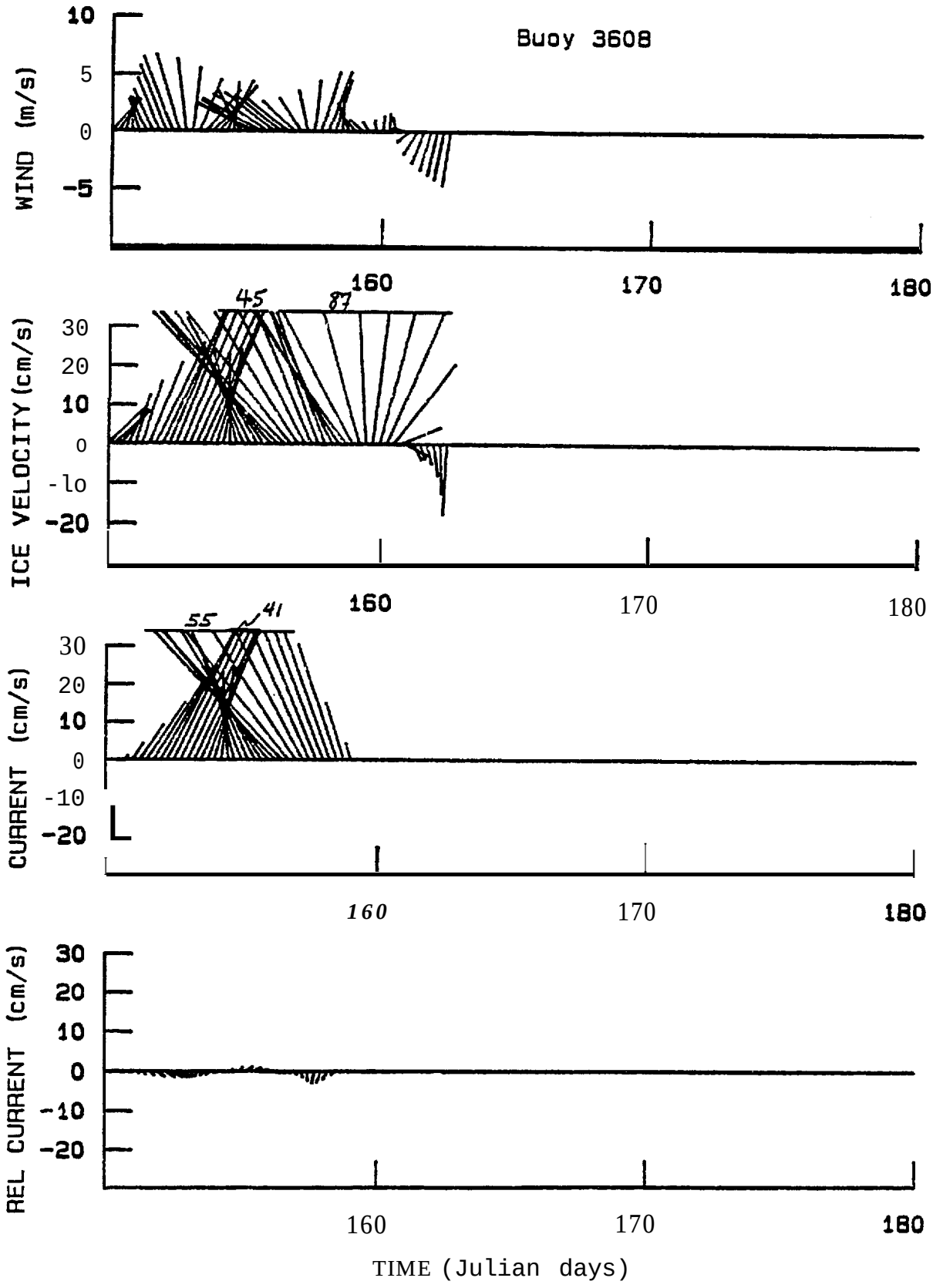

Figure 5.06. Buoy 3608 Stick Plots of Daily Average Wind, Ice Velocity, Current, and Relative Current (concl'd).

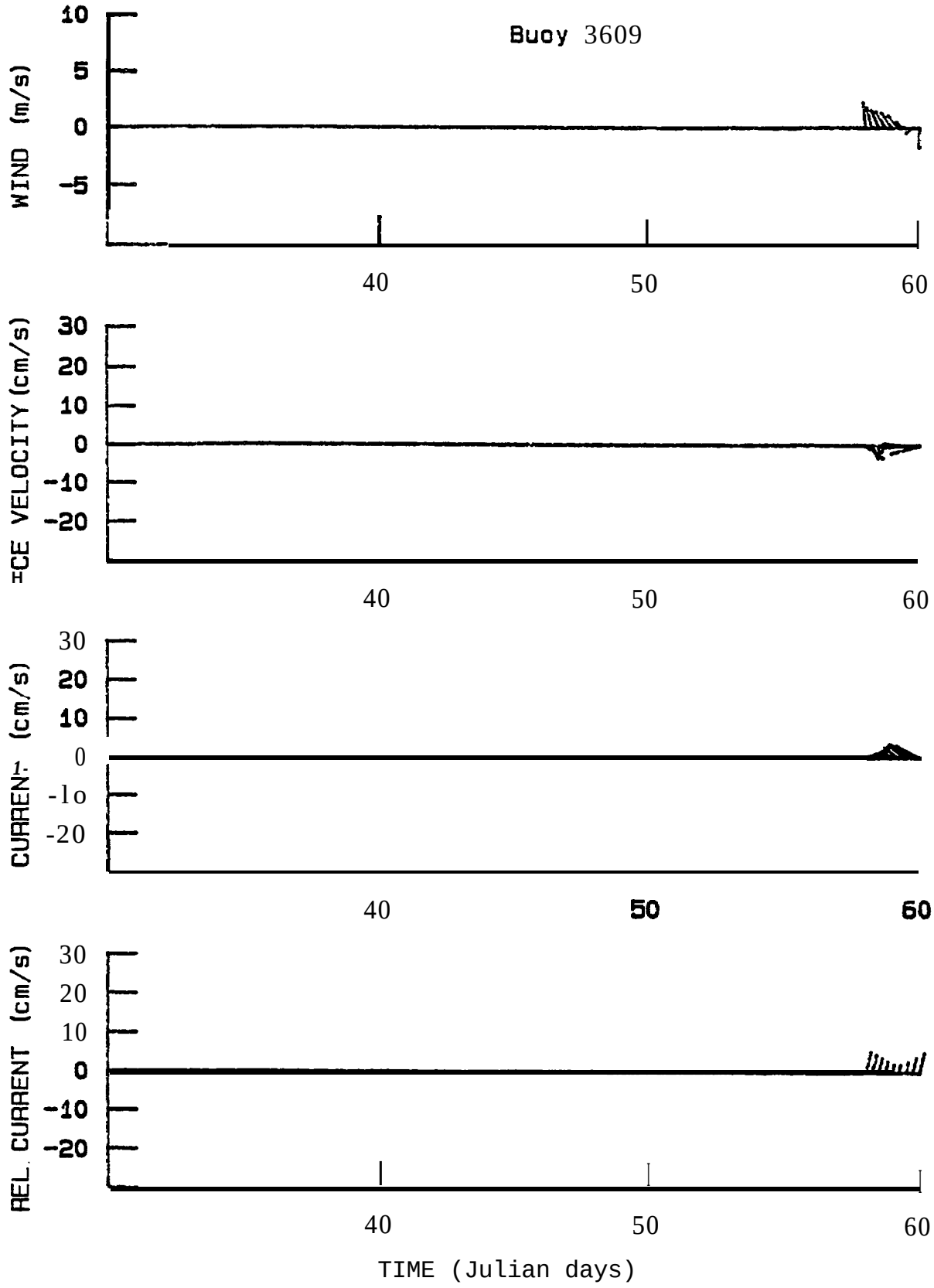

Figure 5.07. Buoy 3609 Stick Plots of Daily Average Wind, Ice Velocity, Current, and Relative Current.

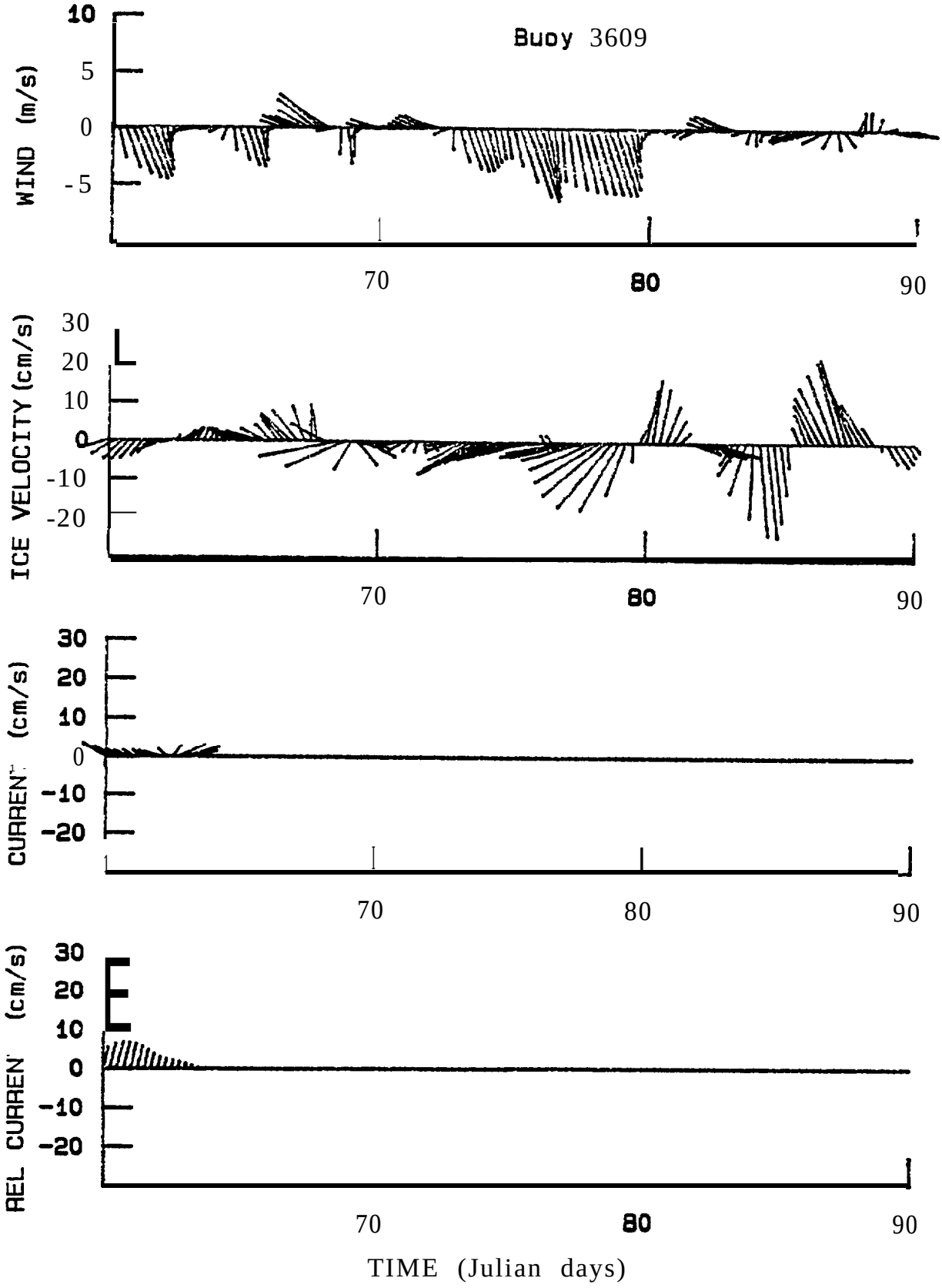

Figure 5.07. Buoy 3609 Stick Plots of Daily Average Wind, Ice Velocity, Current, and Relative Current (cont.).

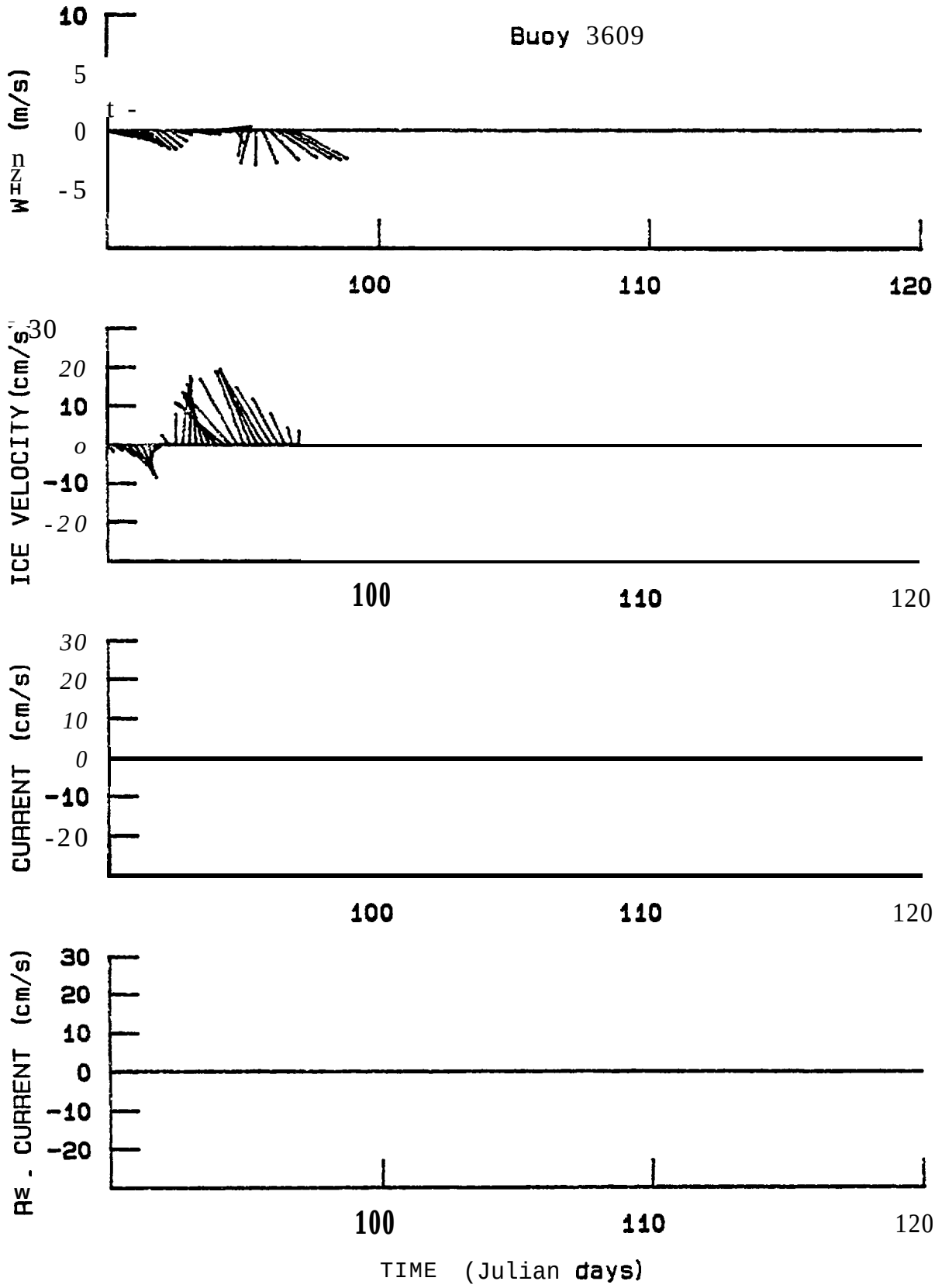

Figure 5.07. Buoy 3609 Stick Plots of Daily Average Wind, Ice Velocity, Current, and Relative Current (concl'd.).

6. RESULTS: CHUKCHI SEA

6.1. Ice Trajectories

Six buoys were deployed during two different time periods. The plan was to measure simultaneously the high speed nearshore motions and also the motions farther offshore that are more representative of the central Chukchi Sea. Multiple deployments were intended to allow buoys to occupy the region of interest for a longer period of time, after the first set drifted away. The ice trajectories for each buoy, obtained after filtering tidal and other high frequency osci nations from the data, are presented in Appendix E. These figures were copied from an earl ier report on this work by Pritchard and Thomas (1985).

In general, the ice cover drifted toward the northwest, moving roughly 650km during a 6-month time period. Near the northwest Alaskan coast, the ice made numerous excursions alongshore, each excursion as large as 100km and lasting from about 3 to 10 days.

Figure 6.01 shows a typical position time history determined from the OI analysis. The shorter-term variations in Chukchi Sea ice motions are quite different from those of Norton Sound ice. The raw data (Figure 6.02) are jumpy, that is, they appear to have random errors on the order of 2km. But these are the same buoys and we expect the measurement error to be about 0.3km. We attribute the jumpiness to local ice deformations associated with rafting and ridging processes. Here the ice is 1-2m thick, even before it is deformed. The ice strength therefore allows ice stress divergence to be large enough that it can alter, or even

dominate, the force balance. Since local deformations can occur in a few hours or less, these processes can generate motions on shorter time scales than do tidal oscillations.

Figure 6.03 shows a plot of (ice)velocity for buoy 3625. The velocity is typically smaller than that for the Norton Sound buoys because tides and inertial oscillations are absent. The power spectral densities for buoys 3423, 3624 and 3625 (Figures 6.04-6.04, respectively> confirm the absence of any significant energy at the tidal or inertial frequencies. Rather, the energy appears to be confined to periods greater than about 2.5 days.

6.2 Wind. Current. and Ice Velocity

Three buoys, 3623, 3624, and 3625 included current meters suspended 10-m below the top surface of the ice, so that relative current measurements as well as position data were obtained. Buoy 3625 also included a barometer. BUOY 3624 drifted offshore of Cape Lisburne and Point Hope. BUOY 3625 drifted in the vicinity of ICY Cape, and buoy 3423 drifted offshore of Wainwright. All were deployed within about 50km of shore and tended to stay within roughly 150km of shore.

Buoy 3623 provided current measurements from February 11 (Jd 42) to March 1(Jd 60), although position data extended until Jd 162. The ice trajectory tended to align with the coast, but with time the buoy migrated offshore, reaching a maximum of about 200 km on Jd 115 before moving back toward shore. From Jd 42 to Jd 60, the winds were typically less than 5m/s, and though variable, tended to align with the coast (Fig. 6.07). The ice moved eastward at up to 25cm/s until Jd 46 and then reversed

direction, slowing to a halt on Jd 50. It began moving eastward again on Jd 52 and again achieved speeds of about 25cm/s. There was no consistent relationship to the wind. Between Jd 42 and Jd 47 the current turned from offshore to northeastward alongshore, reaching a maximum speed of 35cm/s. The current reversed abruptly on Jd 47 and slowed from a maximum of 30cm/s to nearly zero by Jd 50, when it again reversed abruptly and set northeastward at speeds of 35cm/s until the end of the data on Jd 60. The relative current time history closely resembled that of the absolute current, which suggests that ice strength prevented the ice from responding in a free-drift mode to the sharp reversals and high currents.

While at first glance, the pattern of current reversals might correspond to the passage of an eddy, simultaneous current reversals at the locations of buoys 3624 and 3625 point rather to there being a dramatic change in atmospheric pressure and subsequent large-scale response of the ocean current. In fact, the barometer on buoy 3625 registered a low of 1005 mbar on Jd 49 and an increase to 1045 mbar by Jd 54, A barometer on another buoy farther offshore, 3622, registered a similar pattern. Even so, the data indicate that the current rather than the wind dominated the ice motion. Regression of the ice velocity onto the wind and the current showed that the current explained about three times as much of the variability of the ice velocity as did the wind.

Buoy 3624 yielded position and current measurements from February 15 (Jd 46) until May 1 (Jd 121). Over that interval,

the trajectory was characterized primarily by north-south excursions of roughly 200km, but also showed some westward movement . In addition, both wind and current vectors were oriented primarily north-south and displayed several reversals (Fig. 6.08). While there were some wind and ice velocity events which were coincident, there was no consistent relationship between the two. On the other hand, there was clearly a close relationship between the ice velocity and current over the entire data record, and the unambiguous evidence indicates that the current totally dominated the ice motion. One isolated example is that between Jd 46 and Jd 49, both the current and the ice velocity set southward at up to 50cm/s, while the wind was toward the northwest. Calculations over the entire record indicate that the current could account for about 93% of the variance in the ice velocity, while the wind could account for only 2% (see Table 6.1). However, it would be wrong to say that there were no instances in which the wind and current contributions were additive. The general conclusion is that buoy 3624 tracked the barotropic current which represented the oceanic response to large-scale atmospheric pressure fluctuations.

Buoy 3625 provided current measurements from February 16 (Jd 47) to March 8 (Jd 67), although the position data extended longer. Between Jd 52 and Jd 61, the ice moved northeastward alongshore at speeds of 10-20cm/s, and afterwards, it reversed direction and traveled slightly north of westward. The wind was offshore toward the northwest until Jd 61, when it changed direction toward the southwest, approximately alongshore

(Fig. 6.09). Wind speeds were generally in the range of 5-1OIM'S. Currents were northward to northeastward until about Jd 61, when there was a slow shift to northwestward flow. The relative current was variable and weak (less than 5cm/s) until about Jd 61 when it increased to about 10cm/s and became oriented more nearly in opposition to the wind. The change in the wind near Jd 61 was due to the passage of a front which accompanied an eastward moving low-pressure disturbance north of Alaska which was also reflected in the barometer records from buoys 3622 and 3625. Until about Jd 61, the current appeared to dominate the motion of the ice, but after that, the ice motion was clearly dominated by the wind. In fact, the wind and the current each explained about 75% of the variance in the ice velocity. This means that wind and current had nearly equal influence, but this wind correlation probably arose from its correlation with the current.

These three buoys were spaced about 150 km apart along the northwest coast of Alaska, but they still displayed some common behavior. The ice velocity and current reversal on about Jd 50 was reflected clearly in the data from 3623 and 3624, and weakly in the data from 3625. Between Jd 50 and Jd 40, all three buoys executed alongshore motion away from Bering Strait. From the trajectory plots, it is apparent that all three moved alongshore in unison between Jd 90 and Jd 100, and then reversed direction between Jd 100 and Jd 110. Recall that buoy 3608 in the northeast Bering Sea executed these same motions between Jd 90 and Jd 110. While local wind forcing must have some influence,

the evidence is strong that the ice along the coastline from Norton Sound to Barrow responds primarily to very large-scale barotropic current events which are driven by barometric pressure differences.

Table 6.1. Comparison Between Wind, Ice Velocity, and Current for Chukchi Sea Drifting Buoys. Linear Regression Constants for Ice Velocity onto Wind (V-W), Ice Velocity onto Current (U-C), Current onto Wind (C-W), and Relative Current onto Wind (R-W). The parameters in this table satisfy $A = m \exp(i\theta)$ and $B = b_r + ib_i$, where A and B are used in equation (4.25), σ_y^2 and σ_x^2 are the variance of the dependent and independent variable respectively in the linear fit, and f is the fraction of variance of x described by y.

Buoy	N	m	e	b_r	b_i	σ_y^2	σ_x^2	f
3623	18							
V-W		1.48	-46.2	5.09	.30	91.1	8.4	.15
V-C		.32	-13.6	-.70	-.29	91.1	411.8	.44
C-W		2.62	-19.4	15.08	7.83	411.8	8.4	.09
R-W		1.46	7.9	9.99	7.52	243.8	8.4	.02
3624	78							
V-W		.41	-79.3	-2.05	1.91	324.8	62.5	.02
V-C		.89	-10.8	-2.40	.20	324.8	383.9	.93
C-W		.29	-92.8	.14	2.05	383.9	62.5	.00
R-W		.14	130.4	2.19	.14	40.6	62.5	.02
3625	19							
V-W		1.45	-70.8	-.16	-3.10	89.2	33.2	.77
V-C		.99	14.2	1.70	-3.79	89.2	67.8	.72
C-W		1.12	-84.1	-1.03	2.49	67.8	33.2	.60
R-W		.44	145.0	-.88	5.59	27.3	33.2	.19

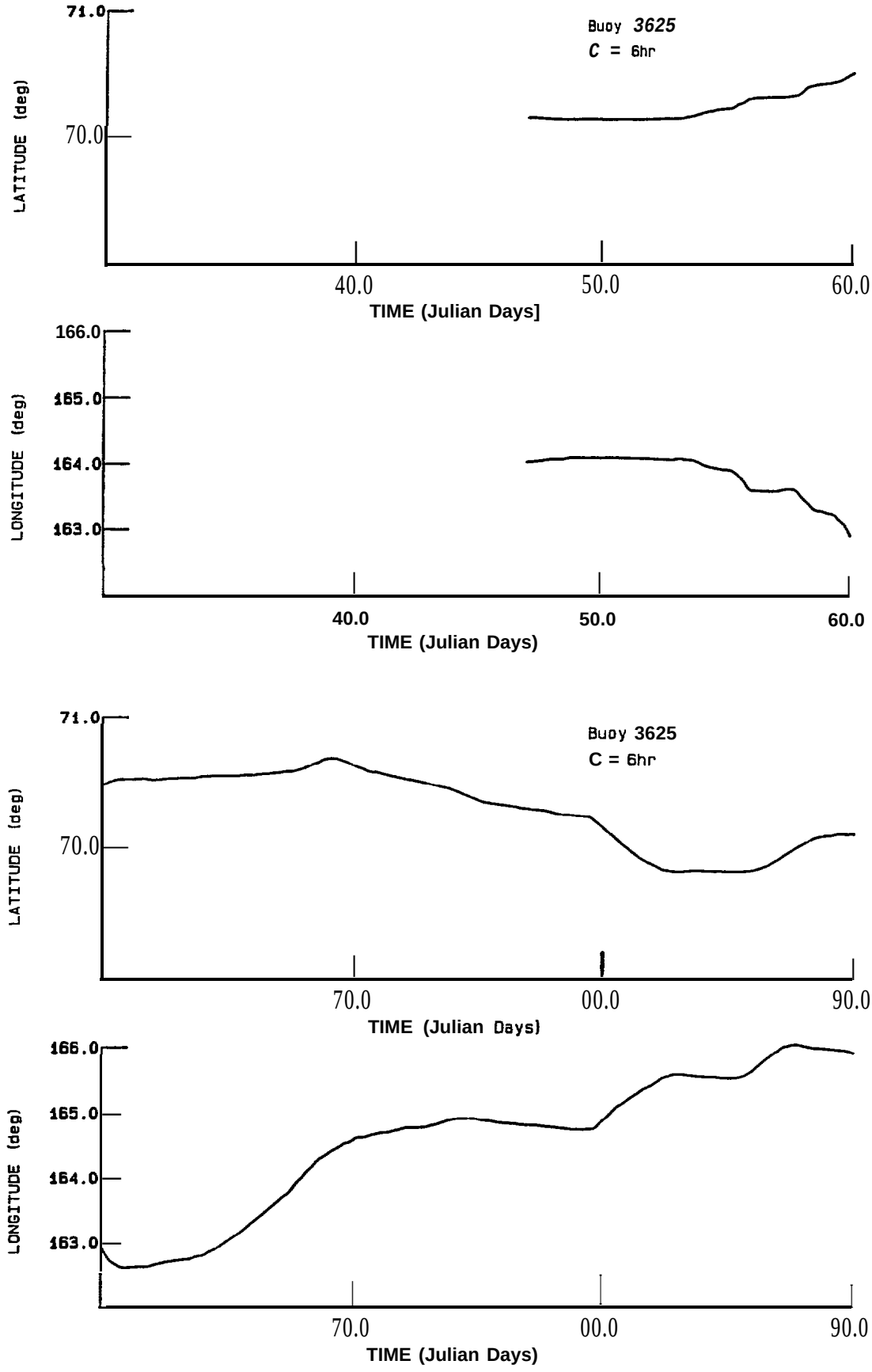

Figure 6.01. Buoy 3625 interpolated Position Time History.

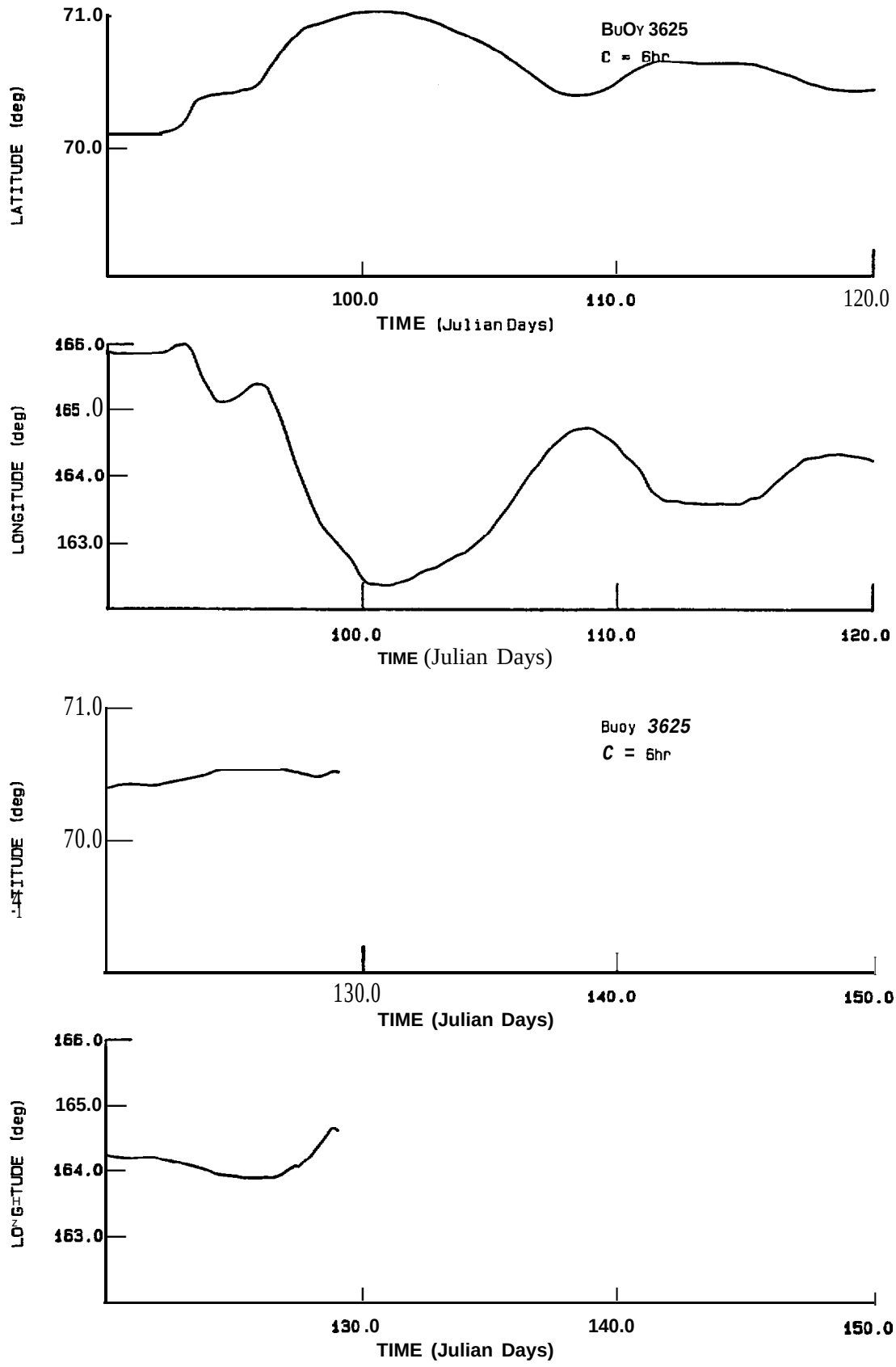

Figure 6.01. Buoy 3625 Interpolated Position Time History (concl'd).

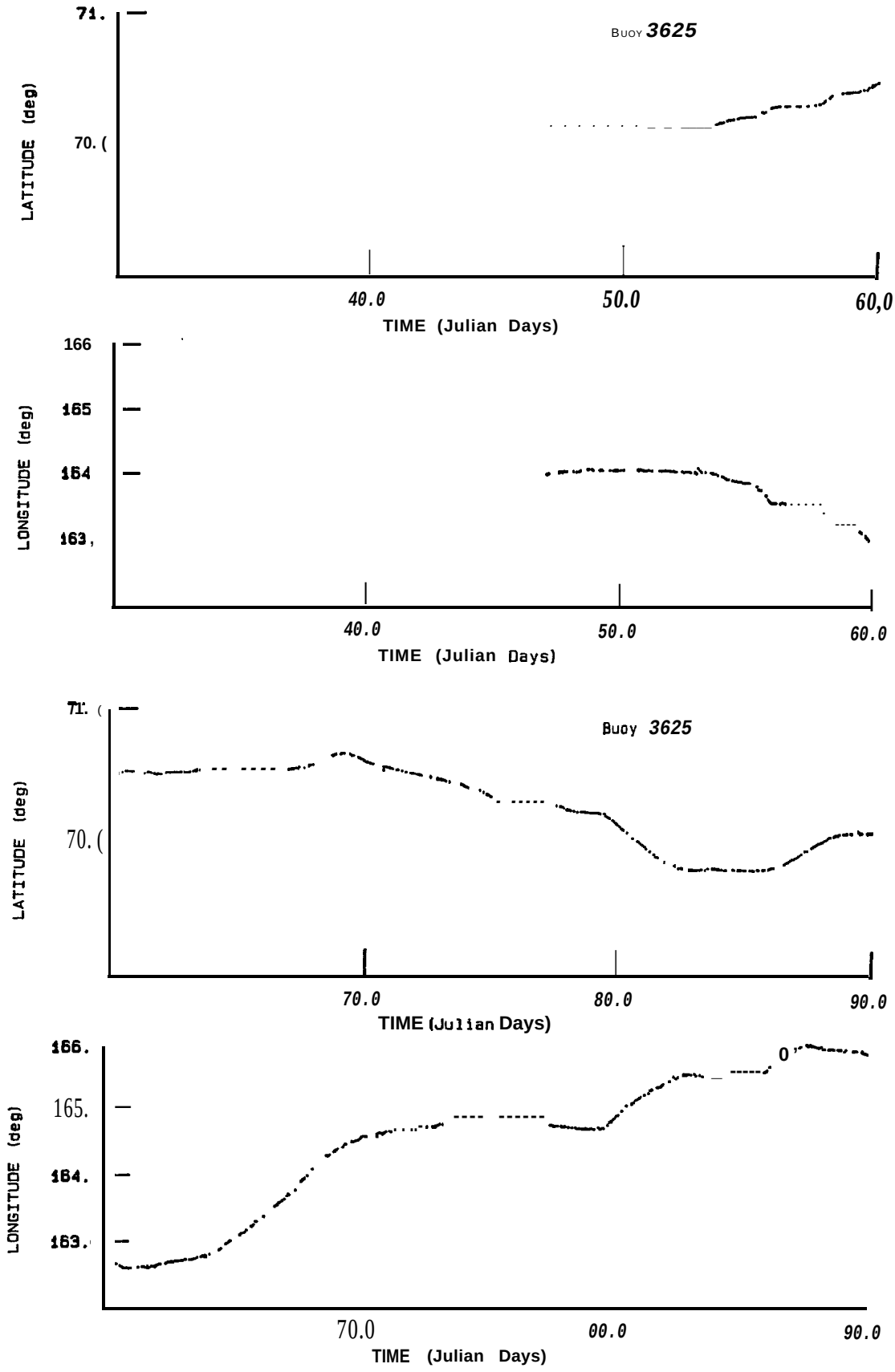

Figure 6.02. Buoy 342S Raw Position Measurements.

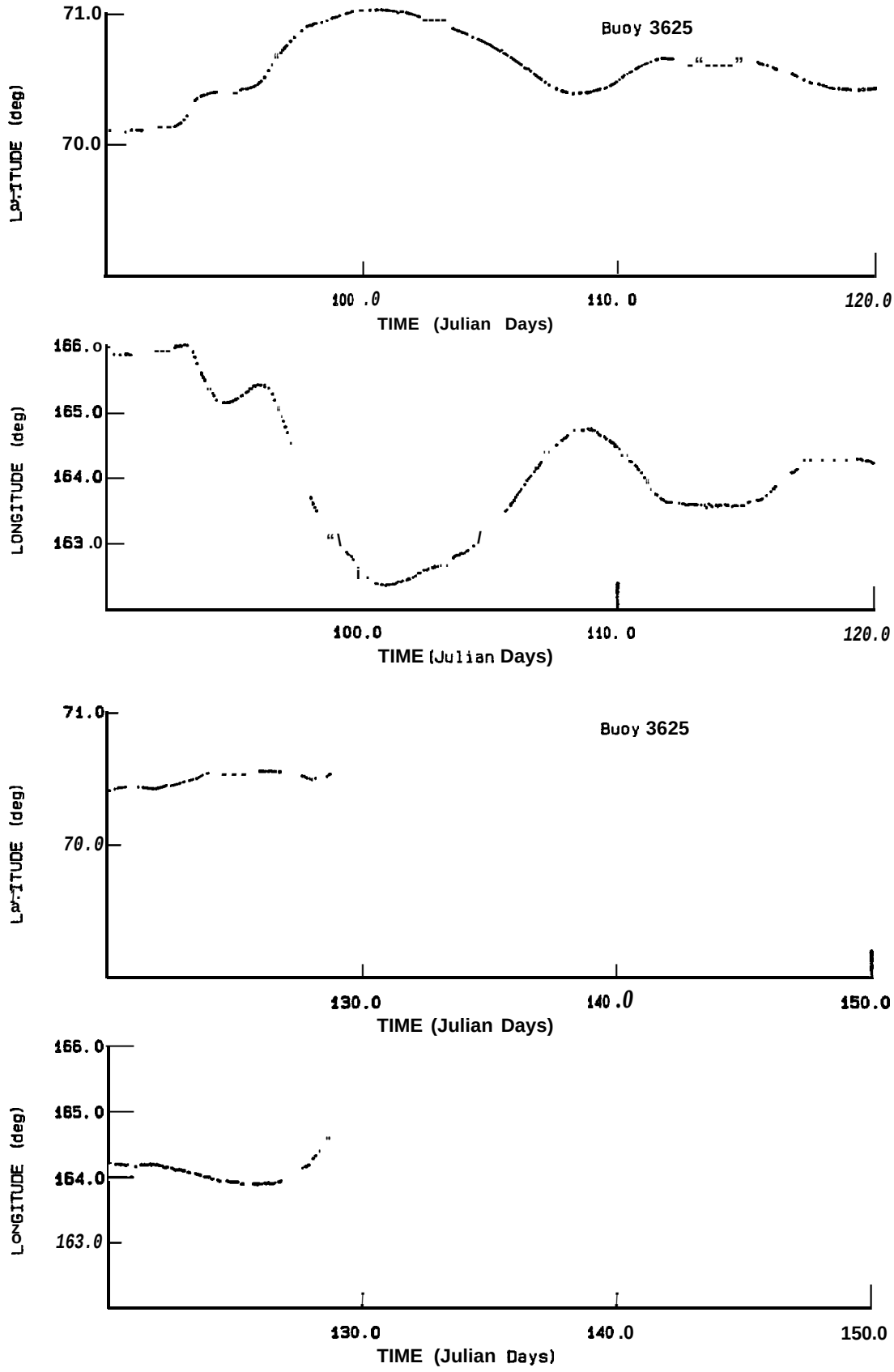

Figure 6.02. Buoy 3625 Raw Position Measurements (concl'd).

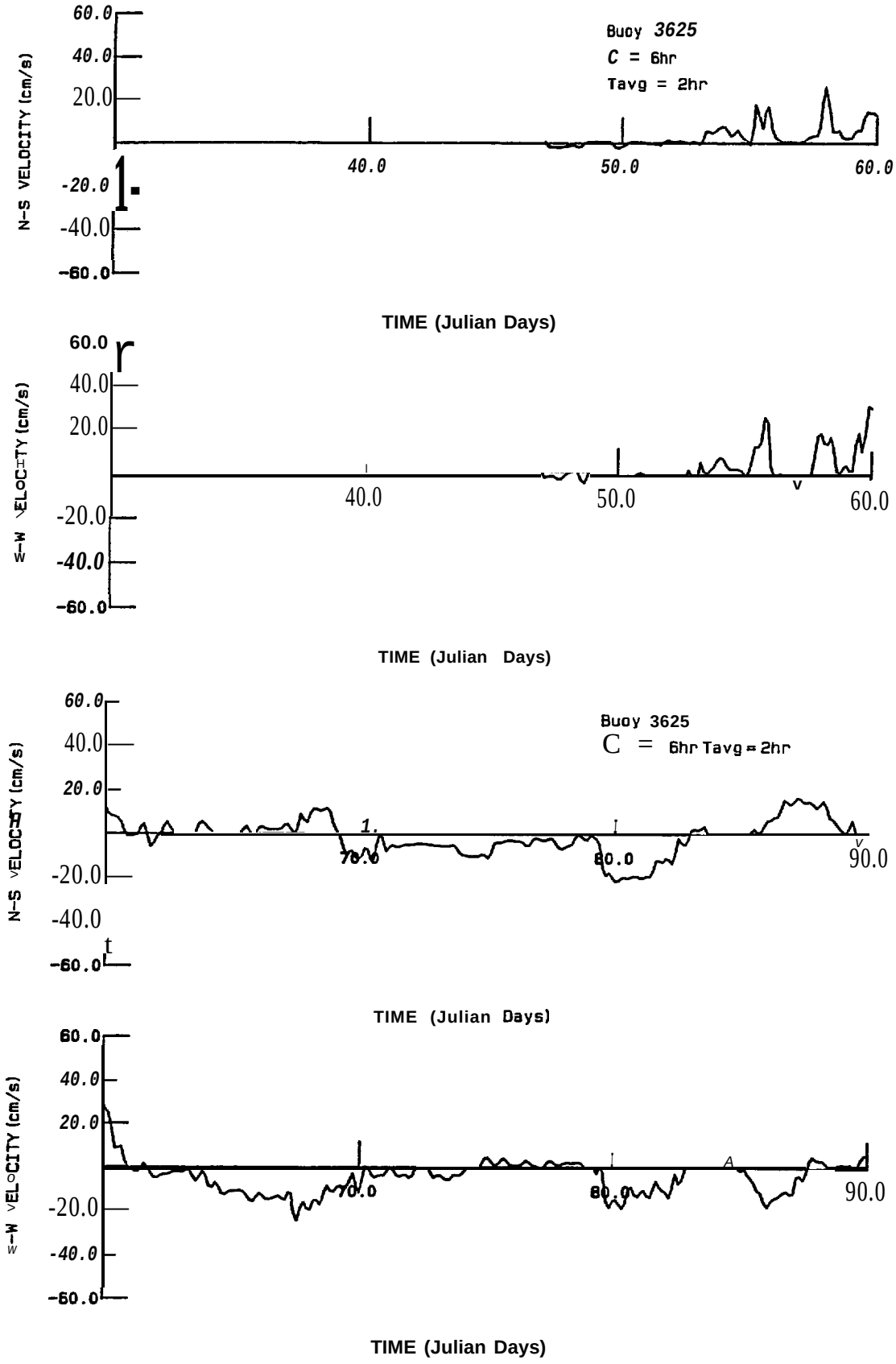

Figure 6.03. Buoy 3625 Velocity Time History Calculated from Interpolated Position History.

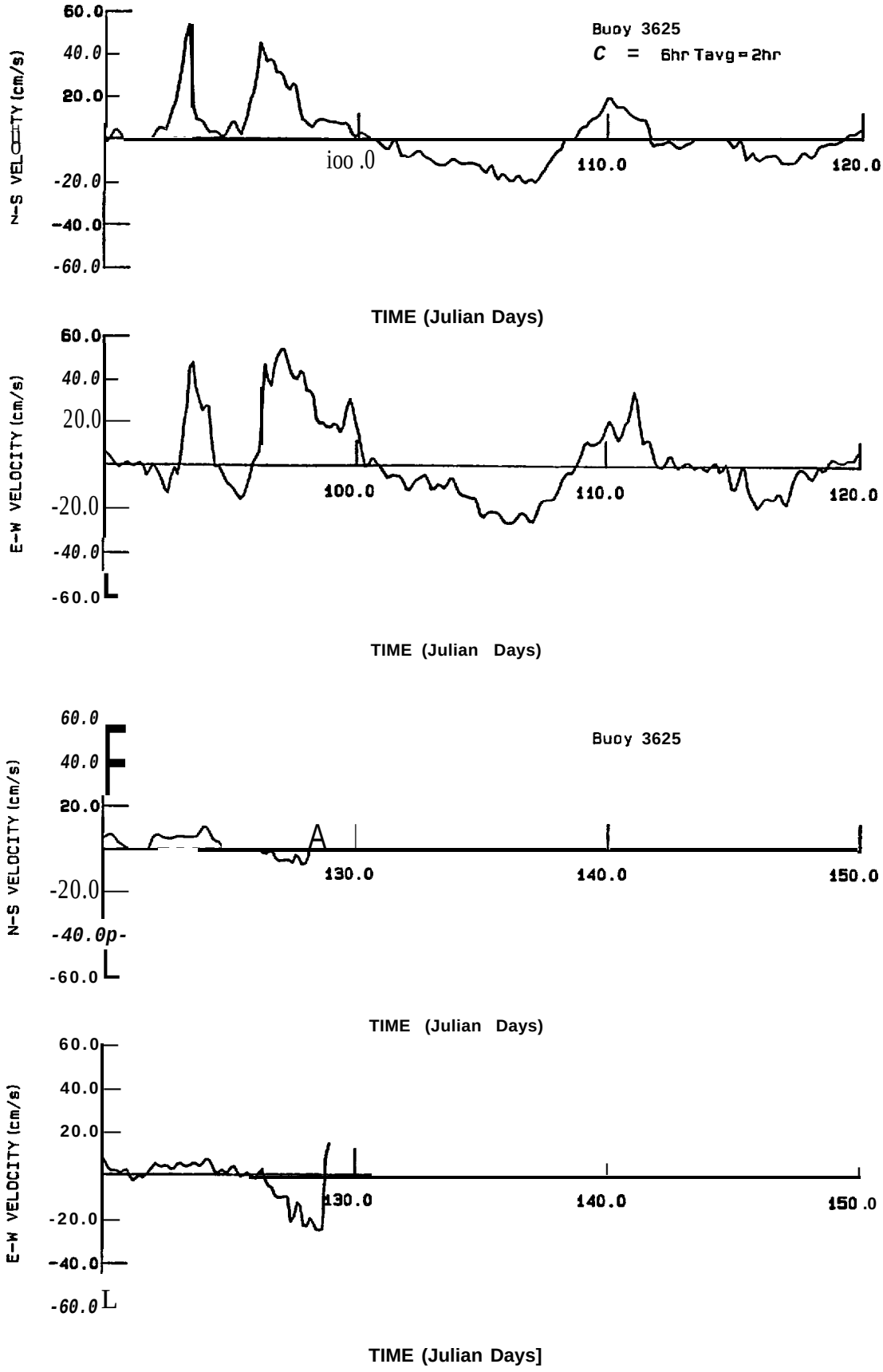

Figure 6.03. Buoy 3625 Velocity Time History Calculated from Interpolated Position History (concl'd).

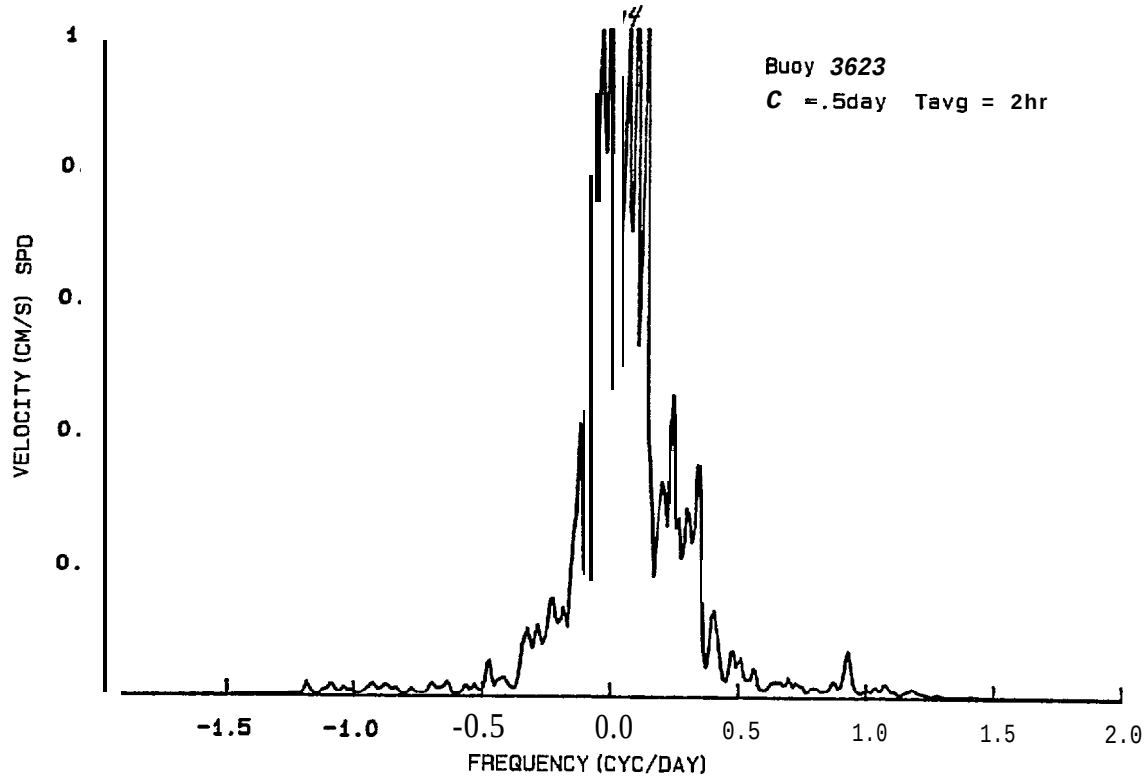

Figure 6.04. Buoy 3623 Ice Velocity Power Spectral Density.

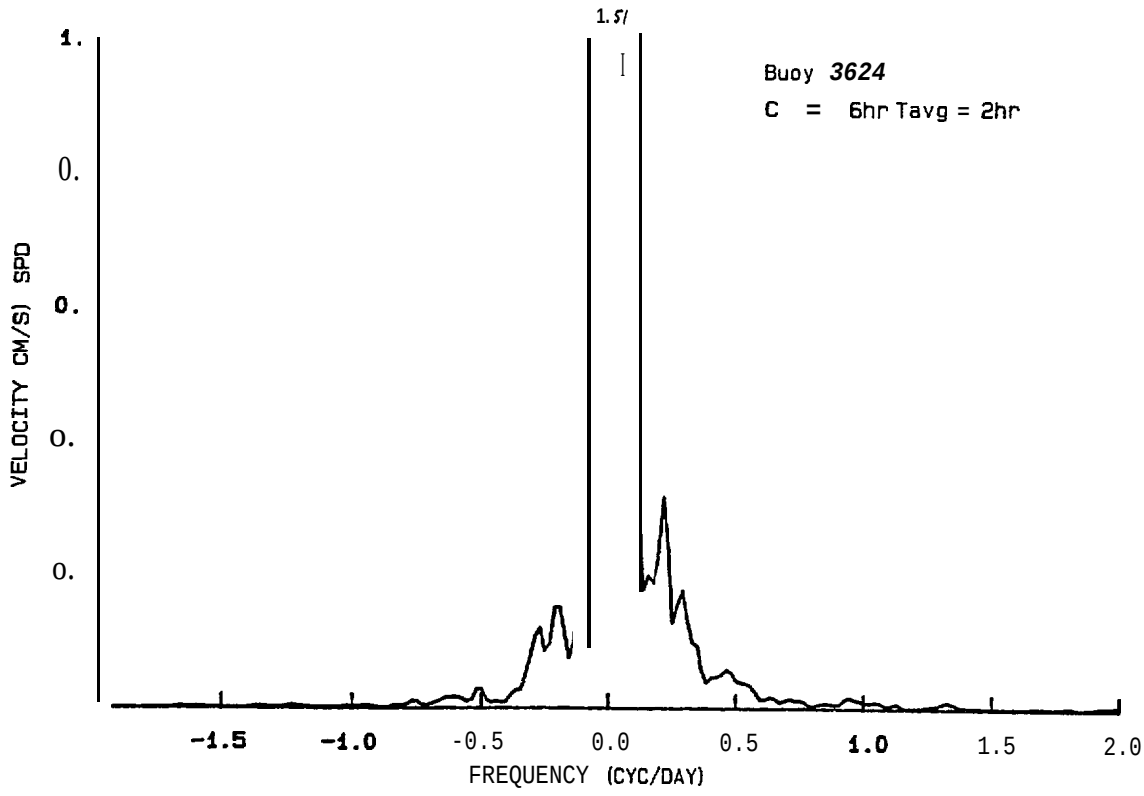

Figure 6.05. Buoy 3624 Ice Velocity Power Spectral Density.

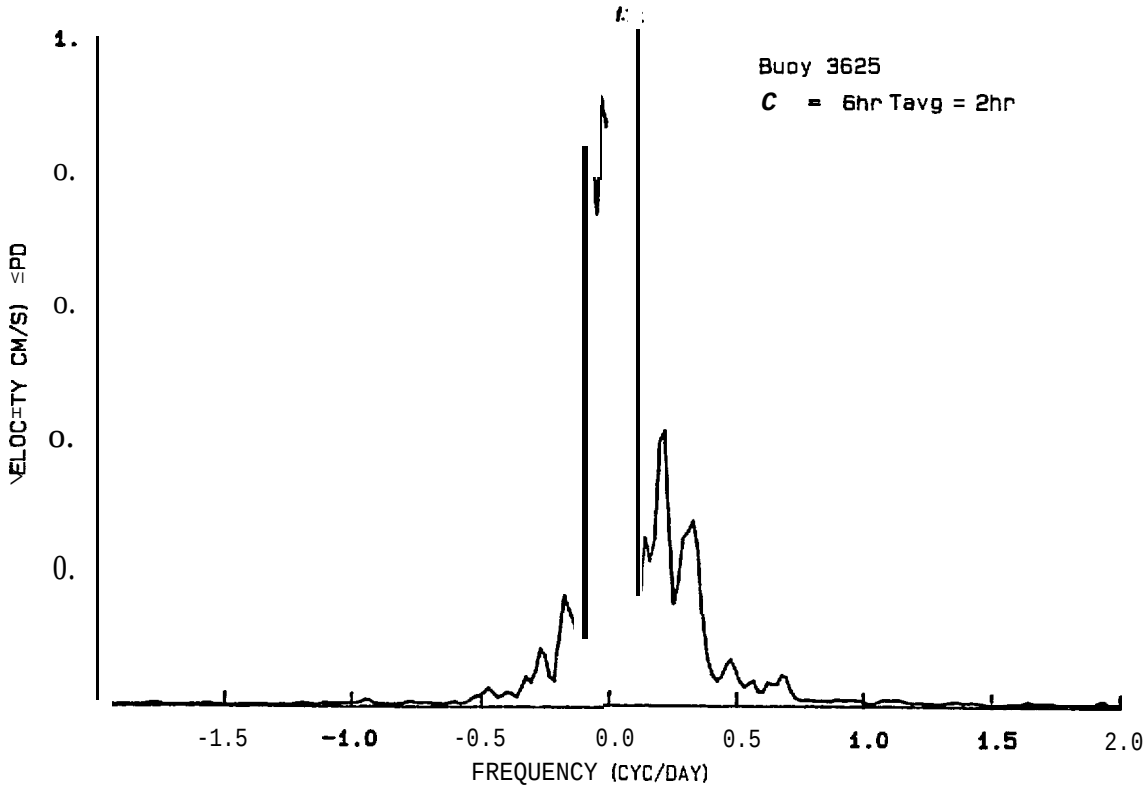

Figure 6.06. Buoy 3625 Ice Velocity Power Spectral Density.

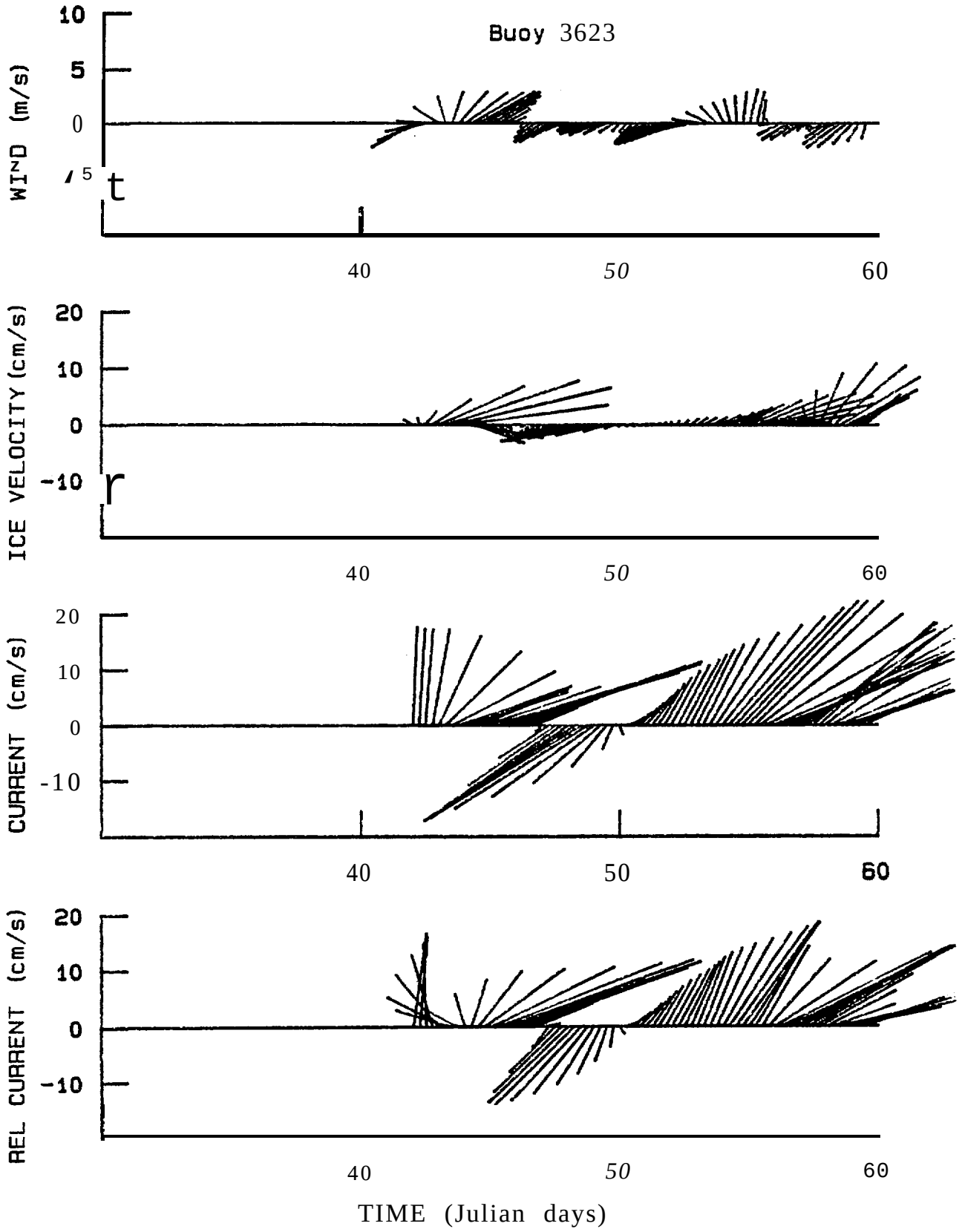

Figure 6.07. Buoy 3623 Stick Plots of Daily Average Wind, Ice Velocity, Current, and Relative Current.

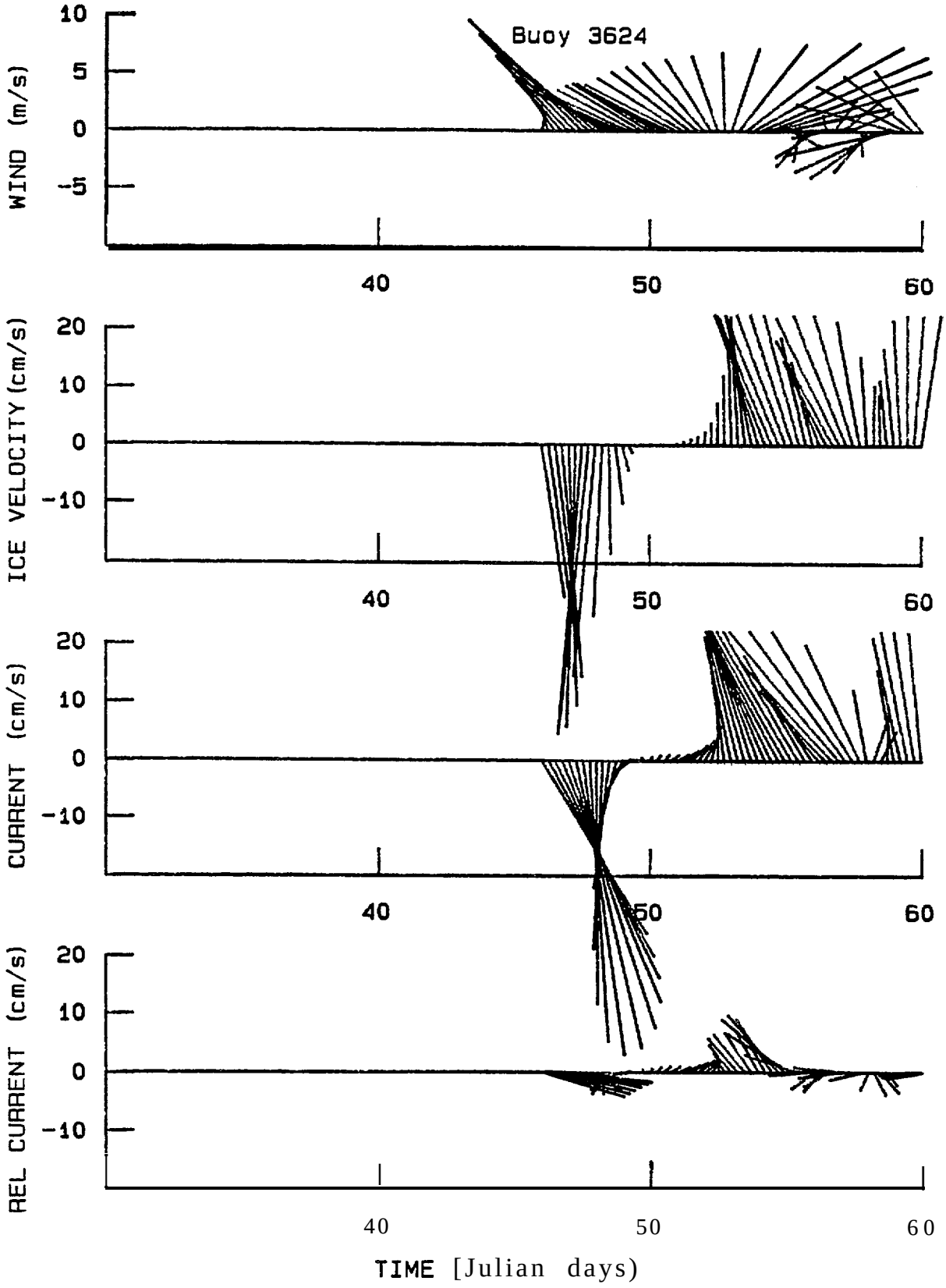

Figure 6.08. Buoy 3624 Stick Plots of Daily Average Wind, Ice Velocity, Current, and Relative Current,

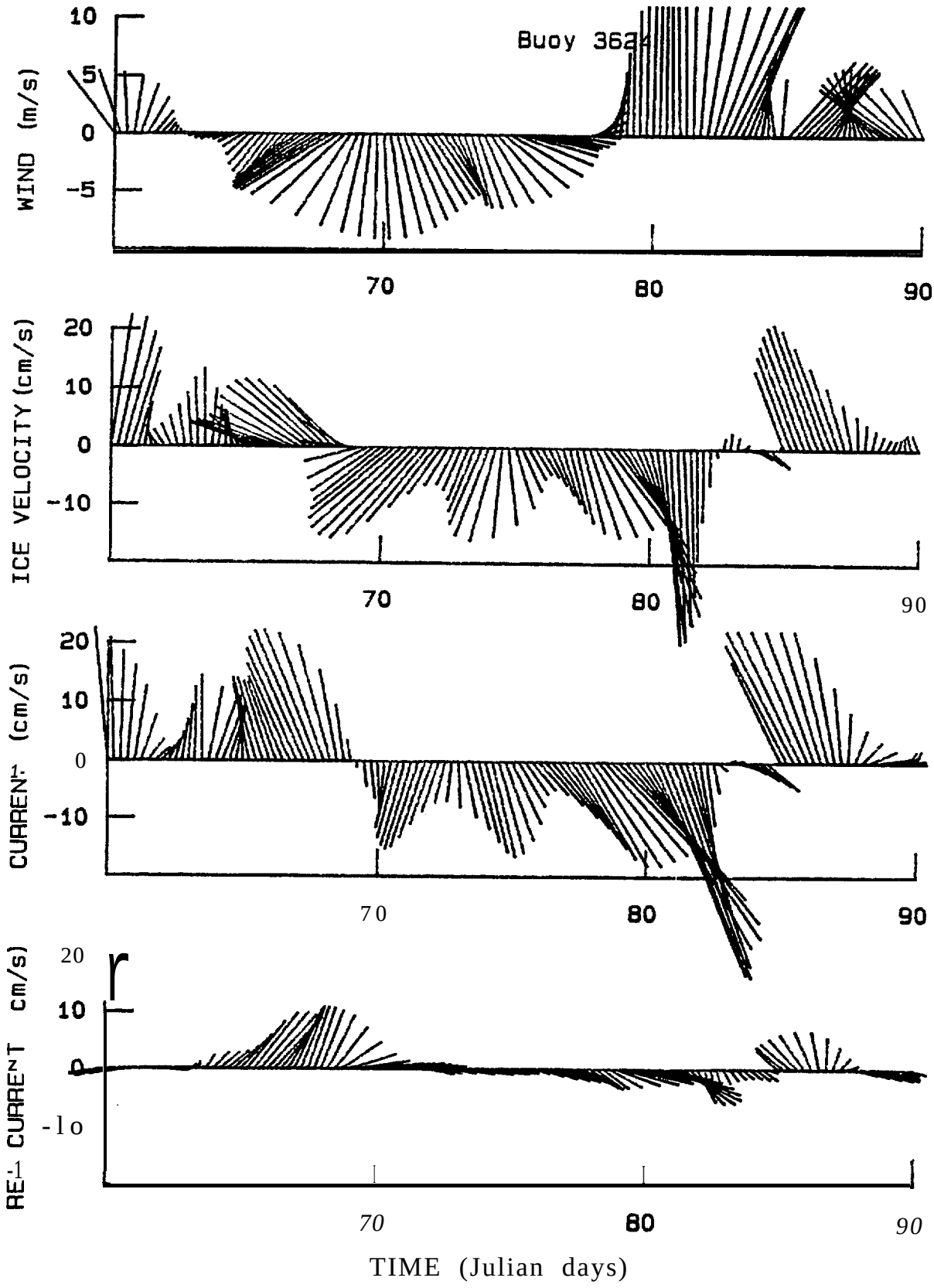

Figure 6.08. Buoy 3624 Stick Plots of Daily Average Wind, Ice Velocity, Current, and Relative Current.

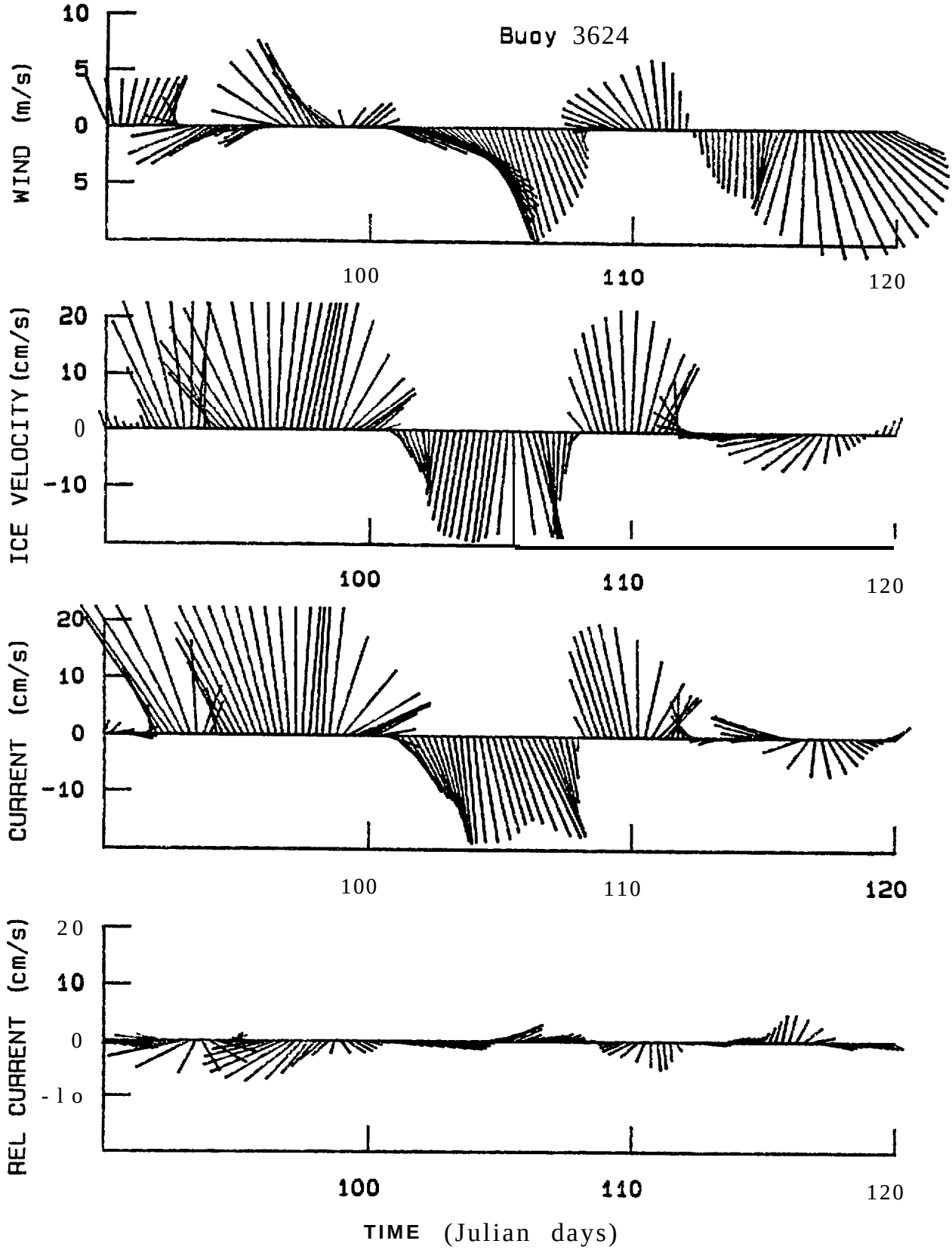

Figure 6.08. Buoy 3624 Stick Plots of Daily Average Wind, Ice Velocity, Current, and Relative Current.

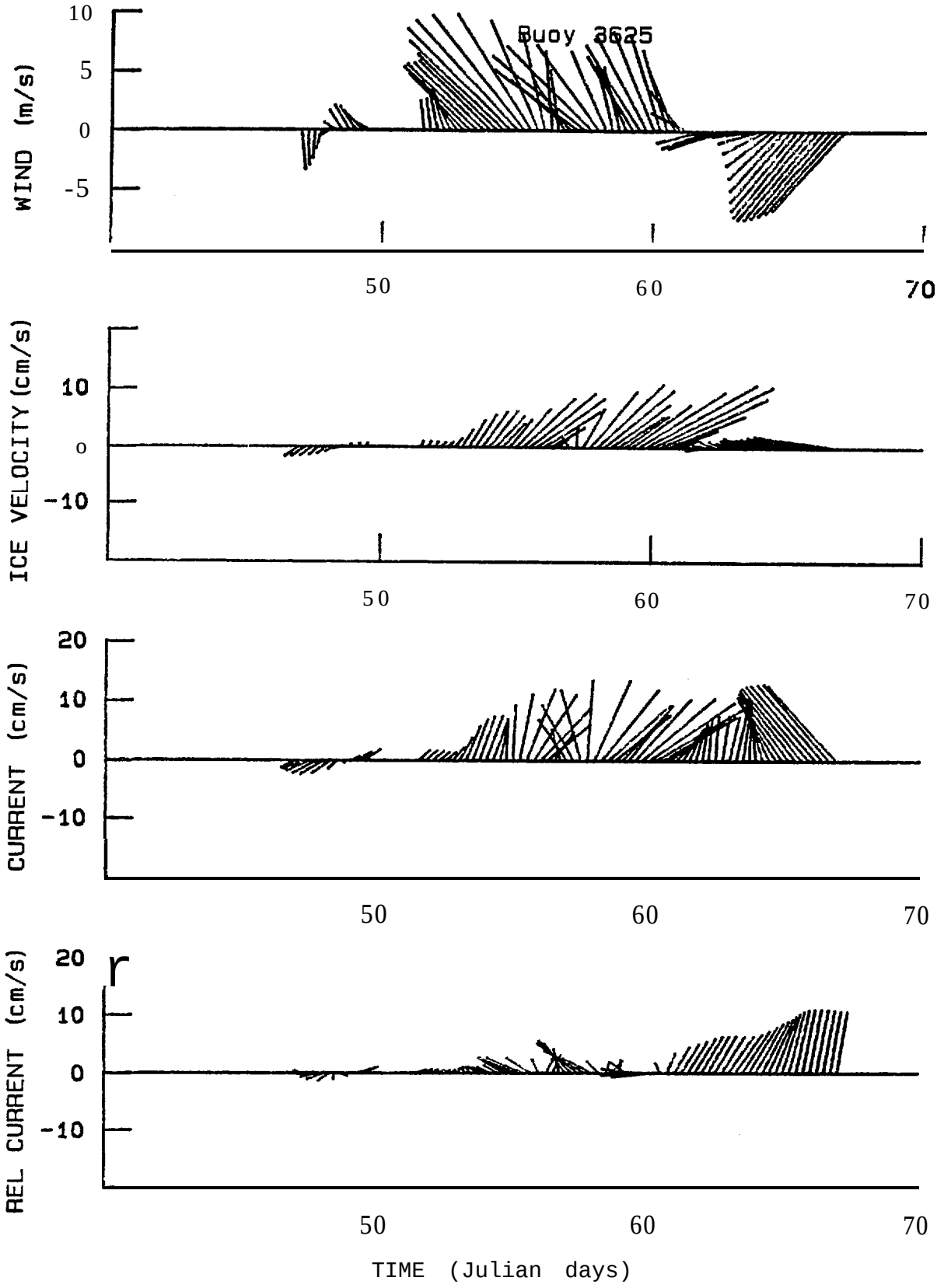

Figure 6.09. Buoy 3625 Stick Plots of Daily Average Wind, Ice Velocity, Current, and Relative Current,

7. SUMMARY

The motions of seventeen Argos buoys deployed on the Norton Sound and Chukchi Sea ice cover have been estimated using the method of optimal interpolation (OI). This is an objective technique that minimizes the expected error in the position estimate, takes account of measurement errors, and calculates the probable error in each position and velocity estimate.

The average ice velocity over a 2-hour time interval was determined as the spatial separation between two successive interpolated positions divided by the time increment. The expected error in these velocity estimates was also minimized by the OI technique. Relative currents were measured by the current meters drifting with the ice. Absolute ocean currents were determined by adding the ice velocity vectors and the relative current vectors.

The position and ice velocity estimates allowed the data to be archived in the new standard format of File Type 154. The existing NODC File Type 156 format was modified to accept ocean current data. A Record Type E was introduced to describe surface conditions, including winds and barometric pressures. A Record Type F was introduced to describe subsurface conditions, including ocean currents, Each data record included a position estimate, and a flag to indicate if this estimate was a measured raw position determined by Service ARGOS or a calculated position estimated by the OI procedure. Ice velocity estimates were included in Record Type F to allow reconstruction of the relative current measured by current meters suspended from the ice.

Ice motion histories show that diurnal tidal oscillations dominate the short-term velocity behavior in Norton Sound. There is a small semi-diurnal tidal component in Norton Sound that increases in the Bering Strait. In contrast, there is no significant tidal velocity component in the Chukchi Sea.

The atmospheric and oceanic conditions that existed during the field program have been described. High frequency variations were removed by filtering with a 48-hour cosine bell filter, and attention was focused on daily and longer behavior. We have analyzed the wind and current data and supplemented them with winds calculated from the NMC barometric pressure maps.

It is generally agreed that on time scales of roughly a day to a few weeks, the winds and currents provide the major external forces that drive the ice. When internal ice stress divergence is negligible, free-drift should provide a good approximation to the force balance. Under free-drift conditions, the ice velocity should be approximately equal to the vector sum of the ocean current and a linear function of the wind."

A complex regression analysis was used to determine what portion of the ice motions were described by the winds and currents using a free-drift model. Specifically, correlations between daily ice velocity and absolute current, and between the relative current (the current relative to the ice velocity) and the wind were determined to characterize the respective portions of the driving force contributed by ocean currents and wind. The three Norton Sound buoys showed that from 56 to 80% of the daily ice velocity variance were explained by the current. The wind contributed 0 to 35%. Similar calculations for the three Chukchi

Sea buoys showed that the current explained from 44 to 93X of the ice velocity variance, while the wind explained from 2 to 19%. In both cases, the current was found to be the more important factor in moving the ice. There was also evidence that some of the current-driven ice drift events were nearly simultaneous from Norton Sound to Barrow, which suggests that the ice was driven by barotropic currents that were caused by large-scale atmospheric pressure differences.

Although we have found that the currents provide the largest driving force to the ice cover in these regions, there remains a substantial part of the velocity variance that is not correlated with the winds or currents. These differences might be attributed to internal ice stress divergence, non-geostrophic currents, or other unknown processes. At this time, we do not know which processes are most important, but all are plausible.

More work is needed to understand how and why the ice behaves as it does, especially in the Chukchi Sea where the ice stress divergence can dominate the force balance. While the scope of the present work was largely limited to providing a basic description of the buoy movements and the concurrent physical setting, it did provide information on the relative importance of winds and currents on ice motions. These results can help guide the more sophisticated numerical studies that are needed to model the essential processes. The longer range goal should be to simulate and predict ice motions in these smaller geographic regions where ice stress divergence is important.

8. REFERENCES CITED

Aagaard, K., A.T. Roach, and J.D. Schumacher (1985) "On the Wind-driven Variability of the Flow through Bering Strait", J. Geophys. Res., vol. 9(I, no. C1, pp. 7213-7221.

Bendat, J. S., and Piersoll, A. G. (1980) Engineering Applications of Correlation and Spectral Analysis, John Wiley & Sons, New York.

Bloomfield, P. (1976) Fourier Analysis of Time Series: An Introduction, John Wiley & Sons, New York.

Colony, R., and Thorndike, A. S. (1985) "Sea Ice Motion as a Drunkard's Walk," J. Geophys. Res., vol. 90, no. C1, pp. 945-97'4.

Gandin, L. S. (1965) "Objective Analysis of Meteorological Fields," translated from Russian by Israel Program for Scientific Translation, Jerusalem, available from NTIS as No. TT65-50007.

Gelb, A., Kasper, J. F., Jr., Nash, R. A., Jr., Price, C.F., Sutherland, A.A., Jr. (1974) Applied Optimal Estimation, The M.I.T. Press, Cambridge, MA.

Kozo, T. L. (1984) "Mesoscale Meteorology of the Norton Sound Region," U.S. Dept. Commerce, NOAA, OCSEAP Final Report 39, pp. 1-102.

Liu, S.-K., and Leendertse, J. J. (1984) "Modeling of the Alaskan Coastal Waters," in Three-dimensional Shelf Models, Americal Geophysical Union, Washington, D.C.

Macklin, S. A., Brown, R. L., Gray, J., and Lindsay, R. W. (1984) "METLIB - II - A Program Library for Calculating and Plotting Atmospheric and Oceanic Fields," NOAA Technical Memorandum ERL PMEL-54, Pacific Marine Environmental Laboratory, Seattle, WA, 53pp.

McPhee, M. G. (1979) "The Effect of the Oceanic Boundary Layer on the Mean Drift of Pack Ice: Application of a Simple Model," J. Glaciol., vol. 9, pp. 388-400.

McPhee, M. G. (1982) "Sea Ice Drag Laws and Simple Boundary Layer Concepts, including Application to Rapid Melting," Report 82-4, Cold Regions Research and Engineering Laboratory, Hanover, NH.

Mofjeld, H. O. (1984) "Recent Observations of Tides and Tidal Currents from the Northeastern Bering Sea Shelf," Pacific Marine Environmental Laboratory, NOAA Technical Memorandum ERL PMEL-57, Seattle, WA.

Overland, J. E. (1985) "Atmospheric Boundary Layer Structure and Drag Coefficients over Sea Ice," J. Geophys. Res., vol. 90, no. C5, pp. 9029-9049.

Pease, C. H., and Salo, S. (1987) "Sea Ice Drift near Bering Strait during 1982," to appear in J. Geophys. Res., Special Issue on Marginal Ice Zones.

Pritchard, R. S. (1979) "Transport and Behavior of a Prudhoe Bay Oil Spill," in Proceedings of a Workshop on Oil in Ice held in Toronto on October 10-11, (Sponsored by University of Toronto and CANMAR).

Pritchard, R. S. (1981) "Mechanical Behavior of Pack Ice," in Mechanics of Structured Media, Part A, (cd) A. P. S. Selvadurai, Elsevier, Amsterdam. pp. 371-405.

Pritchard, R. S. (1984) "Beaufort Sea Ice Motions," in The Alaskan Beaufort Sea, (eds) P. W. Barnes, D. M. Schell, and E. Reimnitz, Academic Press, Orlando, pp. 95-113.

Pritchard, R. S., and Thomas, D. R. (1985) "Chukchi Sea Ice Behavior, 1981-82," Flow Technical Report No. 323, Flow Industries, Kent, WA.

Reynolds, M., and Pease, C. 1-1. (1984) "Drift Characteristics of Northeastern Bering Sea Ice during 1982," NOAA Technical Memorandum ERL PMEL-55, Pacific Marine Environmental Laboratory, Seattle, WA, 135pp.

Stringer, W. J., and Henzler, R. D. (1981) "Ice Displacement Vectors Measured in Norton Sound and the Adjacent Bering Sea 1973-1979," Report to NOAA/OCSEAP on contract no. 03-5-022-55 for RU 267, University of Alaska, Geophysical Institute, Fairbanks, AK.

Thomas, D. R., and Pritchard, R. S. (1979) "Beaufort and Chukchi Sea Ice Motion - Part 1. Pack Ice Trajectories," Flow Research Report No. 133, Flow Research Company, Kent, WA.

Thomas, D. R., and Pritchard, R. S. (1981) "Norton Sound and Bering Sea Ice Motion; 1981," Flow Research Report No. 209, Flow Research Company, Kent, WA.

Thomas, D. R., and Pritchard, R. S. (1982) "The Transport and Behavior of Oil Spilled In and Under Sea Ice," Annual Report to Outer Continental Shelf Environmental Assessment Program on Research Unit 567, National Oceanic and Atmospheric Administration, Boulder, CO.

APPENDIX A

NODC File Type 156 Data Documentation Forms

ACCESSION NUMBER

DATA DOCUMENTATION FORM

NOAA FORM 24-13
(4-77)

U.S. DEPARTMENT OF COMMERCE
NATIONAL OCEANIC AND ATMOSPHERIC ADMINISTRATION
NATIONAL OCEANOGRAPHIC DATA CENTER
RECORDS SECTION
WASHINGTON, DC 20235

FORM APPROVED
O.M.B. No. 41-R2651
EXPIRES 1-S I

(While you are not required tow this form, it is the mmt desirable mechanism for providing the required ancillary information enabling the NODC and users to obtain tbe greatest benefit from yoor data.)

This form should accompany all data submissions to NODC. Section A, Originator Identification, must be completed when the data are submitted. It is highly desirable for NODC to also receive the remaining pertinent information at that time. This may be most easily accomplished by attaching reports, publications, or manuscripts which are readily available describing data collection, analysis, and format specifics. Readable, handwritten submissions are acceptable in all cases. All data shipments should be sent to the above address.

A. ORIGINATOR IDENTIFICATION

THIS SECTION MUST BE COMPLETED BY DONOR FOR ALL DATA TRANSMITTALS

. NAME AND ADDRESS OF INSTITUTION, LABORATORY, OR ACTIVITY WITH WHICH SUBMITTED DATA ARE ASSOCIATED

IceCasting, Inc.
11042 Sand Point Way N.E.
Seattle, WA 981 25-5846

2. EXPEDITION. PROJECT, OR PROGRAM DURING WHICH DATA WERE COLLECTED

Norton Sound and Chukchi Sea

3. CRUISE NUMBER(S) USED BY ORIGINATOR TO IDENTIFY DATA IN THIS SHIPMENT

NORTON or CHUKCHI

4. PLATFORM NAMES 3607, 3608, 3609, 3610, 3611, 3612, 3613, 3614, 3615, 3616, 3617, 3::09 3621, 3622, 3624, &362

5. PLATFORM TYPE(S) (E.G., SHIP, BUOY..ETC.)

Drifting Buoy

6. PLATFORM AND OPERATOR NATIONALITY(IES)

PLATFORM	OPERATOR
USA	USA

7. DATES

FROM: MO/DAY/YR	MO/DAY/YI
1 2/09/81	6/29/82

1. ARE DATA PROPRIETARY?

[X] NO [ ] YES

If YES. WHEN CAN THEY BE RELEASED FOR GENERAL USE? YEAR ___ MONTH _

1. PLEASE DARKEN ALL MARSDEN SQUARES IN WHICH ANY DATA CONTAINED IN YOUR SUEMISSION WERE COLLECTED.

GENERAL AREA

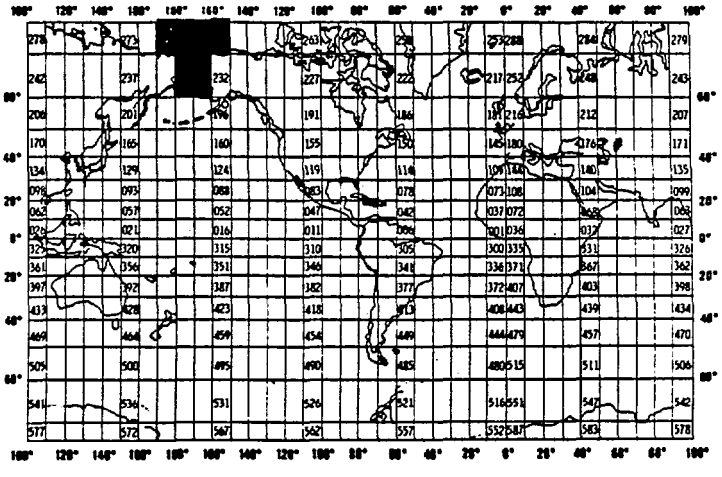

. ARE DATA DECLARED NATIONAL PROGRAM (DNP)?

(I. E., SHOULD THEY BE INCLUDED IN WORLD DATA CENTERS HOLDINGS FOR INTERNATIONAL EXCHANGE?)

[X] NO [ ] YES [ ] PART (SPECIFY BELOW)

. PERSON TO WHOM INQUIRIES CONCERNING DATA SHOULD BE ADDRESSED WITH TELEPHONE NUMBER (AND ADDRESS IF OTHER THAN IN ITEM-1)

Robert S. Pritchard
(206)363-3394

DAA FORM 24-13

B. SCIENTIFIC CONTENT

NAME OF DATA FIELD	REPORTING UNITS OR CODE	METHODS OF OBSERVATION AND INSTRUMENTS USED (SPECIFY TYPE AND MODEL)	ANALYTICAL METHODS (INCLUDING MODIFICATIONS) AND LABORATORY PROCEDURES	DATA PROCESSING TECHNIQUES WITH FILTERING AND AVERAGING
Latitude/ Longitude	Deg,Min,Sec	Raw Position Determined by Service ARGOS. Buoys mfg. by Polar Research Laboratory	Calculated position i determined using Optimal Interpolation to estimate position of sensor data.	Ref: Pritchard and Hanzlick (1987)
Anemometer Ht	Meters	Nominal 3-meter mast ‹ top of ice.		Wind Velocity vector i the average of 32 samples taken during 9-minute period preced ing observation time. Ohs. at 2-hr Intervals
Wind Velocity Speed Direction	m/s deg	Weathermeasure Model W203 Anemomete Model W204 Vane		
Atmospheric Pressure	millibars	Paroscientific barometer		B m p e s g mp ak d g 2 h p d d n m
Air Temperatu e	C	Yellow Springs Instruments Thermolinear Thermistor		Instantaneous sample.
Compass Bearing	Deg	PRL fluxgate compass		Instantaneous sample.
Current Meter Depth	Meters	Nominal length of tether cable from top of ice.		
Ice Velocity Speed Direction	cm/s Deg	Calculated from position.estimated frc Optimal Interpolation.	Values are representative of 2-hr average: centered on ohs. time.	Ref: Pritchard and Hanzlick (1987)

10 AA FORM 24-13

B. SCIENTIFIC CONTENT

AME OF DATA FIELD	REPORTING UNITS OR CODE	METHODS OF OBSERVATION AND INSTRUMENTS USED (SPECIFY TYPE AND MODEL)	ANALYTICAL METHODS (INCLUDING MODIFICATIONS) AND LABORATORY PROCEDURES	DATA PROCESSING TECHNIQUES WITH FILTERING AND AVERAGING
Absolute Current Velc Speed Direction	ity cm/s Deg	Marinco Model Q-9 Savonius Rotor Curren Meter tethered to Drifting Buoy on Ice.	Meter measures curre relative to ice. Abs. current is calculate by adding Ice veloci to rel.current vel. Ref: Pritchard and Hanzlick (1987)	Rel. current speed is average of samples during 9 minutes preceding ohs. time. Rel. current directic is instantaneous sample. Direction is measured relative to buoy orientation and added to compass bearing to obtain Rel. Current Dir.
References ---------- (s Thomas and Pr Pritchard anc Pritchard anc environment the resulti	3 attached lis tchard (1982) Thomas (1985) Hanzlick (198 l conditions c g ice behavio	) escribes the field pr escribes Chukchi Sea describes analytical ring the experiment,	ram and hardware. e motions. ethods, i	

AA FORM 24-13

REFERENCES

Pritchard, R. S., and Hanzlick, D. J. (1987a) "Sea Ice Trajectories and Ocean Currents 1981-1982: Norton Sound and Chukchi Sea," Final Report to OCSEAP/NOAA under Contract WASC-86-00043. Also printed as Technical Report Number ICI-RPT-8701O, IceCasting, Inc., Seattle, WA.

Pritchard, R. S., and Thomas, D. R. (1985) "Chukchi Sea Ice Motions, 1981-82," Flow Technical Report Number 323, Flow Industries, Inc., Kent, WA.

Thomas, D. R., and Pritchard, R. S. (1982) "The Transport and Behavior of Oil Spilled In and Under Sea Ice," Annual Report to OCSEAP on RU567, NOAA, Boulder, CO. Also printed as Flow Research Report Number 240, Flow Research Company, Kent, WA.

C. DATA FORMAT

COMPLETE THIS SECTION FOR PUNCHED CARDS OR TAPE, MAGNETIC TAPE, OR DISC SUBMISSIONS.

1. LIST RECORD TYPES CONTAINED IN THE TRANSMITTAL OF YOUR FILE
GIVE METHOD OF IDENTIFYING EACH RECORD TYPE

HEADER Record	"A" in column 10
LAUNCH SUMMARY Record	"B" in column 10
SURFACE DATA Record	"E" in column 10
SUBSURFACE CURRENT Record	"F" in column 10

2. GIVE BRIEF DESCRIPTION OF FILE ORGANIZATION

Thirty six files on tape. File 1 contains a list of file names. Files 2-I8 contain data for buoys 3607-3625, respectively. Each of these 17 data files is File Type 156. The second set of 18 files is an exact duplicate of the first set of 18 files, to be used in case an original is damaged. The enclosed Table 1 describes the number of lines, words, and bytes in each file.

The tape is UNLABELED.

3. ATTRIBUTES AS EXPRESSED IN ☐ PL-1 ☐ COSIOL ☒ FORTRAN ☐ ALGOL _____ LANGUAGE

4. RESPONSIBLE COMPUTER SPECIALIST:
NAME AND PHONE NUMBER Robert S. Pritchard (206) 363-3394
ADDRESS IceCasting, Inc. 42 and Point Way N.E.
Seattle, WA 98125-5846

COMPLETE THIS SECTION IF DATA AREON MAGNETIC TAPE

5. RECORDING MODE
☐ BCD ☐ BINARY
☐ ASCII ☒ EBCDIC
u _____

6. NUMBER OF TRACKS (CHANNELS)
☐ sEvEN
☒ NINE
☐ _____

7. PARITY
☒ ODD
☐ EVEN

8. DENSITY
☐ 200 BPI ☒ 1600 BPI
☐ 556 BPI
☐ 800 BPI
☐ _____

9. LENGTH OF INTER-RECORD GAP (IF KNOWN) ☒ 3/4 INCH
standard u _____

10. END OF FILE MARK
☐ OCTAL 17
standard ☐ unknown

11. PASTE-ON-PAPER LABEL DESCRIPTION (INCLUDE ORIGINATOR NAME AND SOME LAYSPEC1F1CATIONS OF DATA TYPE, VOLUME NUMBER)
Robert S. Pritchard
IceCasting, Inc.
Ice motion, wind, barometric pressure, and current data from 17 drifting buoys in Norton Sound and the Chukchi Sea during 1981-8:

12. PHYSICAL BLOCK LENGTH IN BYTES
1600

13. LENGTH OF BYTES IN BITS
8

NOAA FORM 24-13

Table 1. A brief description of **files** containing data for drifting buoys 3607-3625.

file #	lines	words	bytes	FILE NAME	Comments
i	18	18	107	list	1st set of files
2	483	4360	39108	n3607	
3	2710	23062	220143	n3608	
4	1011	8393	81876	n3609	
5	64,	396	5169	n3610	
6	417	2625	33762	n3611	
7	1017	6554	82362	n3612	
8	502	3377	40647	n3613	
9	1127	6959	91272	n3614	
10	278	1744	22503	n3615	
11	967	6480	78312	n3616	
12	1076	6514	87141	n3617	
13	20	136	1591	n3620	
14	3075	21476	313846	n3621	
15	2557	18173	207088	n3622	
16	1109	8298	89800	n3623	
17	1783	134S7	144394	n3624	
18	2132	15429	172663	n3625	
19	18	18	107	list	duplicate set of files
20	483	4360	39108	n3607	
21	2718	23062	220143	n3608	
22	1o11	8393	81876	n3609	
23	64	396	5169	n3610	
24	417	2625	33762	n3611	
25	1017	6554	82362	n3612	
26	502	3377	40647	n3613	
27	1127	6959	91272	n3614	
28	278	1744	22503	n3615	
29	967	6480	78312	n3616	
30	107J5	6514	87141	n3617	
31	20	136	1591	n3620	
32	3875	21476	313846	n3621	
33	2SS7	18173	207088	n3622	
34	110?	8298	89800	n3623	
35	1783	134S7	144394	n3624	
36	2132	15429	172663	n3625	

RECORD FORMAT DESCRIPTION

Record Name: HEADER

14. Field Name	15. Position From 1- in Bytes	16. Length Bytes	17. Attributes	18. Use and Meaning
File Type	1	3	A1	'156'
File Identifier	4	6	A6	'NORTON' or 'CHUKCH' depending on location
Record Type	10	1	A1	'A'
Drogue Number	11	5	15	3607, 3608,...3625
Drogue Type	16	5	A5	'NORTN' or 'CHUKC' to identify station
Principal Investigator	21	15	A15	'R.S. Pritchard '
Institution or Agency	36	15	A15	'IceCasting, Inc'
Platform Name	51	12	A12	' ADAP '
Buoy Number	63	4	14	Same as Drogue Number
Blanks	67	14	14X	

RECORD FORMAT DESCRIPTION

Record Name: LAUNCH SUMMARY

14. Field Name	15. Position From 1- in Bytes	16. Length Bytes	17. Attributes	18. Use and Meaning
File Type	1	3	A1	'156'
File Identifier	4	6	A6	'NORTON' or 'CHUKCH' depending on location
Record Type	10	1	Al	'B'
Drogue Number	11	5	15	3607, 3608,...3625
Launch Position				
Latitude	16	7	3I2,A1	DDMMSS plus 'N' or 'S' for hemisphere
Longitude	23	8	I3,2I2,A1	DDDMMSS plus 'E' or 'W' for hemisphere
End Position				
Latitude	31	7	3I2,A1	DDDMMSS plus 'N' or 'S' for hemisphere
Longitude	38	8	13,212,4)1	DDMMSS plus 'E' or 'W' for hemisphere
Launch Date<GMT)	46	6	312	YYMMDD
Launch Time(GMT)	52	4	212	HHXX hours and minutes
End Date(GMT)	56	6	312	YYMMDD
End Time(GMT)	62	4	212	HHXX hours and minutes
Drogue Depth observation	66	4	14	Not Used
Frequency	70	4	I4	Not Used
Blanks	74	7	7X	

RECORD FORMAT DESCRIPTION

Record Name: SURFACE DATA

14. Field Name	15. Position From 1- in Bytes	16. Length Bytes	17. Attributes	18. Use and Meaning
File Type	1	3	A3	'156'
File Identifier	4	6	A6	'NORTON' 01' 'CHUKCH' depending on location
Record Type	10	1	A1	'A'
Drogue Number	11	5	15	3607, 3608,...3625
Position				
Latitude	16	7	3I2,A1	DDMMSS plus 'N' or 'S' for hemisphere
Longitude	23	8	I3,2I2,A1	DDDMMSS plus 'E' or 'W' for hemisphere
Observed Date(GMT)	31	6	312	YYMMDD
Observed Time(GMT)	37	4	212	HHXX hours and minutes
Anemometer Height	41	3	13	xxx-meters to tenths
Wind Speed	44	3	13	xxx-meters/see to tenths
Wind Direction	47	4	14	xxxx-degrees to tenths cw from North , Direction From
Atmospheric Pressure	51	6	I6	xxxxxx-millibars to hundredths
Air Temperature	57	4	14	xxxx-Deg C to tenths
Compass Bearing of Surface Unit	61	4	14	xxxx-degrees to tenths cw from North
Blanks	65	11	1 lx	
Position Code	76	1	A1	'M' for raw position from ARGOS, 'C' for Optimal Interpolation Estimate
Sequence Number	77	4	14	xxxx-data card number, in ascending order

RECORD FORMAT DESCRIPTION

Record Name: SUBSURFACE CURRENT

14.Field Name	15.Position From 1- in Bytes	16.Length Bytes	17.Attributes	18.Use and Meaning
File Type	1	3	A3	'156'
File Identifier	4	6	#M	'NORTON' or 'CHUKCH' depending on location
Record Type	10	1	A1	'F'
Drogue Number	11	5	15	3607, 3608,..,3625
Position				
Latitude	16	7	3I2,A1	DDMMSS plus 'N' or 'S' for hemisphere
Longitude	23	8	I3,2I2,A1	DDDMMSS plus 'E' or 'W' for hemisphere
Observed Date<GMT)	31	6	312	YYMMDD
Observed Time(GMT)	37	4	212	HHXX hours and minutes
Ice Velocity				
Speed	41	5	15	xxxxx-cm/sec to tenths
Direction	46	4	14	xxxx-Degrees to tenths cw from North, Direction Toward
Current Meter Depth	50	4	14	xxxx-meters to tenths
Absolute Current				
Speed	54	5	15	xxxxx-cm/sec to tenths
Direction	59	4	14	xxxx-Degrees to tenths cw from North, Direction Toward
Current Meter Depth	63	4	14	Not Used
Absolute Current				
Speed	67	5	15	Not Used
Direction	72	4	14	Not Used
Position Code	76	1	A1	'M' for raw position from ARGOS, 'C' for Optimal Interpolation Estimate
Sequence Number	77	4	14	xxxx-data card number, in ascending order

APPENDIX B

Sea Ice Trajectories

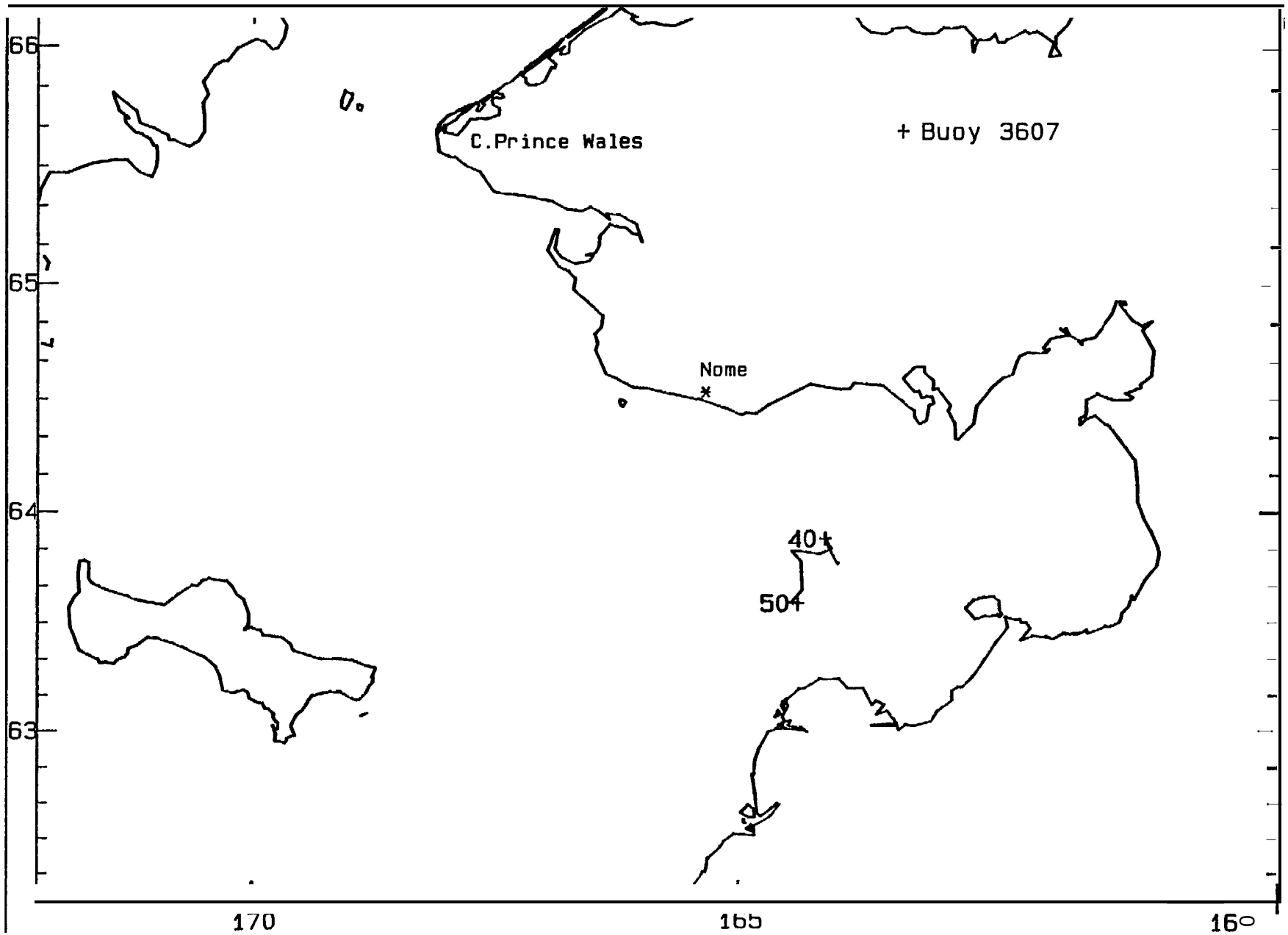
66
65
64
63
170
165
160
C.Prince Wales
+ Buoy 3607
Nome
40
50

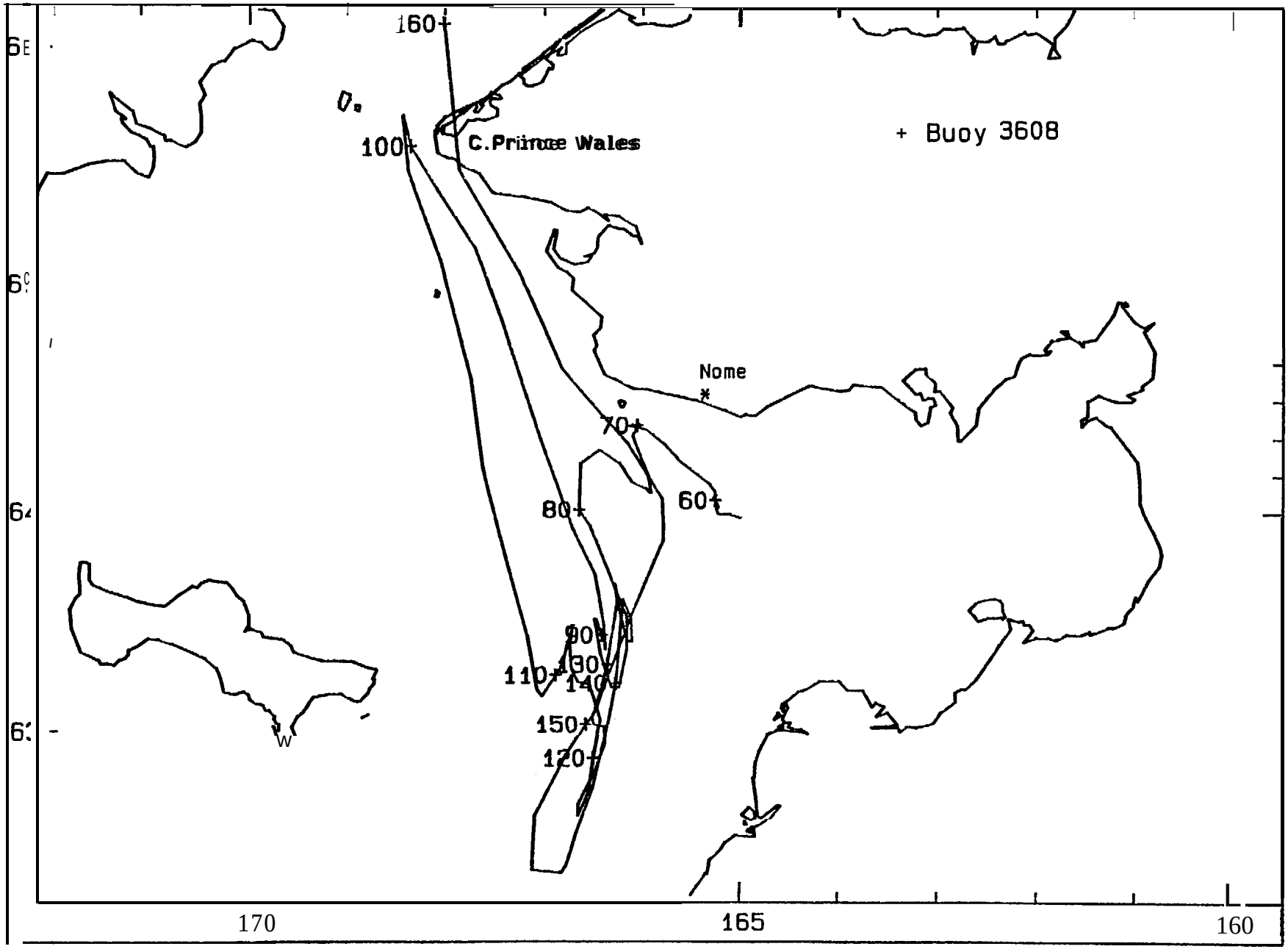
160
100
C.Prince Wales
+ Buoy 3608
Nome
70
60
80
90
110
130
140
150
120
170
165
160

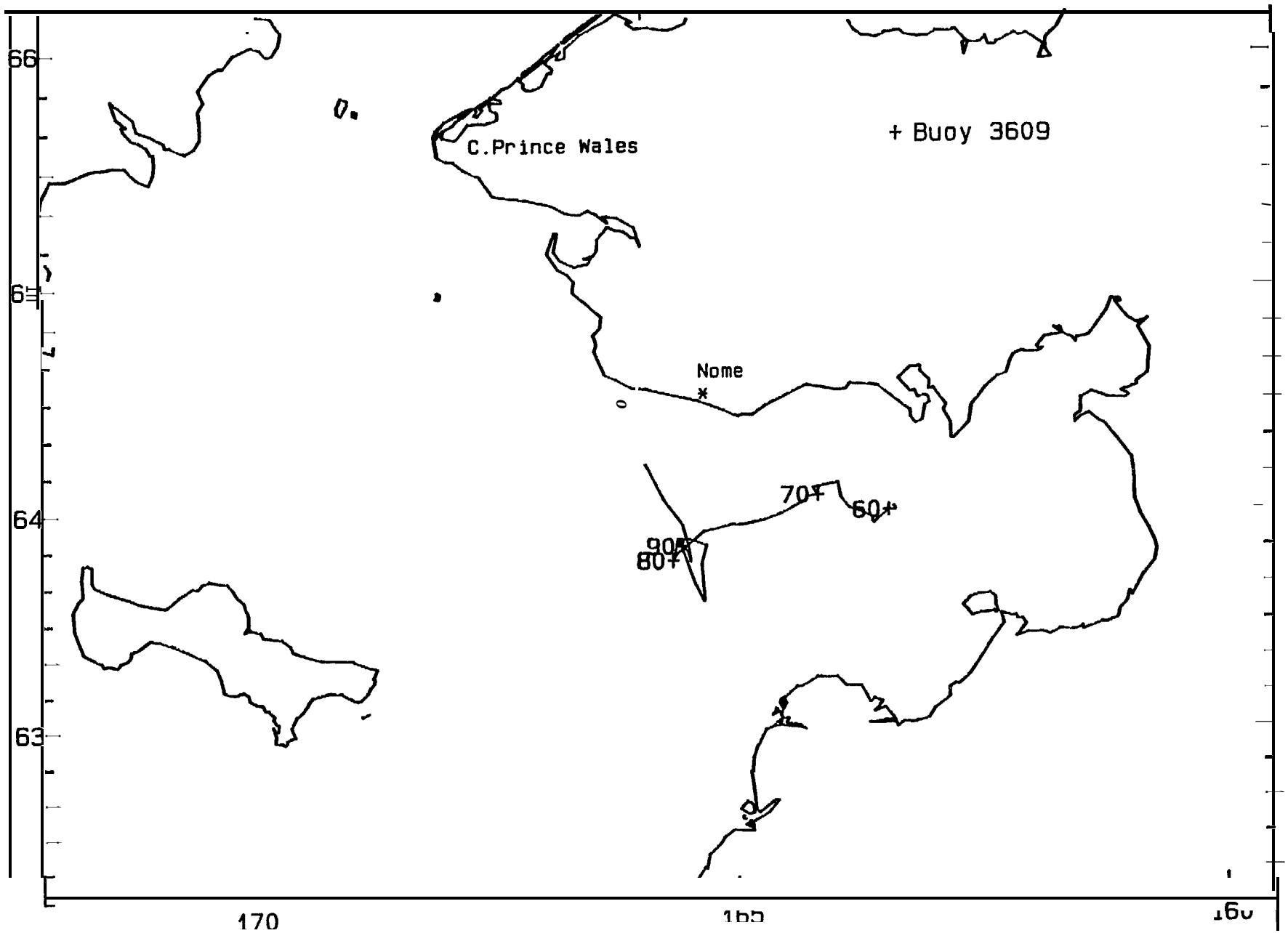
66
65
64
63
170
C.Prince Wales
+ Buoy 3609
Nome
70
60
90
80

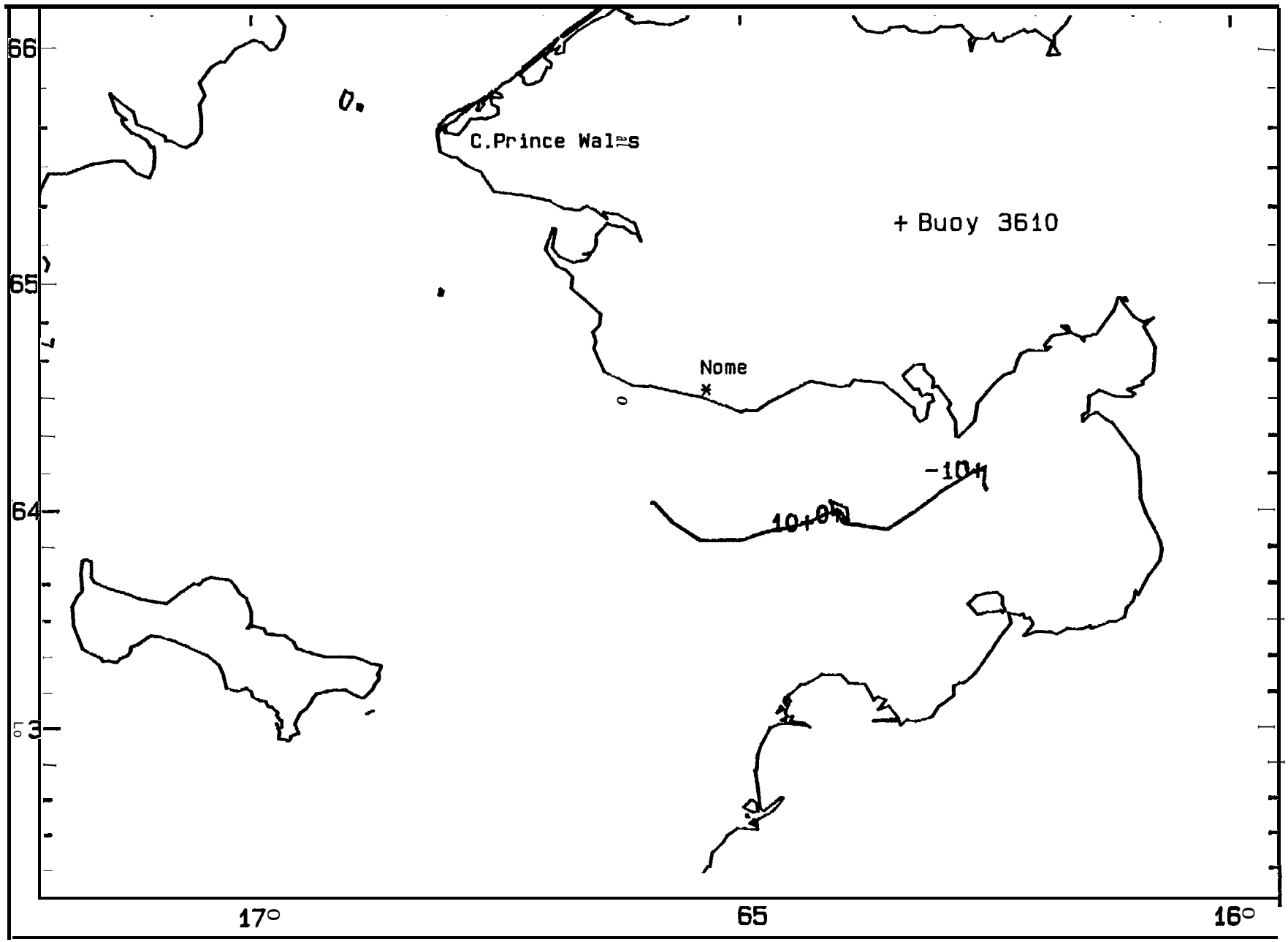
66
65
64
63
17°
65
16°
C.Prince Wales
+ Buoy 3610
Nome
-10
10

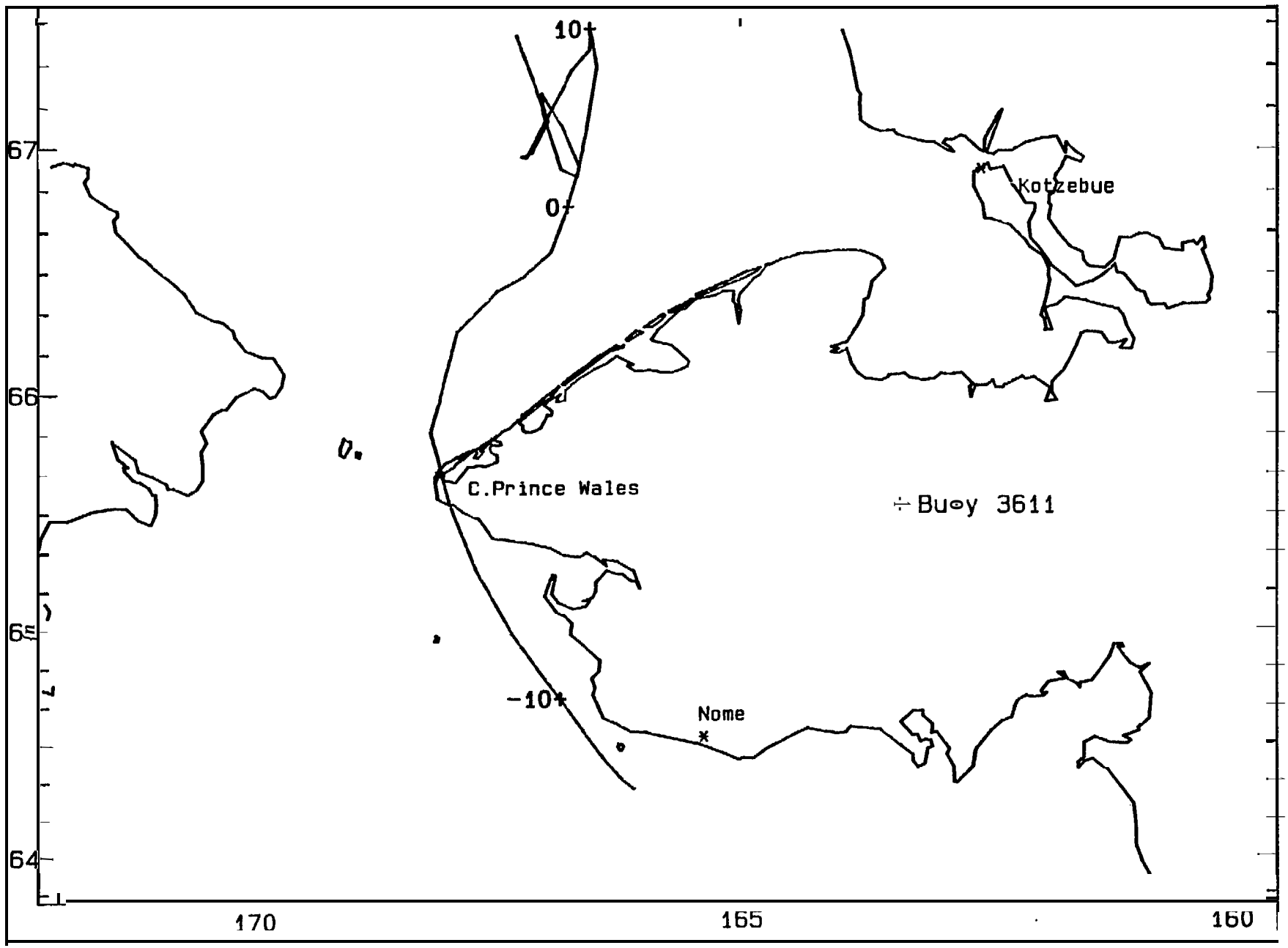
10
0
-10
67
66
65
64
170
165
160
Kotzebue
C.Prince Wales
Buoy 3611
Nome

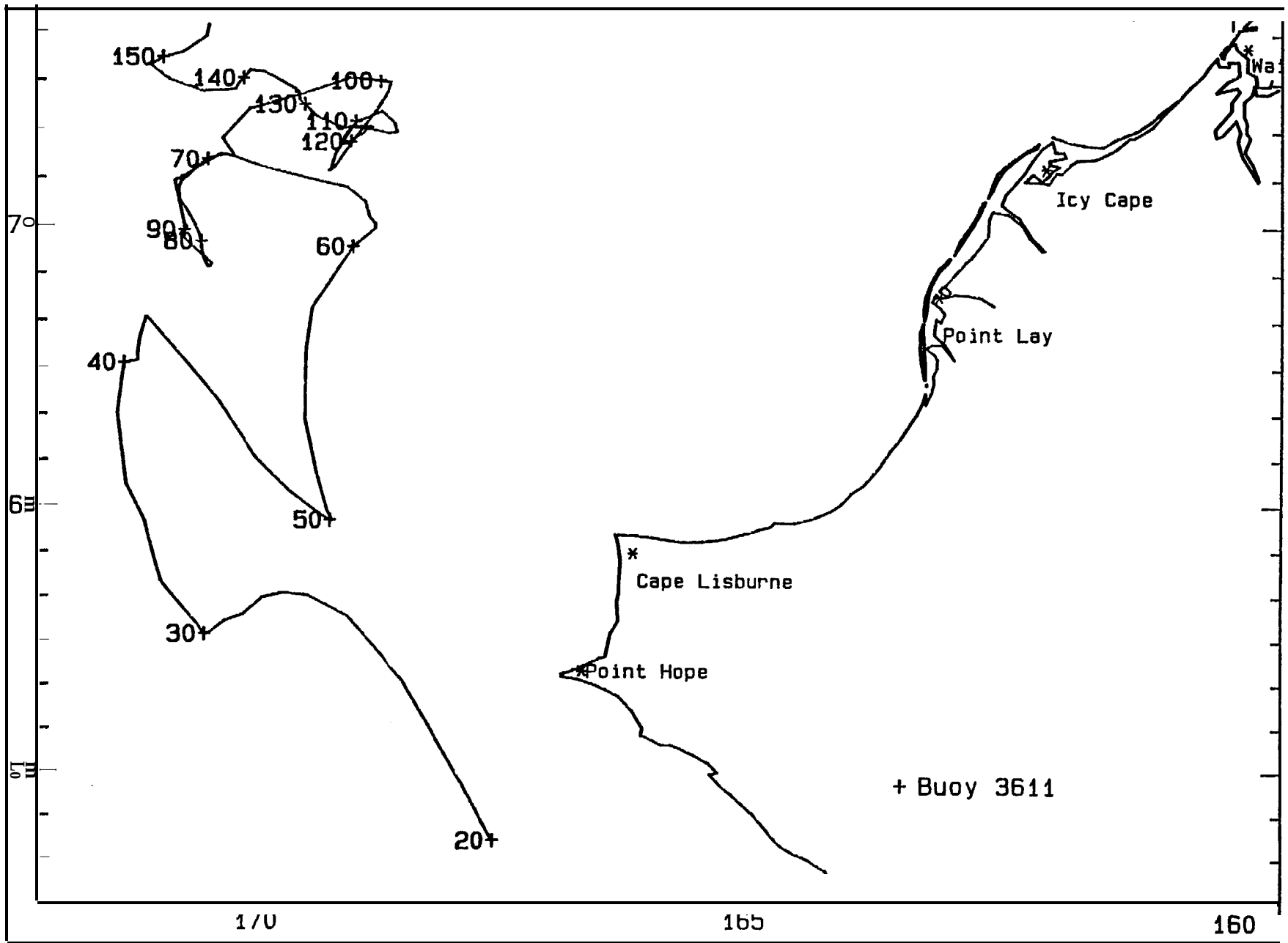
150+
140+
100+
130+
110+
120+
70+
90+
80+
60+
40+
50+
30+
20+
7°
6
10
Icy Cape
Point Lay
Cape Lisburne
Point Hope
+ Buoy 3611
170
165
160

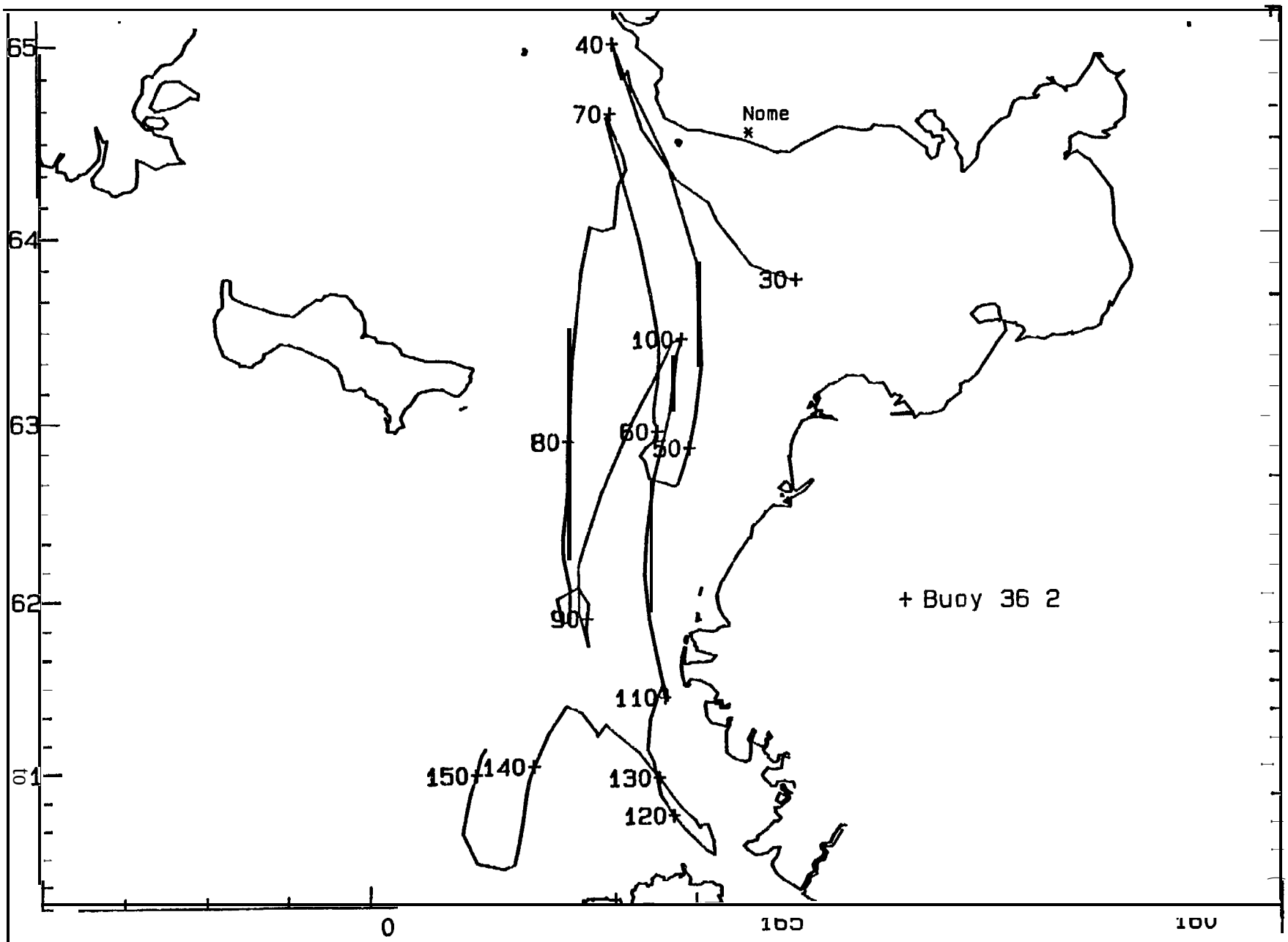
65
64
63
62
61
0
165
160
Nome
40
70
30
100
80
60
50
90
110
150
140
130
120
+ Buoy 36 2

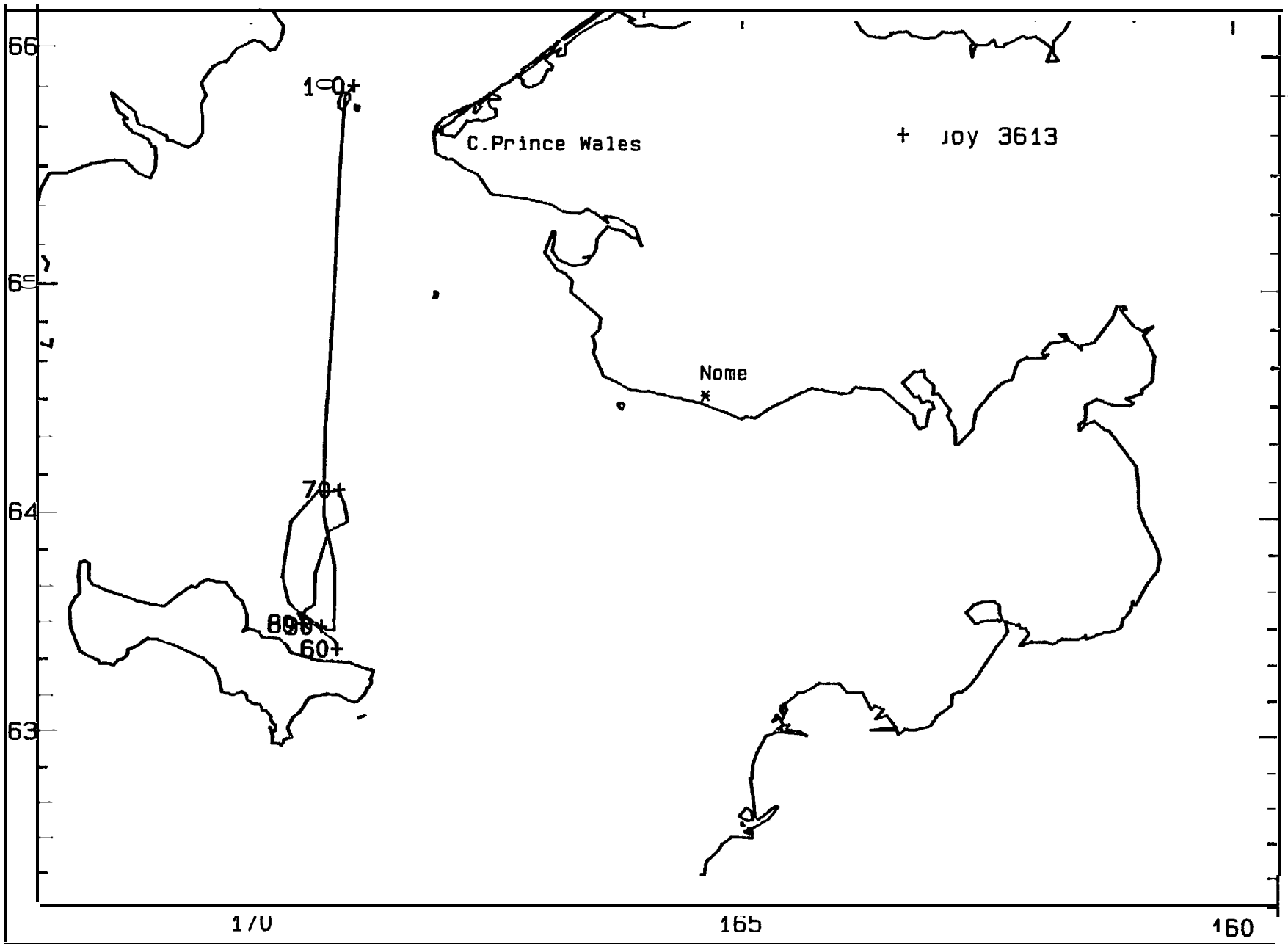
66
65
64
63
170
165
160
C.Prince Wales
+ Joy 3613
Nome
100+
70+
80+
60+

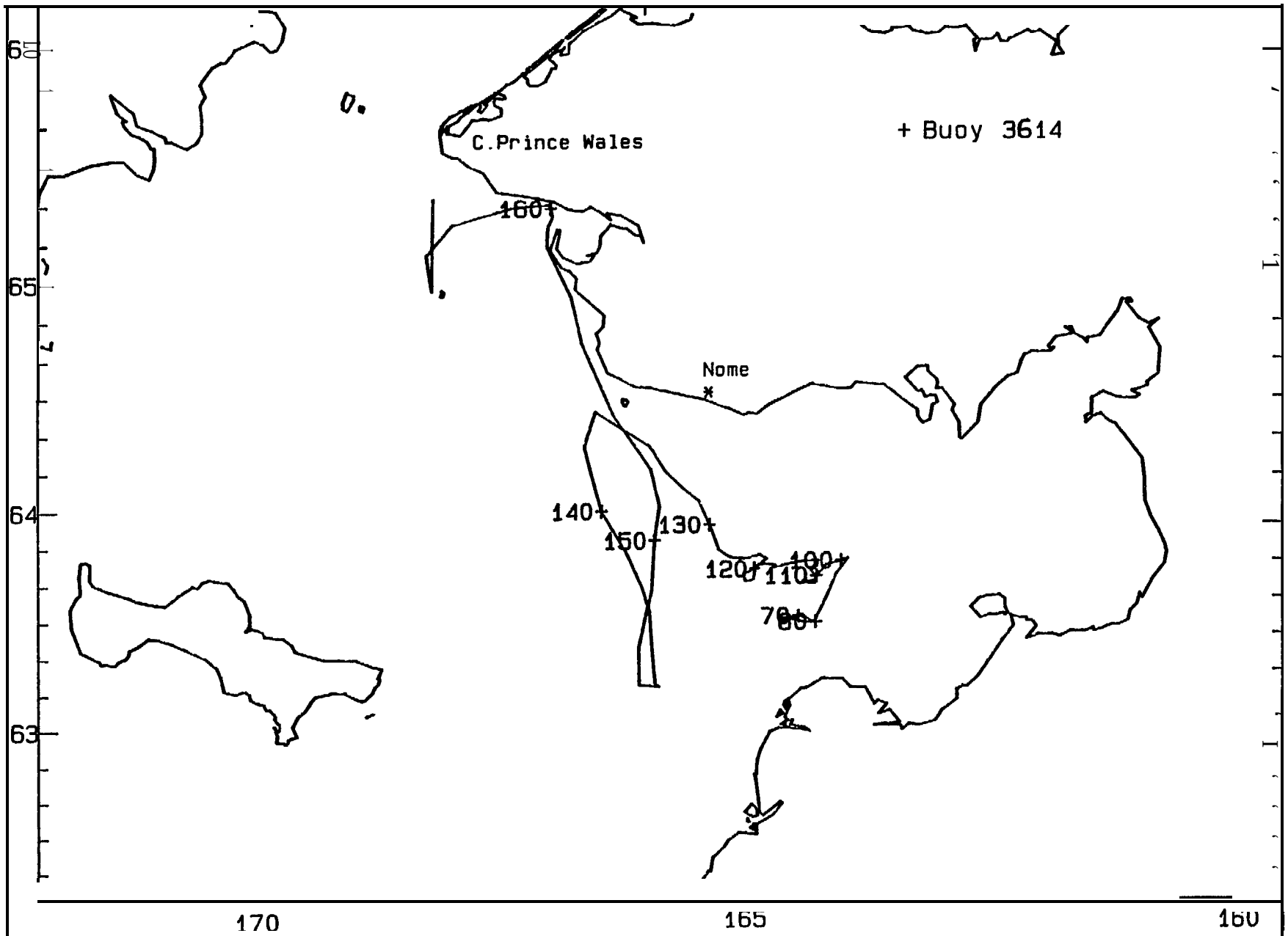
C.Prince Wales
+ Buoy 3614
Nome
160+
140+
150+
130+
120+
110+
100+
70+
80+
65
64
63
170
165
160

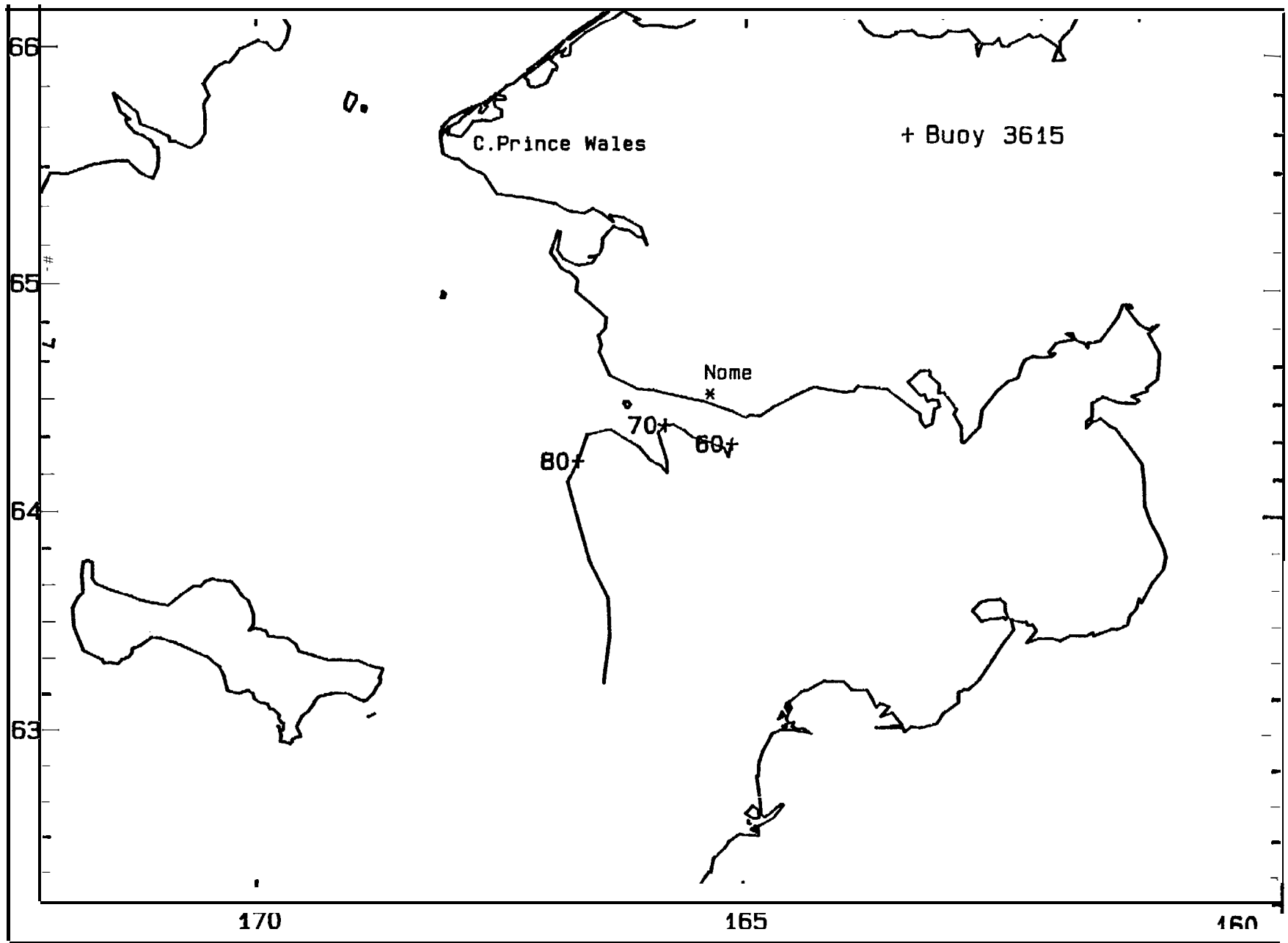
66
65
64
63
170
165
160
C.Prince Wales
+ Buoy 3615
Nome
70+
60+
80+

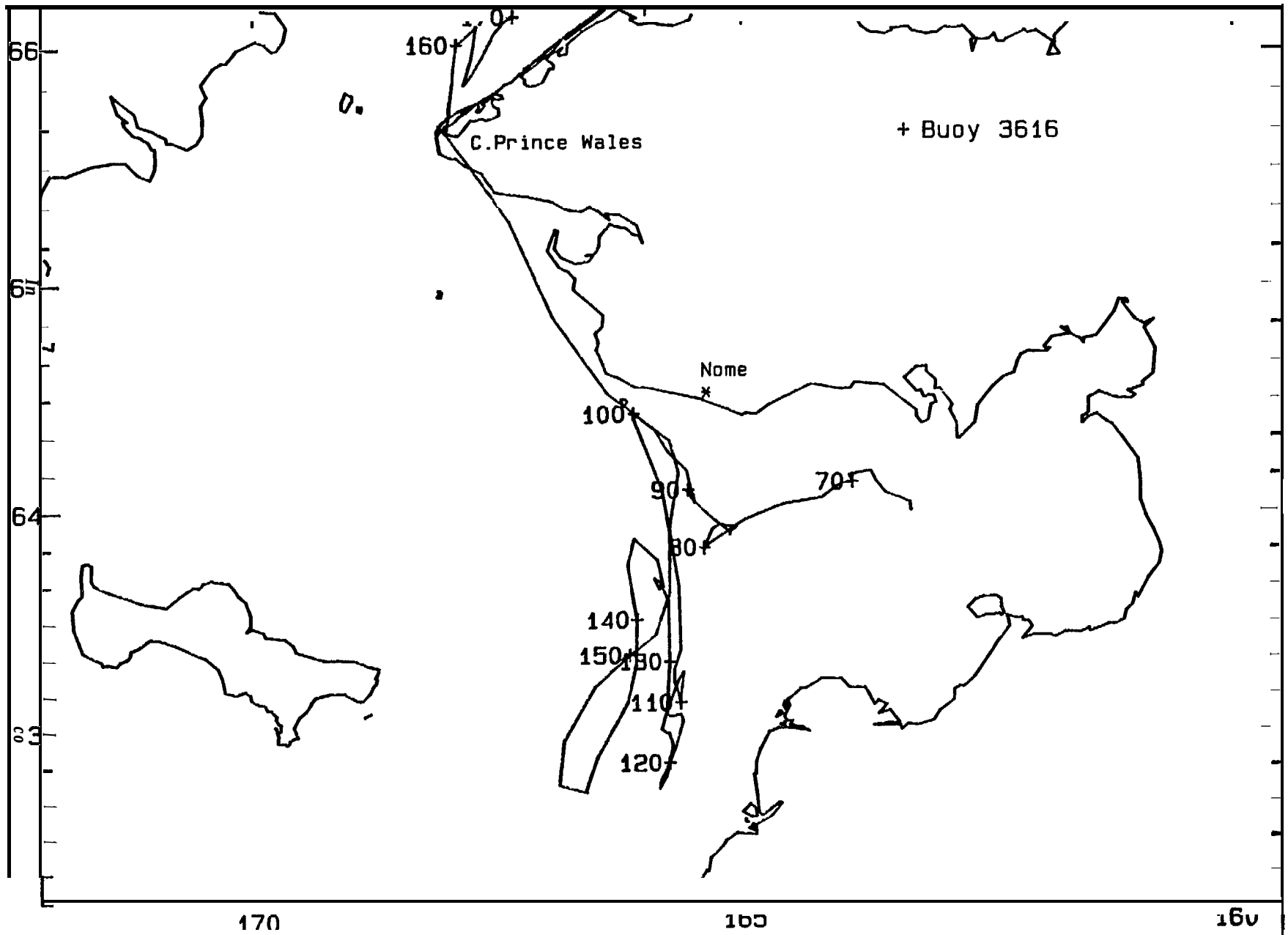
C.Prince Wales
+ Buoy 3616
Nome
160
100
90
70
80
140
150
130
110
120
66
64
170

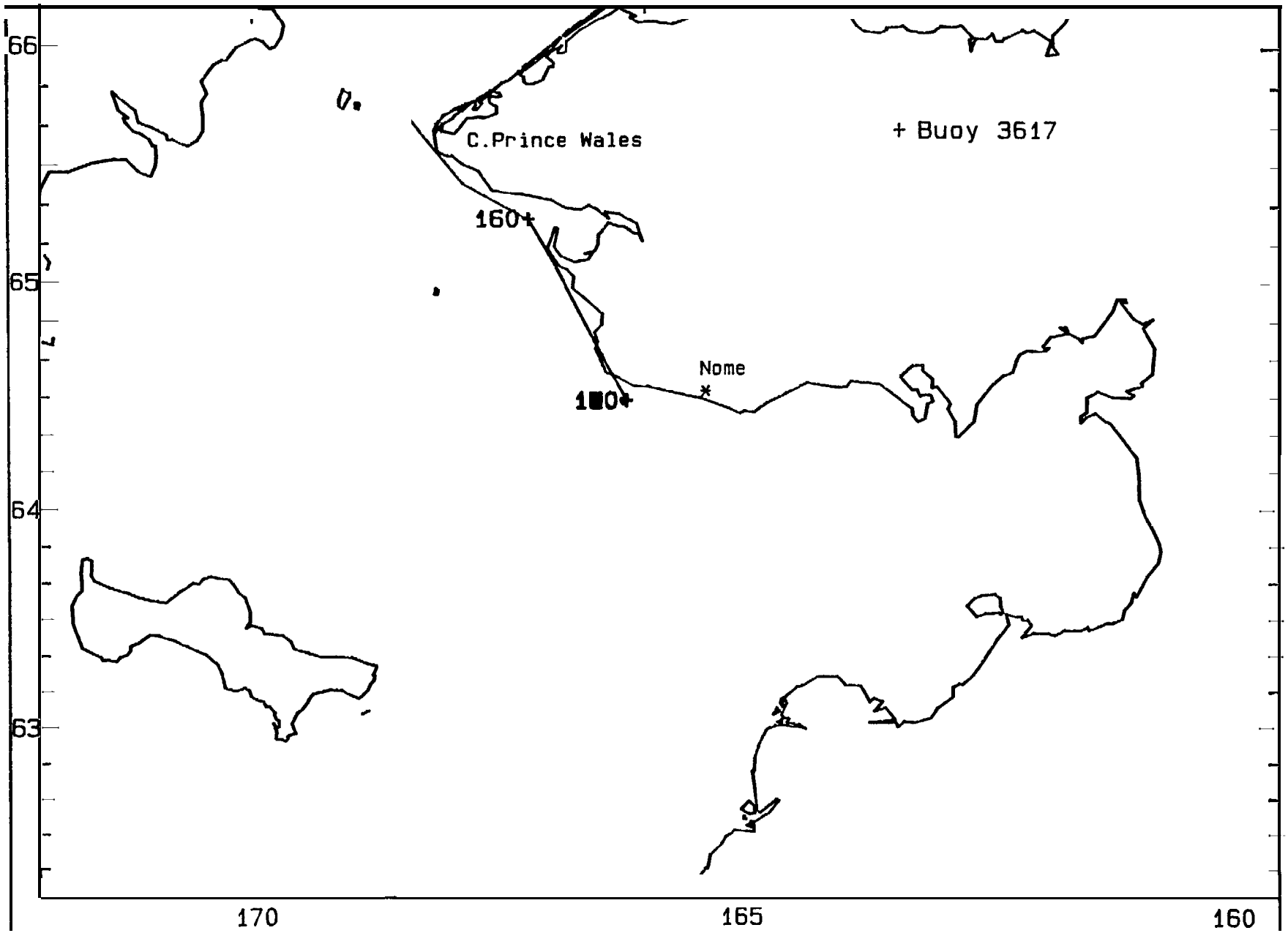
66
65
64
63
170
165
160
C.Prince Wales
+ Buoy 3617
160+
Nome
*

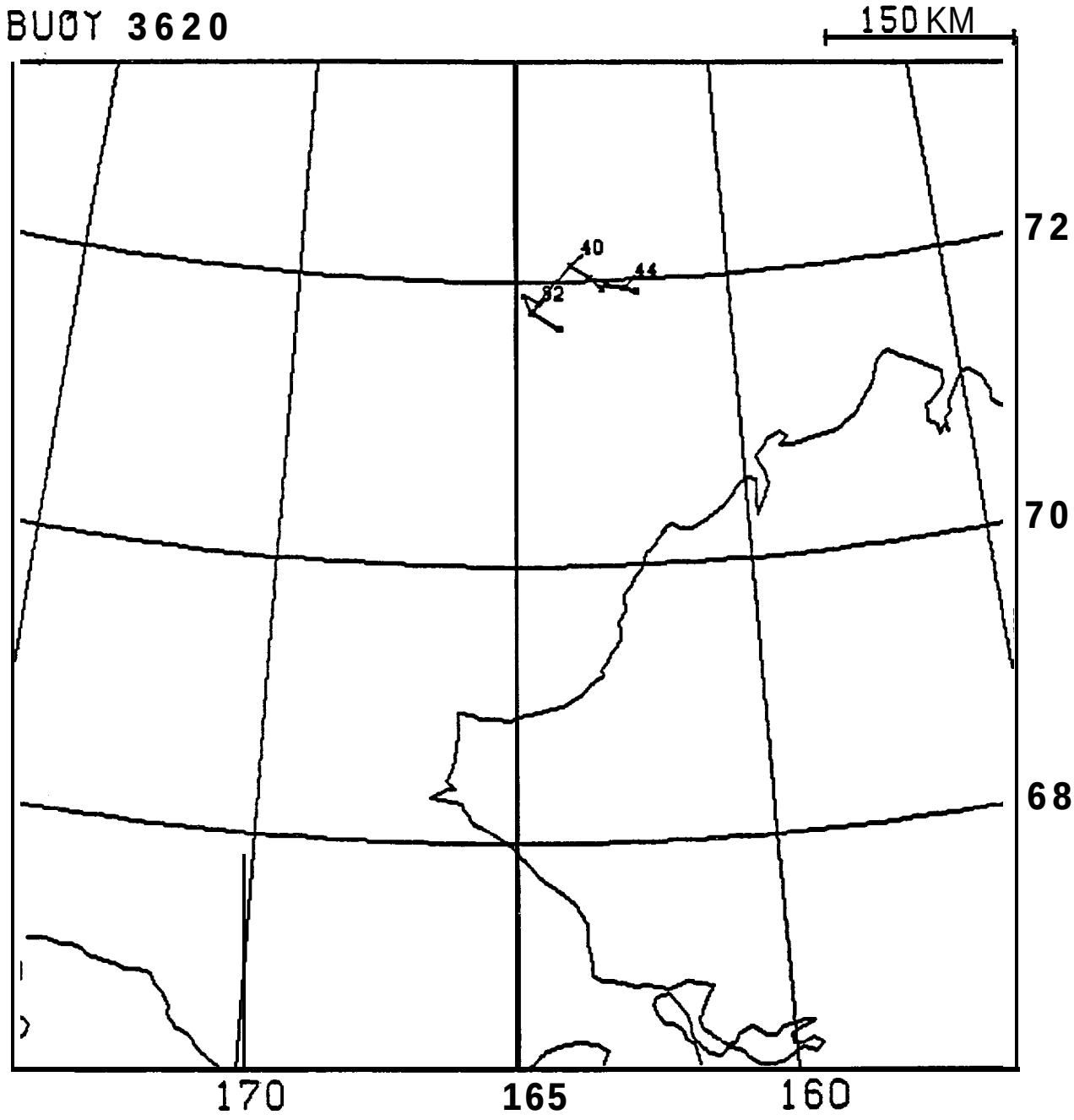
BUOY 3620
150 KM
72
70
68
40
44
32
170
165
160

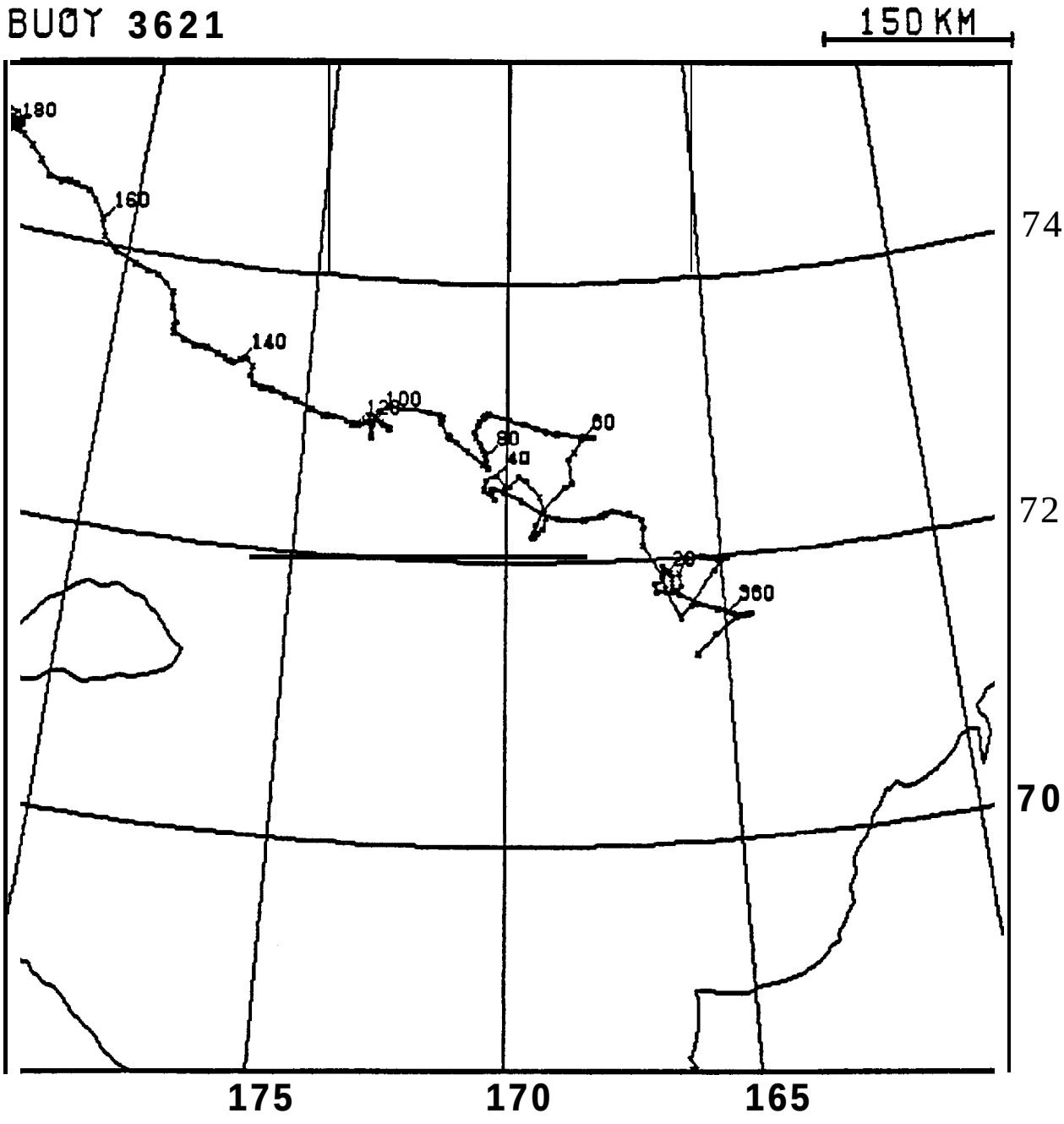
BUOY 3621
150 KM
180
160
140
120
100
80
60
40
20
360
74
72
70
175
170
165

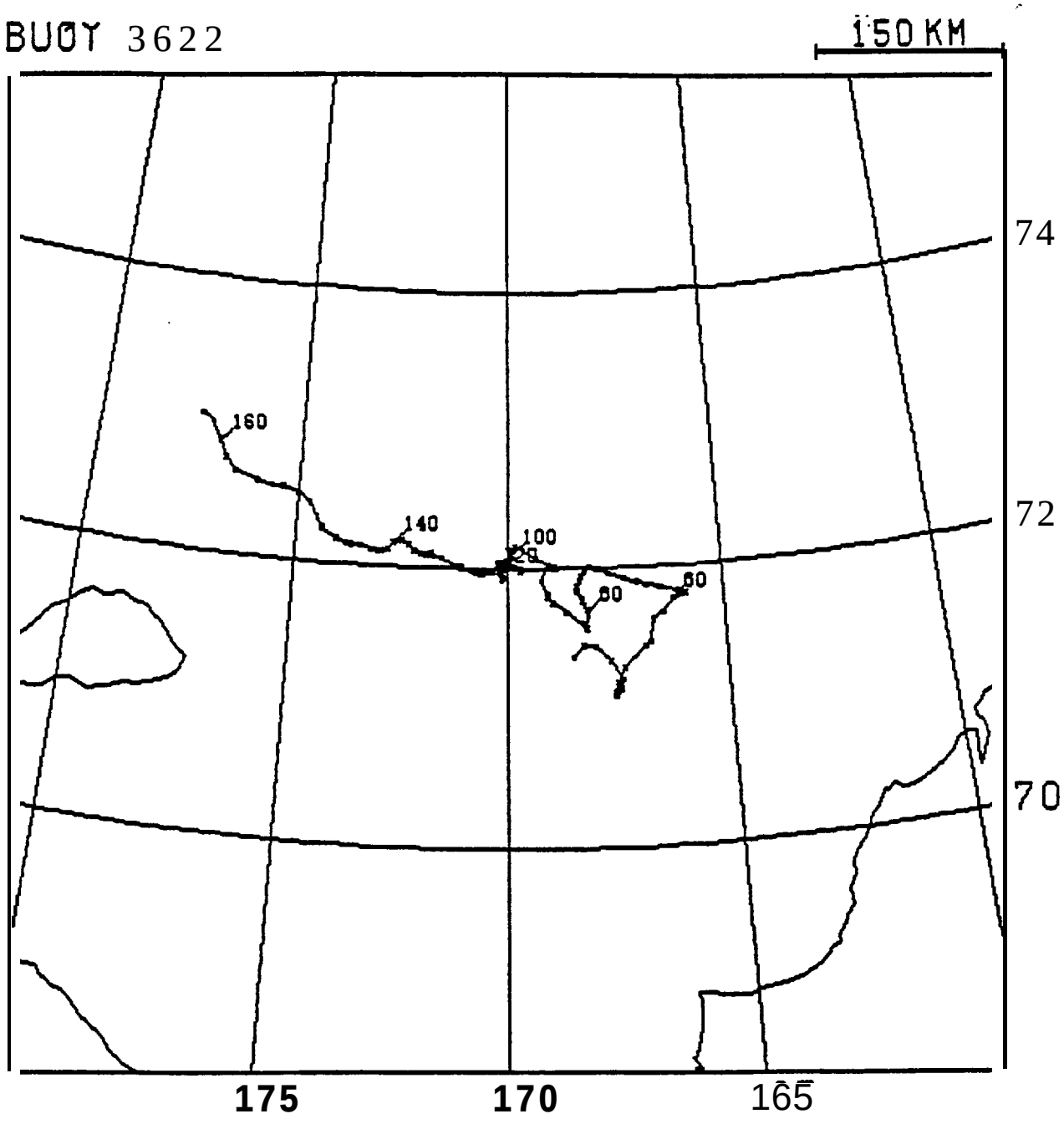
BUOY 3622
150 KM
74
72
70
160
140
100
20
60
60
175
170
165

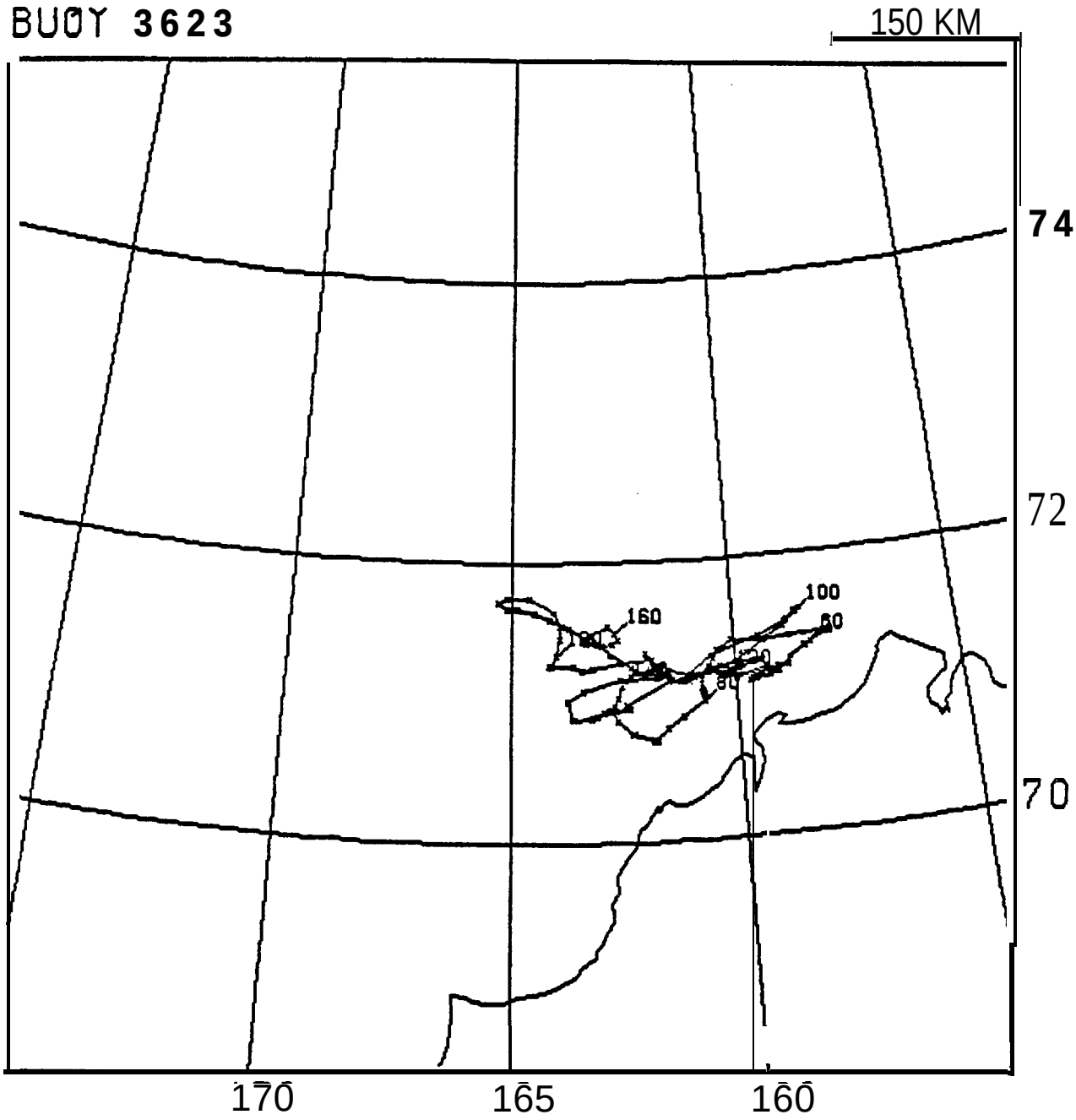
BUOY 3623
150 KM
74
72
70
160
100
60
170
165
160

BUOY 3624

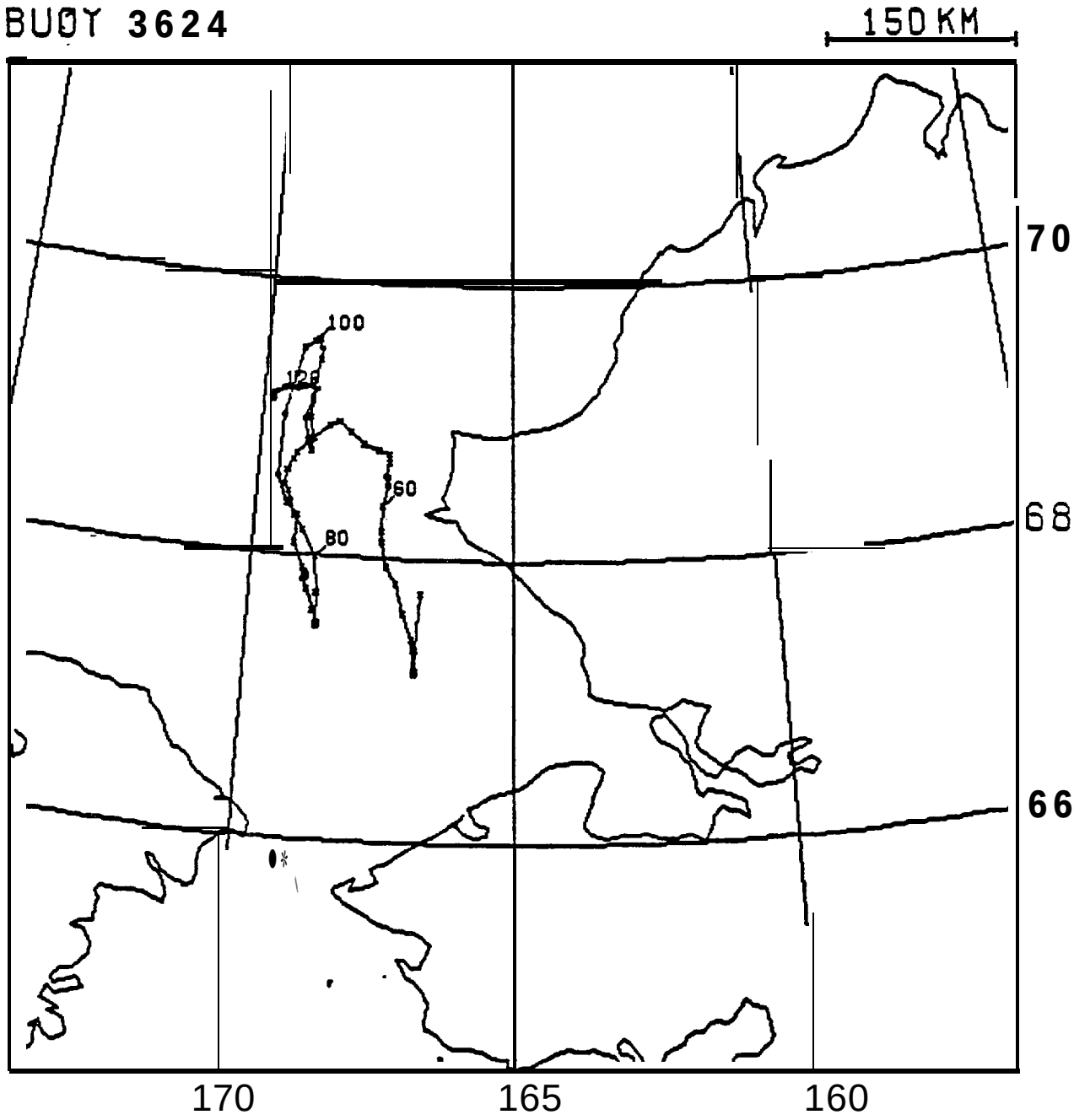

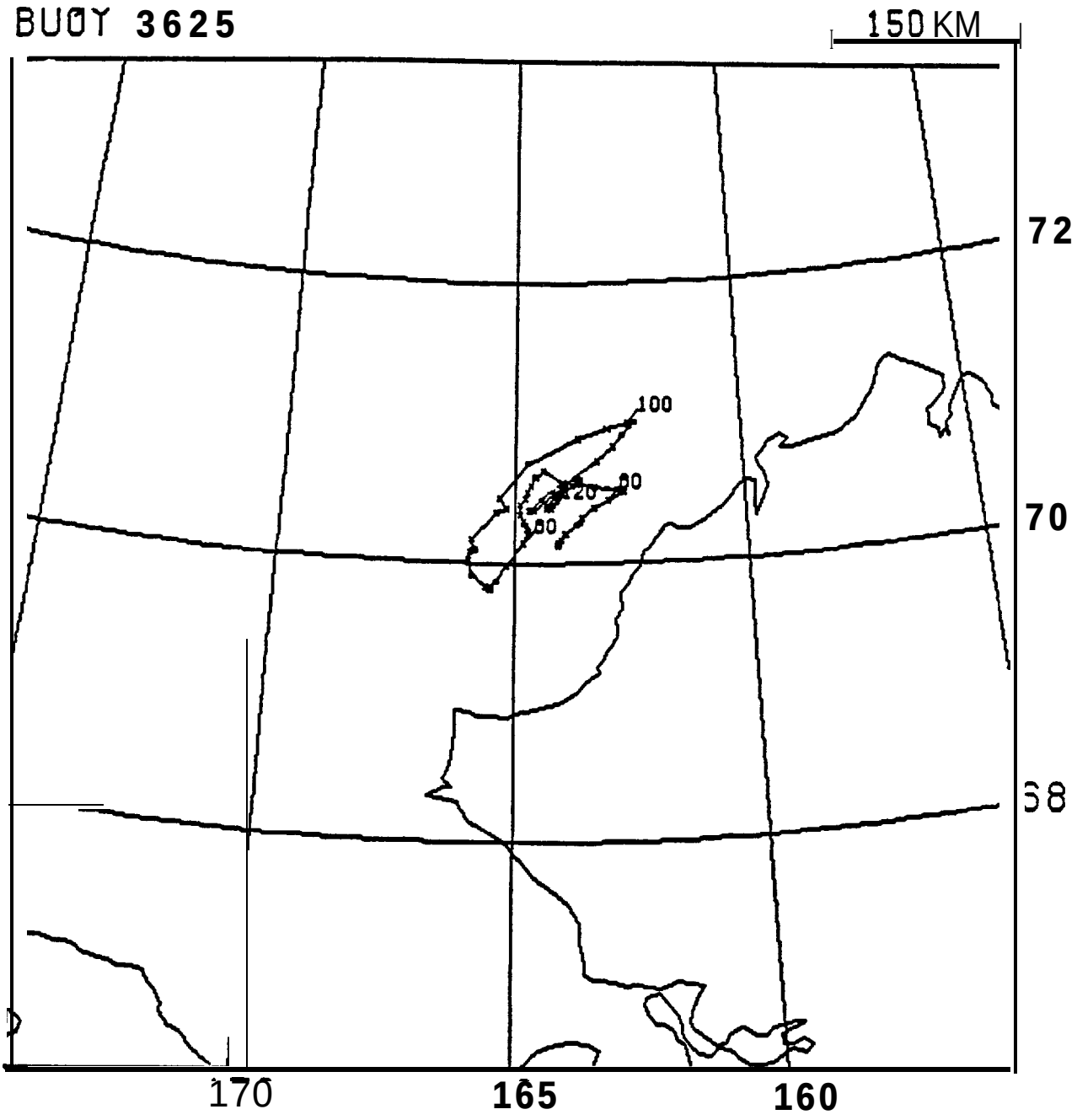
BUOY 3625
150 KM
72
70
68
170
165
160
100
120
80
100